AUBURN UNIVERSITY

SAMUEL GINN
COLLEGE OF ENGINEERING

Research Report

EFFECT OF LIGHTWEIGHT AGGREGATE ON EARLY-AGE CRACKING OF MASS CONCRETE

Submitted to

The Expanded Shale, Clay, and Slate Institute

Prepared by

Aravind Tankasala and Anton K. Schindler

August 2017

Highway Research Center
Harbert Engineering Center
Auburn, Alabama 36849

www.eng.auburn.edu/research/centers/hrc.html

Report No.	2. Government Accession No.	Recipient Catalog No.
Title and Subtitle Effect of Lightweight Aggregate on Early-Age Cracking of Mass Concrete		**Report Date** August 2017 **Performing Organization Code**
Author(s) Aravind Tankasala and Anton K. Schindler		**8. Performing Organization Report No.**
Performing Organization Name and Address Highway Research Center 238 Harbert Engineering Center Auburn University, AL 36830		**Work Unit No. (TRAIS)** **Contract or Grant No.**
Sponsoring Agency Name and Address The Expanded Shale, Clay, and Slate Institute 230E Ohio Street, Suite 400 Chicago, IL 60611-3265		**Type of Report and Period Covered** Technical Report **Sponsoring Agency Code**

Abstract

Early-age cracking in mass concrete structures is a severe problem which could lead to long-term serviceability related problems in the structure. In this project, the effect of using lightweight aggregates on the early-age cracking tendency of mass concrete was evaluated. Concretes were made with 30% Class F fly ash to be representative of mass concrete and the following concrete types were made at water-to-cementitious materials (w/cm) ratios of 0.45 and 0.38: 1) normalweight concrete, 2) internally cured concrete, 3) inverse sand-lightweight concrete, 4) sand-lightweight concrete, and 5) all-lightweight concrete. Rigid cracking frames were used to measure from the time of setting until the onset of cracking the development of concrete stresses caused by autogenous and thermal shrinkage effects. Rigid cracking frame specimens were tested under isothermal and match-cured temperature conditions. The match-cured temperature condition simulated the edge of an 8 × 8 ft mass concrete column.

The maximum in-place concrete temperatures increased as more lightweight aggregates were used in each mixture; therefore, care should be taken when using LWA concrete in mass concrete to make sure that the DEF temperature threshold is not exceeded. The use of lightweight aggregates in concrete with low w/cm is beneficial to control early-age cracking, because it helps to mitigate autogenous shrinkage and lower the modulus of elasticity of the higher strength concrete. The presence of LWA in concrete delayed the time to cracking, with SLW concrete providing the best overall resistance to early-age cracking. Although an increasing amount of LWA in the concrete will increase the maximum concrete temperature in mass concrete applications, the increasing use of LWA will reduce the modulus of elasticity, reduce the coefficient of thermal expansion, and eliminate autogenous shrinkage effects, which all contribute to improve the resistance to early-age cracking

Key Words	Distribution Statement		
Coefficient of thermal expansion, internal curing, shrinkage, temperature, cracking tendency, thermal stress.	No restrictions.		
Security Classification (of this report) Unclassified	**Security Classification (of this page)** Unclassified	**No. of pages** 87	**Price**

Form DOT F 1700.7 (8-72)

Research Report

Effect of Lightweight Aggregate on Early-Age Cracking of Mass Concrete

Prepared by

Aravind Tankasala
Anton K. Schindler

Highway Research Center
and
Department of Civil Engineering
at
Auburn University

August 2017

DISCLAIMERS

The contents of this report reflect the views of the authors, who are responsible for the facts and the accuracy of the data presented herein. The contents do not necessarily reflect the official views or policies of Auburn University. This report does not constitute a standard, specification, or regulation.

NOT INTENDED FOR CONSTRUCTION, BIDDING, OR PERMIT PURPOSES

Anton K. Schindler, Ph.D., P.E.
Research Supervisor

ACKNOWLEDGEMENTS

The authors wish to express their gratitude to the Expanded Shale, Clay, and Slate Institute (ESCSI) for funding this research project. The authors appreciate the lightweight aggregates and chemical admixtures donated by Norlite and BASF Construction Chemicals, respectively. The authors would like to thank the following individuals for their cooperation and assistance towards this research effort:

John P. Ries	ESCSI, Salt Lake City, Utah
Reid W. Castrodale	ESCSI, Concord, North Carolina
Abigail Gabbard	ESCSI, Chicago, Illinois
Bill Wolfe	Norlite, LLC, Cohoes, New York
Kenneth S. Harmon	Carolina Stalite Company, Waleska, Georgia
Michael Robinson	Carolina Stalite Company, Rocky Mount, North Carolina
Jeff F. Speck	Trinity Lightweight, Kennesaw, Georgia
Rickey Swancey	BASF Construction Chemicals, Spring Hill, Tennessee

ABSTRACT

Early-age cracking in mass concrete structures is a severe problem which could lead to long-term serviceability related problems in the structure. In this project, the effect of using lightweight aggregates on the early-age cracking tendency of mass concrete was evaluated. Concretes were made with 30% Class F fly ash to be representative of mass concrete and the following concrete types were made at water-to-cementitious materials (*w/cm*) ratios of 0.45 and 0.38: 1) normalweight concrete, 2) internally cured concrete, 3) inverse sand-lightweight concrete, 4) sand-lightweight concrete, and 5) all-lightweight concrete. Rigid cracking frames were used to measure from the time of setting until the onset of cracking the development of concrete stresses caused by autogenous and thermal shrinkage effects. Rigid cracking frame specimens were tested under isothermal and match-cured temperature conditions. The match-cured temperature condition simulated the edge of an 8 × 8 ft mass concrete column.

The maximum in-place concrete temperatures increased as more lightweight aggregates were used in each mixture; therefore, care should be taken when using LWA concrete in mass concrete to make sure that the DEF temperature threshold is not exceeded. The use of lightweight aggregates in concrete with low *w/cm* is beneficial to control early-age cracking, because it helps to mitigate autogenous shrinkage and lower the modulus of elasticity of the higher strength concrete. The presence of LWA in concrete delayed the time to cracking, with SLW concrete providing the best overall resistance to early-age cracking. Although an increasing amount of LWA in the concrete will increase the maximum concrete temperature in mass concrete applications, the increasing use of LWA will reduce the modulus of elasticity, reduce the coefficient of thermal expansion, and eliminate autogenous shrinkage effects, which all contribute to improve the resistance to early-age cracking

TABLE OF CONTENTS

LIST OF TABLES

LIST OF FIGURES

Chapter 1

Introduction

1.1 BACKGROUND

Mass concrete is defined by ACI 207.1R (2012) as “any volume of concrete with dimensions large enough to require that measures be taken to cope with the generation of heat from hydration of the cement and attendant volume change to minimize cracking”. Mass concrete construction began in the United States with the construction of large scale concrete structures such as dams and foundations. In 1930, the ACI committee 207 was formed to examine and solve problems related to cracking of dams. Today, mass concrete includes dams, bridge elements as shown in Figure 1-1, mat foundations, etc.

With regard to size, the least dimension of the concrete element is important in deciding if the element can be categorized as mass concrete (Gajda and VanGeem 2002). Most states and agencies designate mass concrete as elements with least dimension equal to or greater than 4 feet (Jahren et al. 2014).

Hydration of cementitious materials in concrete is an exothermic process, and a considerable quantity of heat is generated during the early stages of concrete construction (Neville 2011). The result is a significant rise in temperature at the core of element, and a temperature difference between the interior and exterior of the element due to the heat transfer at the edge with the environment. Two unique types of distresses can develop due to the high early-age temperatures that develop in mass concrete. The first of these—known as thermal cracking—is primarily attributed to a large difference between the concrete temperature at the core and edge of the element. Cracking occurs in the concrete when stresses in the concrete exceed the tensile strength of the concrete (Mehta and Monteiro 2013). If the concrete member is subjected to differential heating and cooling, stresses are induced in the concrete and as a result, it can lead to early-age thermal cracking of the concrete member (Emborg 1989). Concrete stresses are dependent on many factors such as the tensile strength, coefficient of thermal expansion, restraint conditions, modulus of elasticity, creep (relaxation), and temperature history (Emborg 1989). Effective control of early-age cracking can result in reduced cracking at later ages, more durable concrete with lower overall porosity, and extended service life of the structure (Bentz and Weiss 2011). Figure 1-2 is an example of thermal cracking in a bridge column in Texas.

Figure 1-1: Bridge column wrapped with insulating blankets (Jahren et al. 2014)

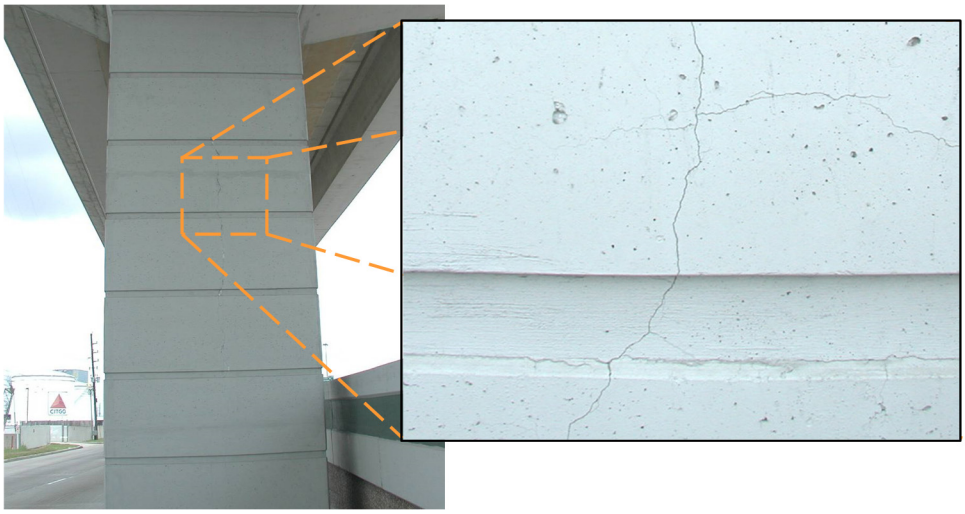

Figure 1-2: Thermal cracking of a bridge column in Texas (Photo courtesy of Dr. J.C. Liu)

The second type of distress of potential concern in mass concrete is known as delayed ettringite formation (DEF). DEF is a form of internal concrete sulfate attack, which is triggered by high early-age temperatures, the availability of moisture, and the availability of sulfate that is internally present in the concrete (Taylor et al. 2001). DEF causes an expansion in the concrete and this can lead to cracking, as shown in Figure 1-3.

Figure 1-3: Cracking due to DEF at the San Antonio Y overpass (Thomas et al. 2008)

1.2 LIGHTWEIGHT AGGREGATES

Lightweight aggregates (LWAs) have been used over the past 100 years from building ships to various structures. Though found in nature, manufactured LWAs are becoming increasingly popular in the concrete industry. Rotary kilns are used to produce lightweight aggregate (LWA) from shale, slate, and clay rocks under controlled conditions (Bremner and Ries 2009). While the addition of LWAs reduces the density of concrete, an additional and valuable property is its ability to absorb large quantities of water. The high internal pore volume of the LWAs acts as internal water reservoirs and when saturated the LWAs can supply water to the concrete to promote hydration of the cementitious materials, hence the term “internal curing of concrete” (Bentz and Weiss 2011).

Different classifications of concrete are obtained when adding LWA to concrete, and the commonly used ones include sand-lightweight concrete (SLWC), all-lightweight concrete (ALWC), and “internally cured” concrete (ICC). SLWC contains coarse LWA and normalweight fine aggregate, while ALWC contains both coarse and fine LWA. ICC generally involves replacing a portion of fine aggregate with fine LWA. Internal curing takes place in all concretes containing pre-wetted LWAs.

Lightweight aggregate has a higher insulating ability when compared to normalweight aggregate (Maggenti 2007) and concretes containing LWA have been found to reach higher maximum in-place

temperatures due to hydration, as shown in Figure 1-4 (Tankasala et al. 2017). Early-age cracking and the associated cracking risk of concrete are affected by several factors; therefore, a higher temperature difference alone does not render the concrete as more prone to early-age cracking (Byard and Schindler 2010). An earlier study concluded that the use of LWAs in bridge deck applications resulted in a significant improvement in resistance to early-age cracking when compared to normalweight concrete (Byard and Schindler 2010). This improved behavior was observed in internally cured (IC), sand-lightweight (SLW), and all-lightweight (ALW) concretes, and was attributed to an increase in tensile strength and a decrease in modulus of elasticity, coefficient of thermal expansion (CTE), and autogenous shrinkage. The study further concluded that although SLW and ALW concretes experienced higher peak temperatures, this did not translate to an increase in early-age cracking in bridge deck applications, and the reduction in CTE and elasticity modulus led to a significant overall delay of early-age cracking in bridge deck applications. Hence from an initial assessment, it would appear that the compounded benefits associated with LWA could be beneficial to mass concrete placements; however, verification of this concept by laboratory and field tests or by more sophisticated analysis has not yet been conducted.

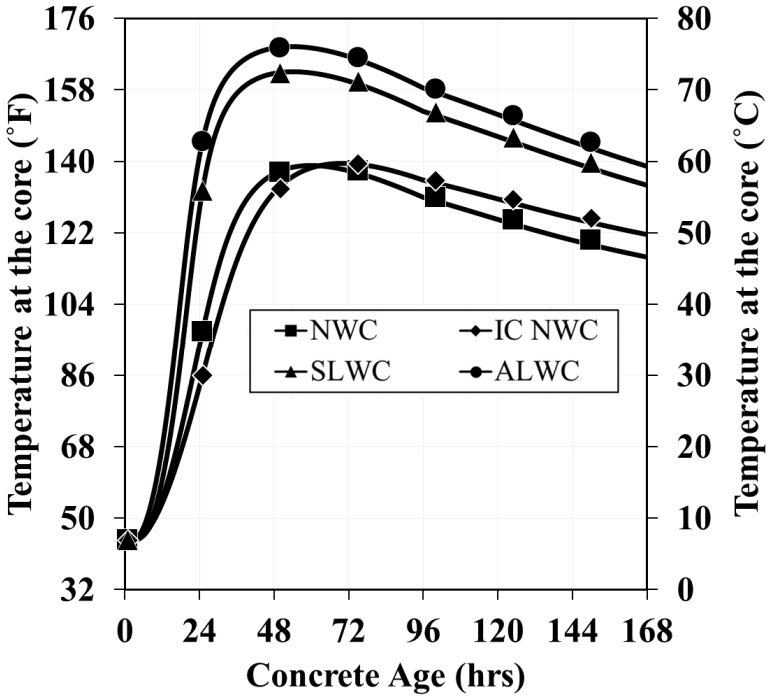

Figure 1-4: Comparison of simulated core concrete temperatures for normalweight concrete (NWC), internally cured normalweight concrete (IC NWC), sand-lightweight concrete (SLWC), and all-lightweight concrete (ALWC) for an 8×8 ft cross-section size column (Tankasala et al. 2017)

1.3 PROJECT OBJECTIVES

The primary objective of this study is to assess the effect of using lightweight aggregate on the early-age cracking tendency of mass concrete. The impact of using ICC, inverse sand-lightweight concrete (ISLWC), SLWC, and ALWC on the early-age cracking of mass concrete relative to normalweight concrete will be quantified. The secondary objectives of this study are as follows:

- Evaluate the effect of using lightweight aggregate on the development of concrete temperatures in mass concrete applications,
- Evaluate the compressive strength, splitting tensile strength, modulus of elasticity, coefficient of thermal expansion, and thermal diffusivity and determine their effect on the early-age cracking tendency of mass concrete,
- Evaluate the effect of water-to-cementitious-materials ratio (*w/cm*) in concrete containing lightweight aggregates on the cracking tendency of mass concrete,
- Compare the measured modulus of elasticity values to estimates from ACI 318 (2014) and AASHTO LRFD Bridge Design Specifications (2016) expressions, and
- Compare the measured splitting tensile strength values to estimates from ACI 207.2R (2007) and ACI 207.1R (2012) expressions, and evaluate the applicability of lightweight modification (λ) factor to estimate the splitting tensile strength recommended by Green and Graybeal (2013).

1.4 RESEARCH APPROACH

Rigid cracking frames (RCF), as shown in Figure 1-5, were used to evaluate the development of early-age concrete stresses from the time of initial set to cracking (Mangold 1998). Rigid cracking frames can measure the early-age development of thermal and autogenous stresses in hardening concrete. The cracking frames can be programmed to simulate a unique temperature history, thereby allowing researchers to gain detailed information about the combined effect of the heat of hydration, modulus of elasticity, creep (relaxation), coefficient of thermal expansion, tensile strength, and restraint on the cracking tendency of concrete. In this project, the cracking tendency of concretes was measured in the RCF, using a temperature profile to simulate mass concrete placement. A detailed discussion of the rigid cracking frame is provided in Section 3.4.3.

In addition to the cracking behavior of concrete specimens, the unrestrained free shrinkage was also determined using free-shrinkage frames (FSF), as shown in Figure 1-6. A detailed discussion of the free-shrinkage frame is provided in Section 3.4.4.

The time-depended development of mechanical properties were determined by performing compressive, splitting tensile, and modulus of elasticity tests at various ages as per ASTM C39 (2014), ASTM C496 (2014), and ASTM C469 (2014), respectively. The cylinders used to test the time-depended development of mechanical properties were match cured to the temperature of the RCF specimens. Semi-adiabatic calorimetry was used to characterize the heat of hydration and thermal diffusivity of each concrete

as discussed in Sections 3.4.1 and 3.4.2, respectively. The coefficient of thermal expansion of each concrete was determined as per AASHTO T336 (2009).

Two groups of concretes, each with a *w/cm* of 0.38 and 0.45 were tested. Each group of concretes contained five mixtures: a reference normalweight concrete, internally cured concrete, inverse sand-lightweight concrete, sand-lightweight concrete, and all-lightweight concrete. Ten concretes were thus produced under laboratory conditions and evaluated in this study. The use of two different *w/cm* concretes allows one to assess the effect of *w/cm* on the cracking tendency and stress development of the lightweight aggregate and reference concrete mixtures. For the lower *w/cm* concrete mixtures, the development of stress due to autogenous shrinkage were recorded under isothermal conditions. In order to be representative of mass concrete, Class F fly ash at a 30% (by mass) cement replacement level was used in all mixtures.

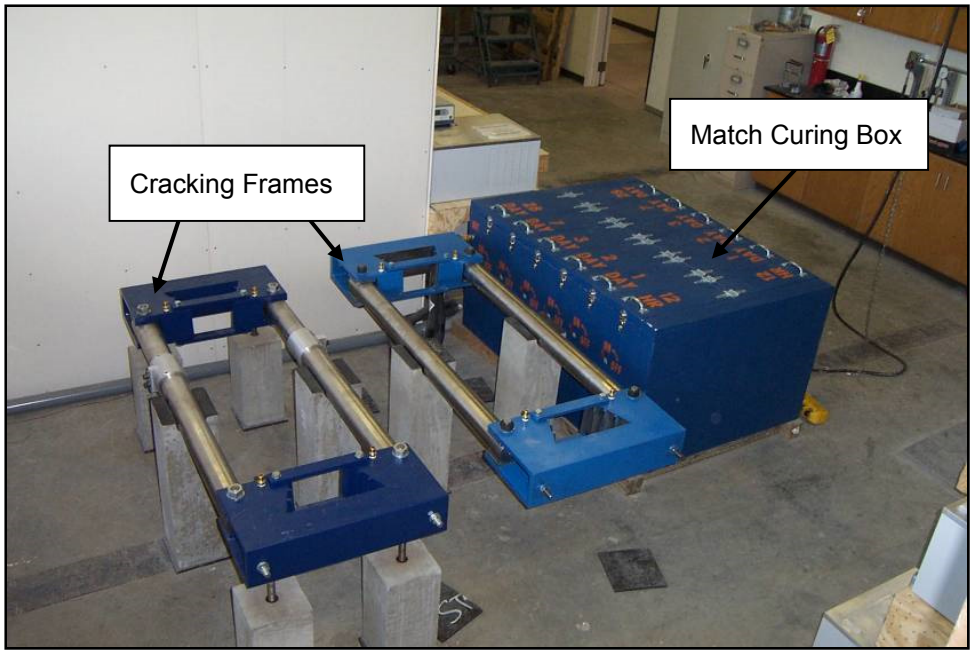

Figure 1-5: Rigid cracking frames used to evaluate the cracking potential of concretes (Byard and Schindler 2010)

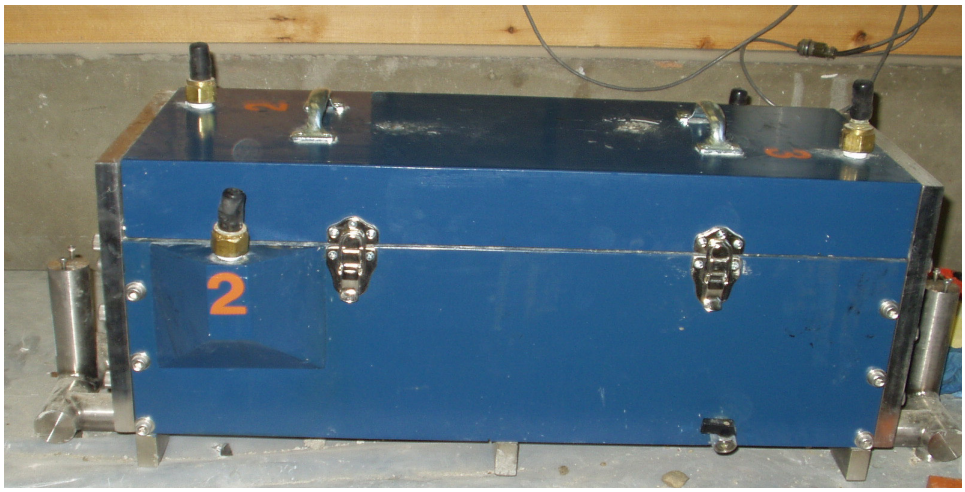

Figure 1-6: Free-shrinkage frame used to evaluate the unrestrained free shrinkage of concretes (Byard and Schindler 2010)

1.5 REPORT OUTLINE

This report contains six chapters. A literature review regarding early-age cracking, unique mass concrete issues, internal curing, lightweight aggregates, properties of lightweight aggregate, and the beneficial effects of lightweight aggregate in concrete is presented in Chapter 2. The experimental testing program to evaluate the early-age stress development of concrete and properties is covered in Chapter 3. In addition, the methods to assess the early-age stress development of concrete, temperature modeling of concrete, and properties of the materials used in the study are covered in Chapter 3. The results of the experimental work performed for this study are presented in Chapter 4. A discussion and synthesis of results are presented in Chapter 5. The summary, conclusions, and recommendations of this research project are presented in Chapter 6.

Chapter 2

Literature Review

A summary of the available research literature relevant to this project is provided in this chapter. The review includes a review of the factors responsible for early-age cracking, an overview of mass concrete structures and their associated temperature issues, lightweight aggregates, and the effects of internal curing on chemical and autogenous shrinkage along with its potential benefits for mass concrete applications.

2.1 EARLY-AGE CRACKING

Early-age cracking is primarily affected by the following factors (Emborg and Bernander 1994):

- Temperature development in the structure,
- Autogenous shrinkage associated with low *w/c* ratios,
- Early-age creep effects,
- Mechanical properties of the young concrete, and
- Restraint of the structure.

The effect of these factors on early-age cracking will be discussed in the remainder of this section.

2.1.1 Temperature and Thermal Stress Development

The thermal stresses can be computed from Equation 2-1 (Emborg and Bernander 1994). Creep (or relaxation) effects at early ages need to be accounted for to obtain an accurate estimate of the stress developments (Emborg 1989).

$$\text{Thermal Stress} = \sigma_T = \Delta T \times CTE \times K_r \times E_c \quad \text{..... (Equation 2-1)}$$

where,

ΔT = temperature change = $T_{zero\text{-}stress}$ - T_{min} (˚F),
CTE = coefficient of thermal expansion (strain/˚F),
K_r = degree of restraint factor,
E_c = creep adjusted elasticity of modulus (psi),
$T_{zero\text{-}stress}$ = concrete zero-stress temperature (˚F), and
T_{min} = minimum concrete temperature (˚F).

In order to gain an understanding of the evolution of early-age thermal stresses and how it is impacted by concrete temperatures and mechanical properties, a fully restrained element with an uniaxial stress state is considered in Figure 2-1. The concrete is placed in its fresh state under hot summer field

conditions. Initially the concrete is in a plastic state and hence no stresses are present. However, after final set is achieved, represented by time t_{fs}, stresses begin to develop in the concrete. The concrete hydration process is an exothermal reaction, and hence the concrete temperature begins to rise rapidly, starting from temperature at final set $T_{final\text{-}set}$ to a maximum temperature T_{max} (line B). The continued rise in temperature initially induces compressive stresses in the concrete; however, due to early-age relaxation effects the compressive stresses are reduced in magnitude (Emborg 1989; Westman 1999). When a concrete specimen is subjected to constant strain, creep manifests itself in the form of a progressive decrease in stress over time, and this phenomenon is known as relaxation (Neville 2011). The mechanical properties such as the strength and stiffness of the concrete starts to develop at final set, t_{fs}, and develops rapidly thereafter. After the maximum temperature is reached, the temperature begins to drop and the concrete begins to contract as a result. This results in the decrease of compressive stresses which eventually reaches a zero value at time t_{zs}. The corresponding temperature is known as zero-stress temperature T_{zs}. The zero-stress temperature is often considerably higher than the final set temperature T_{fs}. Beginning from time t_{zs} the stresses in concrete change from compression to tension for the first time. After further cooling, the stresses begin to increase (tensile), and once the stresses exceed the tensile strength of the concrete, cracking occurs and the time of cracking is denoted as t_c (Springenschmidt, Breitbucher and Mangold 1994). Therefore, only the portion of tensile stresses, which develop after the zero-stress temperature is unfavorable and results in thermal cracks.

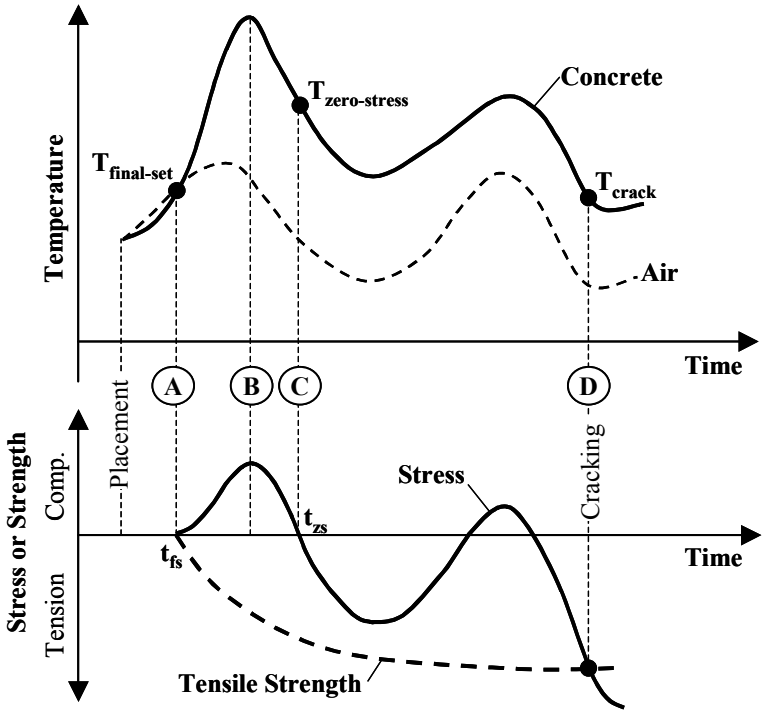

Figure 2-1: Evolution of early-age thermal stresses (Schindler and McCullough 2002)

2.1.2 Autogenous Shrinkage

The phenomena wherein the absolute volume of cement plus water decreases progressively with hydration is known as chemical shrinkage (Tazawa 1998; Holt 2001). Before setting, this phenomenon results in volumetric change, however, no stresses are generated since the concrete is still in a plastic state (Holt 2001). At setting, enough hydration products have formed to provide a self-supporting skeletal framework in the paste matrix. Water filled capillary voids are present in between the framework of solids. As water is consumed by the ongoing hydration process, the voids empty and capillary tensile stresses are generated, resulting in volumetric shrinkage (Tazawa 1998; Lura et al. 2003). The concrete volume change that occurs without mass loss, temperature variation, external force application, or restraint is called autogenous shrinkage (Tazawa 1998). At early concrete ages, viscous behavior is quite pronounced and the smallest stresses make way for large deformations (Lura et al. 2003). Stresses related to autogenous shrinkage may contribute significantly to early-age cracking (Tazawa 1998).

For higher *w/c*m, generally above 0.42, autogenous shrinkage and related stresses are not a major concern (Holt 2001). A graphical illustration of the relationship between chemical and autogenous shrinkage (horizontal direction) is shown in Figure 2-2, where *C* is the cement volume, *W* is the volume of water, H_y is the volume of hydration products, and *V* is the volume of voids.

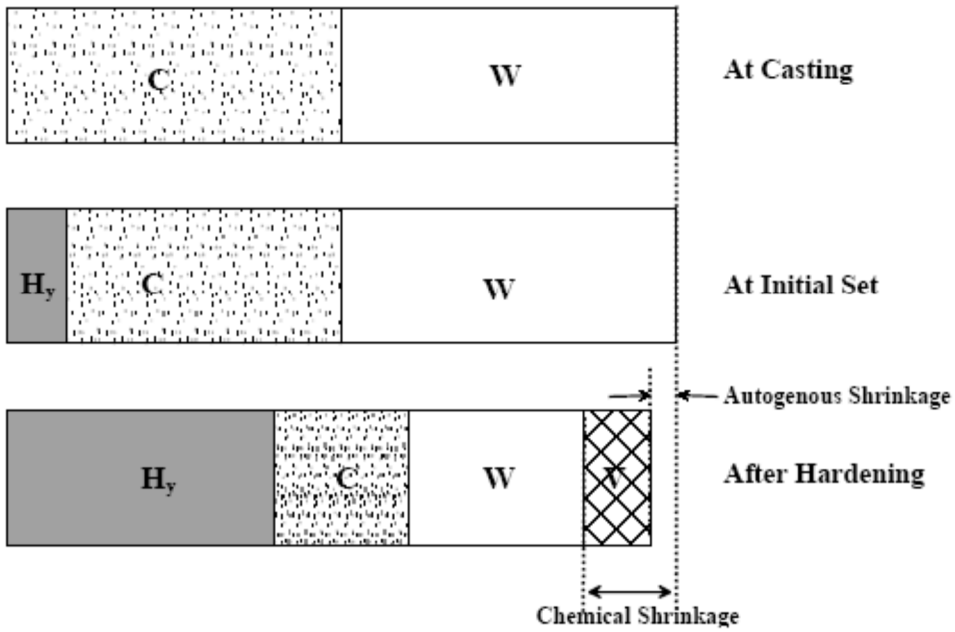

Figure 2-2: Volume reduction because of autogenous shrinkage (Tazawa 1998)

2.1.3 Early-age Creep or Relaxation

Creep can be defined as a gradual increase in strain with time under loading, i.e., an increase in strain under a sustained stress. Alternatively, if the concrete is restrained in such a manner that it is subjected only to a constant strain, then creep manifests itself in the form of a gradual decrease in stress over a period

and this phenomenon is known as relaxation (Neville 2011). Early-age creep or relaxation is generally beneficial in reducing early-age stresses and consequently cracking in concrete (Atrushi 2003).

Creep tends to be influenced by a mixture of intrinsic and extensive factors. Intrinsic factors include the strength, modulus of elasticity of aggregate, fraction of aggregate in the concrete mixture, and the aggregate size. An increase in any of these factors results in a decrease in creep (Bažant 1982). Extensive factors include temperature, pore water content, age at loading, etc. and their influence on creep is complicated (Bažant 1982). Early-age creep data are scarce in literature owing to the complexity of testing concrete creep at early ages. Compressive and tensile creep tends to increase with a rise in temperature; however, this is offset by an increase in hydration rate, which in turn reduces creep (Umehara et al. 1994; Bažant 1982).

2.1.4 Mechanical Properties of Concrete

2.1.4.1 Compressive Strength

The compressive strength of concrete depends on many factors: the water-to- cementitious materials-ratio (*w/cm*), curing conditions, total air content, aggregate type, aggregate size, and rate of loading to name a few (Mehta and Monteiro 2013). Numerous expressions exist for modeling the compressive strength of concrete (Hedlund 2000); however, for this study the exponential equation, Equation 2-2, developed by Freiesleben Hansen and Pederson (1977) is used.

$$f_c(t_e) = f_{cult} \times exp\left(-\left(\frac{\tau_s}{t_e}\right)^{\beta_s}\right) \quad \text{(Equation 2-2)}$$

where,

$f_c(t_e)$ = compressive strength at equivalent age t_e (psi),

f_{cult} = ultimate compressive strength parameter (psi),

τ_s = strength development time parameter (hrs),

β_s = strength development slope parameter (unitless), and

t_e = equivalent age (hrs).

2.1.4.2 Splitting Tensile Strength

The tensile strength depends on similar factors as compressive strength; however, it is more sensitive to the quality of bond between the aggregate and paste. Higher tensile strength values at early ages are desired to improve resistance to early-age cracking. Splitting tensile strength can be estimated by Equation 2-3 (ACI 207.2R 2007), provided the compressive strength is known. ACI 207.1R (2012)

adopted an expression from Raphael (1984), which is shown in Equation 2-4 for estimating the splitting tensile strength for mass concrete structures from a known compressive strength.

$$f_{ct}=6.7\times(f_c)^{0.5} \quad \text{(Equation 2-3)}$$

$$f_{ct}=1.7\times(f_c)^{\frac{2}{3}} \quad \text{(Equation 2-4)}$$

where,

f_{ct} = splitting tensile strength (psi), and

f_c = concrete compressive strength (psi).

Greene and Graybeal (2013) also developed an expression, shown in Equation 2-5, to estimate the splitting tensile strength from known compressive strength values using a lightweight modification factor (λ). The lambda modification factor is determined from the concrete density, as shown in Equation 2-6.

$$f_{ct}{}''=0.212\times\lambda\times(f''_c)^{0.5} \quad \text{(Equation 2-5)}$$

$$0.75\leq\lambda=7.5\times w_c{}''\leq 1.0 \quad \text{(Equation 2-6)}$$

where,

w''_c = density of normalweight concrete or equilibrium density of lightweight concrete (kcf),

f''_{ct} = splitting tensile strength (ksi),

f''_c = concrete compressive strength (ksi), and

λ = lightweight modification factor (unitless).

2.1.4.3 Modulus of Elasticity

The modulus of elasticity is affected by the type of aggregate and the volume proportion of aggregate in the concrete (Neville 2011). Equation 2-7 from ACI 318 (2014) is used to estimate the modulus of elasticity from the known density and compressive strength. Recently, AASHTO (2016) adopted a new expression for determining the modulus of elasticity of concrete from known density and compressive strength values, and this expression is shown in Equation 2-8. From both these equations, it can be seen that a decrease in concrete density results in a decrease in modulus of elasticity. Lower modulus of elasticity of concrete will reduce early-age stresses and contribute to reduced cracking at early ages (Bentz and Weiss 2011; Byard et al. 2012).

$$E_c=33\,(w_c)^{1.5}(f_c)^{0.5} \quad \text{(Equation 2-7)}$$

$$E_c{}''=120{,}000\,K_1(w_c{}'')^{2.0}\left(f_c{}''\right)^{0.33} \quad \text{(Equation 2-8)}$$

where,

E_c = modulus of elasticity (psi),

E''_c = modulus of elasticity (ksi),

f_c = concrete compressive strength (psi),

w_c = density of normalweight concrete or equilibrium density of lightweight concrete (lb/ft^3),

f''_c = concrete compressive strength (ksi),

w_c'' = density of normalweight concrete or equilibrium density of lightweight concrete (kips/ft^3), and

K_1 = aggregate correction factor (unitless)

2.1.5 Degree of Restraint

Degree of restraint is the ratio of the actual stress resulting from volume change to the stress that would be present if full restraint was present. All concrete elements are restrained to a certain degree either by supporting elements or by different parts of the element itself (ACI 207.2R 2007). Restraint of an element is impacted by many factors, with the important ones being its own modulus of elasticity, the modulus of elasticity of the restraining element, and the geometry of the structure (usually the cross-sectional area) (ACI 207.2R 2007). While restrained volume change may induce a tensile, compressive or flexural state of stresses in concrete elements, those restraint conditions leading to a tensile state of stress in concrete are of concern due to their contribution to concrete cracking (ACI 207.2R 2007). Lower restraint leads to lower stresses and various models for modeling of restraint are available in literature (Larson 2003; ACI 207.2R 2007).

2.2 UNIQUE MASS CONCRETE ISSUES

Thermal stresses arising because of temperature differences between the zero-stress temperature and the temperature at cracking were discussed in the previous section. However, unique temperature issues related to mass concrete exist. An important distinction between normal concrete elements and mass concrete elements is their size and the thermal behavior. Mass concrete is defined by ACI (ACI 207.2R 2007) as “any volume of concrete with dimensions large enough to require that measures be taken to cope with the generation of heat and attendant volume change to minimize cracking”. The minimum dimension for a structure to be defined as mass concrete varies across state agencies, but according to ACI 301 (2016), if the least dimension of the concrete structure is greater than 4 ft, it can be considered a mass concrete structure. Because of their size, high temperatures develop at the core of the mass concrete element which leads to increased risk of: 1) delayed ettringite formation (DEF), and 2) thermal cracking.

2.2.1 Delayed Ettringite Formation

Delayed ettringite formation (DEF) can be described as the formation of ettringite after the concrete hardening process is completed and in which none of the sulfate which causes the ettringite formation comes from external sources (Taylor, Famy, and Scrivener 2001). It is a form of internal concrete sulfate attack, which is triggered by high temperatures and availability of sulfate, which is internally present in the concrete. Owing to their large size and high heat of hydration, mass concrete with only plain portland cement, that experiences temperatures more than 158˚F (70°C), are generally susceptible to DEF formation (Sylla 1988; Folliard et al. 2006; Livingston et al. 2006). Distresses due to DEF may include map cracking, fracture of surfaces, and deterioration of strength in the concrete due to formation of ettringite crystals (Livingston et al. 2006). Figure 2-3 shows a column of the San Antonio Overpass damaged because of DEF (Folliard et al. 2006). Various state agencies place a restriction on the maximum concrete temperature, generally 160˚F, to prevent DEF (Jahren et al. 2014). Incorporation of sufficient amounts of various supplementary cementitious materials (SCMs) helps in preventing DEF and the maximum temperature regulations may be relaxed in such cases (ACI 301 2016). For example, if the cementitious content includes 25 percent (by mass) of cement replacement with Class F fly ash, then the concrete maximum temperature limit may be increased to 185°F to mitigate DEF (ACI 301 2016).

Figure 2-3: Cracking observed in a mass concrete column due to DEF (Folliard et al. 2006)

2.2.2 Thermal Cracking

Thermal gradient can be defined as a temperature change along a specific path through the concrete structure (ACI 207.2R 2007). There are two types of thermal gradients, mass and surface gradients. The mass gradient refers to the long-term maximum internal temperature change of a large concrete mass as it cools from an internal peak temperature to a stable temperature equal to approximately the average

ambient temperature. Surface gradients refers to the temperature differences between the core and the surface of the concrete member (ACI 207.2R 2007). Due to their large size, and other factors such as thermal conductivity, specific heat, and density, the heat generated in the interior of a mass concrete member is not easily transferred through the concrete and thus high temperatures are sustained in the core for extended durations (ACI 207.1R 2012). Also, heat generated at the surface can quickly be dissipated to the surroundings resulting in a lower surface temperature. This difference in temperature between the surface and the core can cause large thermal gradients leading to severe cracks, which may reduce the long-term durability of the mass concrete element (ACI 207.1R 2012). An example of thermal cracking is provided in Figure 2-4.

Figure 2-4: Thermal cracking observed in a thick slab (Gajda 2007)

Most state agencies limit the thermal gradients to 35˚F, and it is the most commonly used temperature differential limit in mass concrete projects (Jahren et al. 2014). This approach was resorted to as a precautionary measure to prevent thermal cracking after early research projects involving dams in Europe used this 35°F limit (FitzGibbon 1976; Bamforth 1981). Nonetheless, no readily available laboratory or field research evidence confirms the suitability of a maximum temperature differential of 35˚F for all concretes. The use of supplementary cementitious materials, reduced concrete placement temperatures, and favorable ambient temperature are some of the factors which can reduce thermal gradients in a mass concrete structure.

2.3 LIGHTWEIGHT AGGREGATES

Lightweight aggregate (LWA) occurs in nature and is found as pumice and scoria and have been used in lightweight concrete for over 100 years (Bremner and Ries 2009). Modern LWA is manufactured from special deposits of shale, clay, or slate. The diagram shown in Figure 2-5, taken from ESCSI Reference Manual (Holm and Ries 2007), details the LWA production process. The raw materials for LWA are mined from deposits of clay, shale, slate, etc. They are then crushed and sized (stored if necessary) and sent via a conveyor belt into a rotary kiln. They are produced by heating graded particles into the high end of the rotary kiln, to a temperature of 2100˚F. The rotary kiln is generally 60 to 225 ft in length with diameters varying between 6 to 12 ft. The LWA spends 30 to 60 minutes in the kiln, with gradual heating occurring in the first 2/3rd of the kiln length and rapid heating in the final 1/3rd of the kiln length. Upon heating the pyroplastic mass, gases are liberated which cause expansion, and the expansion is retained upon cooling. After cooling the expanded particles have a unique vesicular structure and contain pores that have a size range of approximately 5 to 300 µm developed in a continuous, crack-free, high-strength vitreous phase. After the cooling process the aggregates are crushed to appropriate gradations and shipped to concrete production plants (Holm and Ries 2007; ACI 213R 2013).

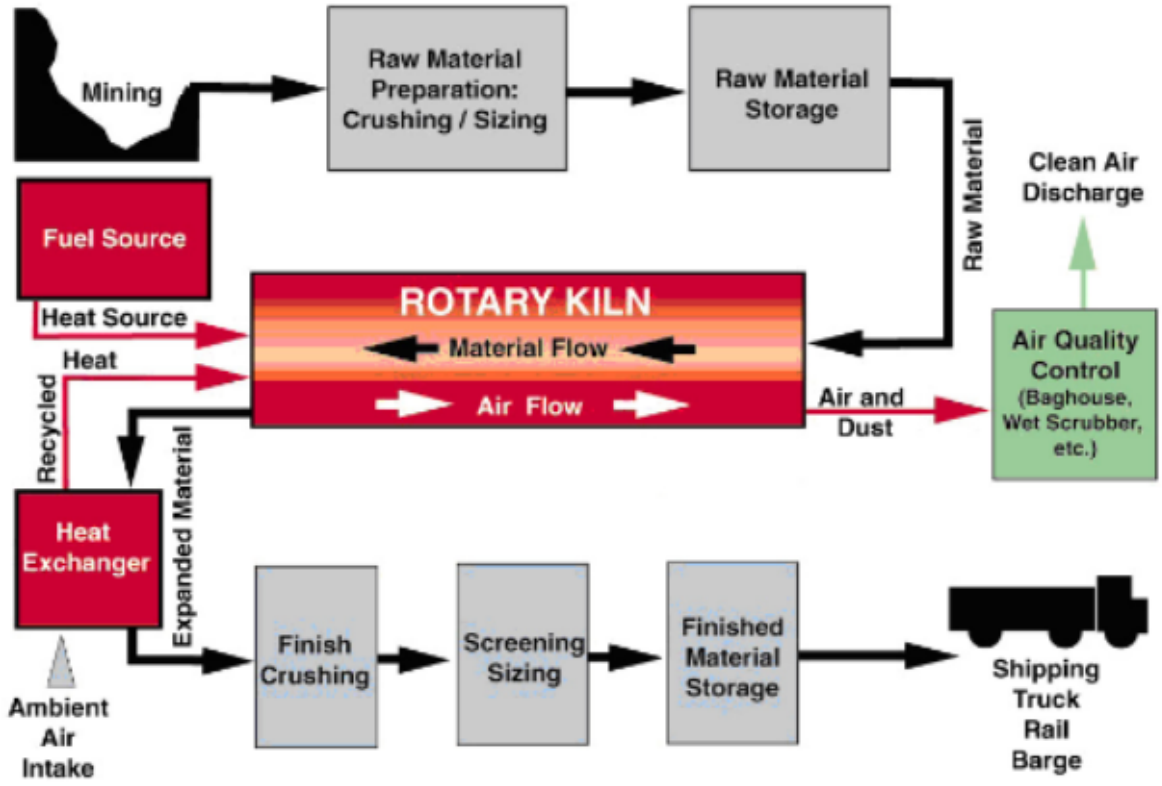

Figure 2-5: Production of rotary kiln lightweight aggregate (Holm and Ries 2007)

Pores close to the surface are readily permeable and rapidly absorb water within the first few hours of exposure to moisture; however, interior pores fill extremely slowly. Non-interconnected interior pores, which form a small fraction of the total pores, are never filled even after years of immersion in water (Holm and Ries 2007).

2.4 INTERNAL CURING

Internal curing was originally defined by the American Concrete Institute (ACI) as "supplying water throughout a freshly placed cementitious mixture using reservoirs, via pre-wetted lightweight aggregates, that readily release water as needed for hydration or to replace moisture lost through evaporation or self-desiccation." In 2013, ACI changed the definition of internal curing to “a process by which the hydration of cement continues because of the availability of internal water that is not part of the mixing water” (ACI CT 16). The first published acknowledgement of internal curing dates to 1957, when LWA was used in production of concrete (Klieger 1957).

During the hydration of cementitious materials, capillary pores are created. Water present in the capillary pores continues to deplete as a result of hydration or due to external drying. This results in the formation of partially-filled pores within the microstructure, leading to the development of air-water menisci. Capillary pressure is induced as a result, and concurrently a measurable stress is present. These stresses are usually of concern when the *w/cm* is low (Lura et al. 2003). LWA due to its high-water absorption capacity when pre-wetted and introduced in the concrete, can desorb water into the cement paste and as a result can relieve the concrete from autogenous shrinkage stresses (Bentz et al. 2005; Byard et al. 2012).

The addition of pre-wetted LWA to concrete has been shown to enhance hydration, improve internal water movement, and mitigate autogenous deformation due to the availability of moisture provided by the aggregates (Bentz and Weiss 2011; RILEM TC 196 2007; Byard et al. 2012). While other materials such as wood pulp fibers, perlite, and super absorbent polymer (SAP) may be used for internal curing, LWA also contributes to the load carrying capacity of the structure and its availability in the U.S. market makes it an attractive option to provide internal curing in concrete (Delatte et al. 2008).

Different classifications of concrete are obtained when adding LWA to concrete, and the commonly used ones are sand-lightweight concrete (SLWC), all-lightweight concrete (ALWC), and “internally cured” (IC) concrete. The latter generally involves replacing a portion of fine aggregate with fine LWA. This name is commonly used in literature (RILEM TC 196 2007) even though internal curing takes place in all concrete containing pre-wetted lightweight aggregates. For the sake of clarity, the term normalweight concrete (NWC) is used herein for concrete that does not contain any lightweight aggregate.

It is estimated that the desorbed water can travel 0.07 in. into the paste from (around) each aggregate particle (Henkensiefken et al. 2011). Therefore the use of fine LWA is preferred for internal curing when compared to coarse LWA, as it allows for an improved spatial distribution of moisture throughout the microstructure of the concrete.

Proportioning of concrete for internal curing requires that an adequate amount of internal water be provided to overcome the effects of autogenous shrinkage. A simplified method to determine the amount of LWA needed to provide internal curing is provided with Equation 2-9 (Bentz et al. 2005). The quantity of internal curing water required to achieve total saturation within the hydrating cement paste, is estimated as the amount required to compensate for chemical shrinkage occurring at the maximum expected degree of hydration. While the goal of the method is to provide sufficient moisture to prevent autogenous shrinkage (self-desiccation), it actually provides enough internal curing water to mitigate chemical shrinkage, because it is difficult to only estimate the amount of autogenous shrinkage. Hence, this method is conservative, since autogenous shrinkage is always less than chemical shrinkage (Tazawa 1998).

$$M_{LWA} = \frac{C_f \times CS \times \alpha_{max}}{S \times \emptyset_{LWA}} \quad \text{..... (Equation 2-9)}$$

where,

M_{LWA} = oven-dry weight of LWA (lb),

C_f = cement content (lb/yd^3),

CS = chemical shrinkage (lb of water/lb of cement),

α_{max} = maximum degree of cement hydration (0 to 1),

S = degree of saturation of aggregate (0 to 1), and

Φ_{LWA} = absorption of LWA (lb water / lb dry LWA).

Chemical shrinkage can be computed by determining the mass composition of the Bogue components within the cement (generally provided by manufacturer) and the chemical shrinkage coefficients provided in Table 2-1 (Bentz et al. 2005). For *w/cm* less than 0.36, the maximum degree of hydration can determined as (*w/cm)*/0.36. When the *w/cm* is greater than 0.36, it is assumed that the maximum degree of hydration is unity (Bentz et al. 2005).

Table 2-1: Coefficients for chemical shrinkage (Bentz et al. 2005)

Bogue Compounds	Coefficient (lb of water/ lb of solid cement phase)
C_2S	0.0704
C_3S	0.0724
C_3A	0.115*
C_4AF	0.086*

Note: * Denotes assuming total conversion of the aluminate phases to monosulfate.

An important consideration when using LWA is the amount of water that can be readily desorbed into the cement paste at high relative humidity values (i.e., ≥ 93% RH) (Castro et al. 2011). When pre-soaked LWA is added to the concrete mixture, the extra water is initially drawn from the larger pores in the

LWA and subsequently from the relatively smaller pores (Lura et al. 2003). Various commercially available LWAs desorb between 85 to 98% of the absorbed water at 93% relative humidity (Castro et al. 2011). Desorption of water depends on the aggregate pore size distribution, the porous nature of the paste, and the internal relative humidity (RILEM TC 196 2007). Table 2-2 provides the absorption values and desorption coefficient values for the LWA used in this study. Desirable LWAs for internal curing generally have high absorption capacities, usually 10 to 30 percent by weight and high desorption capacities (Castro et al. 2011).

Table 2-2: LWA absorption and desorption coefficients (Castro et al. 2011)

Item	Lightweight Aggregate - Shale
Supplier Source	Norlite (Albany, NY)
Desorption coefficient at 93% relative humidity	0.955
Absorption capacity at 24 h (%)	18.1
Absorption capacity after vacuum (%)	21.2

2.5 EFFECT OF LWA ON CONCRETE PROPERTIES

2.5.1 Autogenous Shrinkage

Numerous studies have concluded that incorporation of LWA in concrete can lead to increased availability of moisture in the concrete leading to minimal or zero autogenous shrinkage and related stresses (RILEM TC 196 2007; Weiss and Bentz 2010; Byard et al. 2012). Replacement of fine aggregate with levels ranging from 7 to 33% (on a volume basis) of fine LWA has been shown to reduce or eliminate autogenous shrinkage (Henkensiefken et al. 2009). In the case of sand-lightweight and all-lightweight concretes, autogenous shrinkage stresses were insignificant (close to zero), thus relieving a major component of early-age stresses for the concrete (Byard et al. 2012).

2.5.2 Coefficient of Thermal Expansion

Lightweight aggregates in general have lower coefficient of thermal expansion when compared to normal-weight aggregates (Neville 2011). A major reason is the phase transformation undergone by lightweight aggregates in their manufacturing process (Chandra and Berntsson 2003). Concrete containing larger proportion of lightweight aggregates, including internally cured concrete, have lower coefficient of thermal expansion values (Byard et al. 2012). A reduction in coefficient of thermal expansion is beneficial in reducing stresses due to thermal effects (Byard et al. 2012).

2.5.3 Mechanical Properties

The effects of internal curing on the mechanical properties of the concrete depend on mixture proportions, curing conditions, and testing age. In IC concrete, due to increased availability of moisture, the degree of hydration is higher than normalweight concrete (NWC) (Byard et al. 2012). However, some LWAs are inherently weaker than their natural gravel or limestone counterparts owing to their porous structure (Mehta and Monteiro 2013.) Thus, there are two competing effects which affect the mechanical properties of concretes made with LWA.

Schittler et al. (2010) found that when the replacement levels of sand with fine LWA is at 11 and 24 percent (volume basis) in IC concretes, the 28-day compressive strengths were similar when compared with NWC. Whereas they found, the tensile strengths of the IC concretes with a 20 percent (weight basis) replacement with LWA is higher than NWC by nearly 10 percent. Sand-lightweight concrete was found to have enhanced compressive and tensile strengths than NWC at 28 days (Byard et al. 2012). One of the reasons is the densification of the interfacial transition zone (ITZ), wherein water from the local LWA promotes hydration thus resulting in a stronger bond between the aggregate and the paste matrix (Neville 2011). There have also been studies (Raoufi 2011) which indicate that increasing replacement levels of LWA lead to an overall reduction in tensile strength. This can be attributed to the different types of LWA available in the market. All-lightweight concrete generally has lower compressive and tensile strengths due to a larger proportion of LWAs used in this concrete type (Byard et al. 2012).

The modulus of elasticity of concretes containing LWAs is significantly lower than NWC. The decrease in modulus of elasticity with concrete density can be estimated with either Equation 2-7 or 2-8. This is primarily because lightweight aggregates are less dense and have a porous structure (Neville 2011; Chandra and Berntsson 2003). Therefore, concretes containing large amounts of LWAs, specifically sand-lightweight and all-lightweight concrete, show a marked decrease in modulus of elasticity when compared with NWC (Raoufi 2011; Byard et al. 2012). This reduction in modulus of elasticity is beneficial in reducing concrete stresses due to restraint, thermal, drying, and autogenous shrinkage effects (Byard et al. 2012).

2.5.4 Creep

While many factors affect creep, the water content and the effect of aggregates are most important (Neville 2011). LWA being softer aggregates impose reduced restraint to cement paste movements, so creep is expected to increase (Byard 2011). The compliance with normalized elastic response of normalweight and slate lightweight mixtures with *w/c* of 0.42 loaded at 0.5 day is shown in Figure 2-6. It can be observed that the compliance (i.e. creep) is higher for the SLW and ALW concretes that contains large amounts of LWA (Byard 2011). On average, lightweight concrete (LWC) experiences higher creep than NWC (Clarke 2002). This may be attributed to the lower modulus of elasticity in LWA concrete. High creep (or relaxation) will reduce early-age stresses (Mehta and Monteiro 2013).

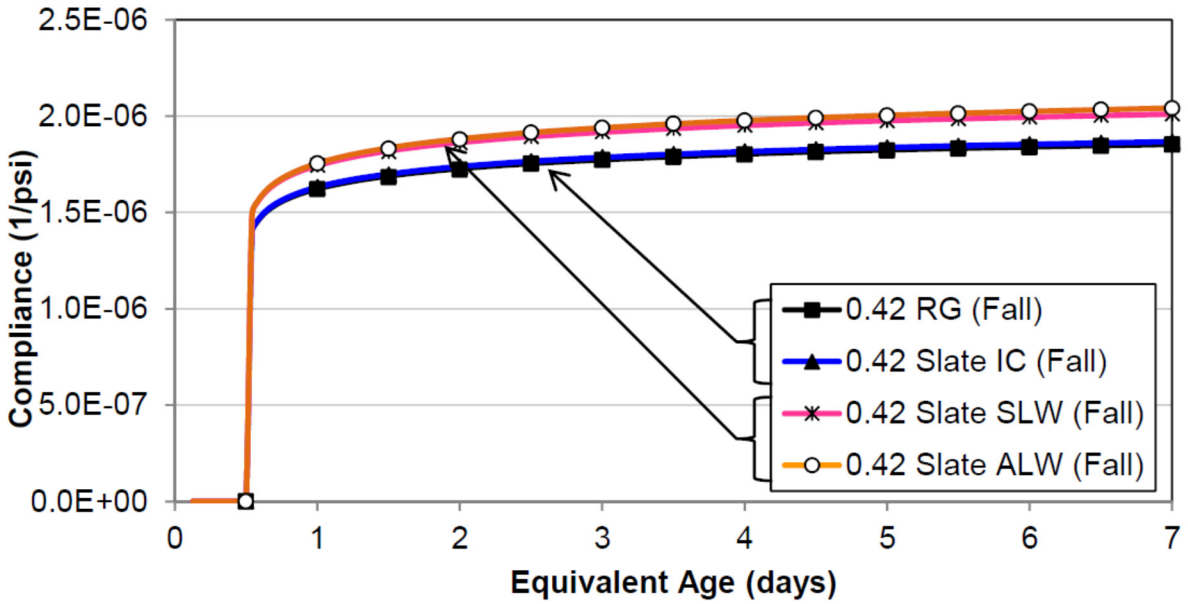

Figure 2-6: Compliance with normalized elastic response of normalweight and slate lightweight concretes with *w/c* of 0.42 loaded at 0.5 days (Byard 2011)

2.5.5 Thermal Conductivity

Thermal conductivity refers to the ability of the material to conduct heat. The mineralogical composition of the aggregate significantly affects the thermal conductivity of the concrete. For example, the higher the crystalline content, the higher its thermal conductivity (Neville 2011). LWA has a porous structure, is less crystalline, and hence has a lower thermal conductivity than its normalweight counterparts (Neville 2011; Chandra and Berntsson 2003). During the pours for mass concrete piers, Maggenti (2007) reported a higher temperature rise throughout the hydration process for concrete containing LWA when compared to concrete containing normalweight aggregates with identical cementitious and fine aggregate content. This higher temperature rise can be attributed to a lower thermal conductivity and due to a lower density of concrete containing LWA (Chandra and Berntsson 2003).

Chapter 3

Experimental Work

3.1 EXPERIMENTAL PROGRAM

Concrete containing various amounts of lightweight aggregate and cured under conditions simulating mass concrete were tested to assess their early-age cracking behavior. These results were then compared to the response of a normalweight concrete made with river gravel and river sand as coarse and fine aggregate, respectively. This mixture will be referred to as the reference mixture and did not contain any lightweight aggregates.

Two rigid cracking frames (RCF) and one free-shrinkage frame (FSF) were used for evaluating the cracking tendency and cylinders were match-cured simultaneously to test the time-dependent development of mechanical properties. A schematic of the test equipment and procedure is shown in Figures 3-1 and 3-2. Figure 3-1 schematically shows the match-cured temperature conditions used to test all concretes. Concrete in the match-cured RCF was cured to mass concrete (column) conditions and the thermal and autogenous stresses were recorded. The concrete in the second RCF, as shown in Figure 3-2, was tested under isothermal conditions; therefore, only stresses developing because of autogenous shrinkage were recorded. The FSF recorded the free-shrinkage strains for the match-cured specimens, with the concrete cylinder specimens match-cured in a similar fashion.

The typical water-to- cementitious materials (*w/cm*) for mass concrete construction varies between 0.38 and 0.55, hence two groups of concrete mixtures with *w/cm* mixtures of 0.38 and 0.45 were tested. Autogenous shrinkage development is important only for the low *w/cm* mixtures because for higher *w/cm* mixtures autogenous shrinkage is not a concern (Weiss and Bentz 2010).

Class F fly ash is used increasingly in mass concrete mixtures since it decreases the heat of hydration (Schindler and Folliard 2005). In this project, Class F fly ash at a cement replacement level of 30 percent by mass was used, because a large amount of mass concrete construction used fly ash in the range of 25 to 30 percent and many state agencies have a minimum requirement of approximately 25 to 30 percent (by mass) of fly ash for mass concrete construction (Jahren et al. 2014).

Each group of *w/cm* mixtures contained five concrete mixtures, and they comprised of a reference concrete mixture and four concretes containing varying amounts of lightweight aggregate. The use of two different *w/cm* mixtures allows one to assess the effect of *w/cm* on the cracking tendency and stress evolution of the lightweight aggregate and control concrete mixtures. The ConcreteWorks program developed at UT Austin (Poole et al. 2006) was used to predict the concrete temperature development for each specific concrete mixture. Since ACI 301 (2016) recommends that an element with least dimension of 4ft or greater be designated as mass concrete, the 8×8 ft column modeled in this study is representative of mass concrete. The temperature development was modeled for an 8 × 8 ft size column for both *w/cm* concretes. The temperature modeling is discussed in detail in Section 3.5.

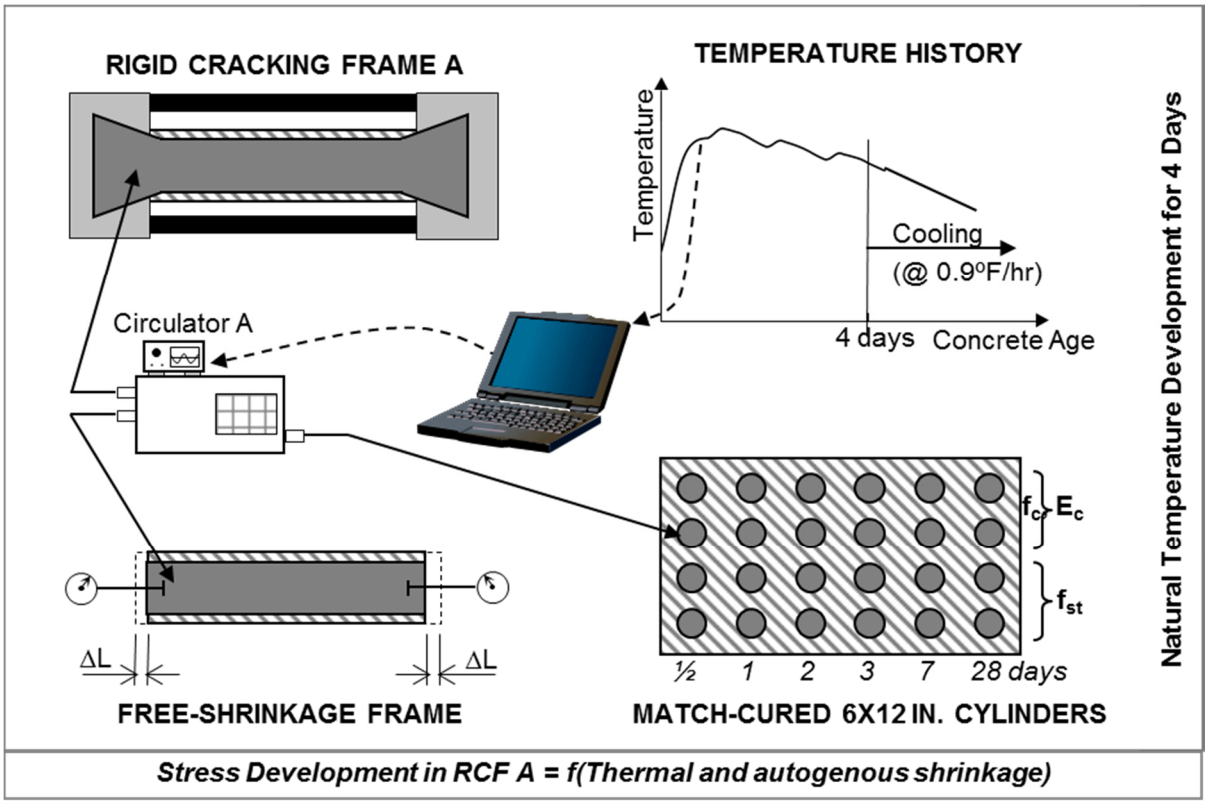

Figure 3-1: Mass-concrete curing test setup

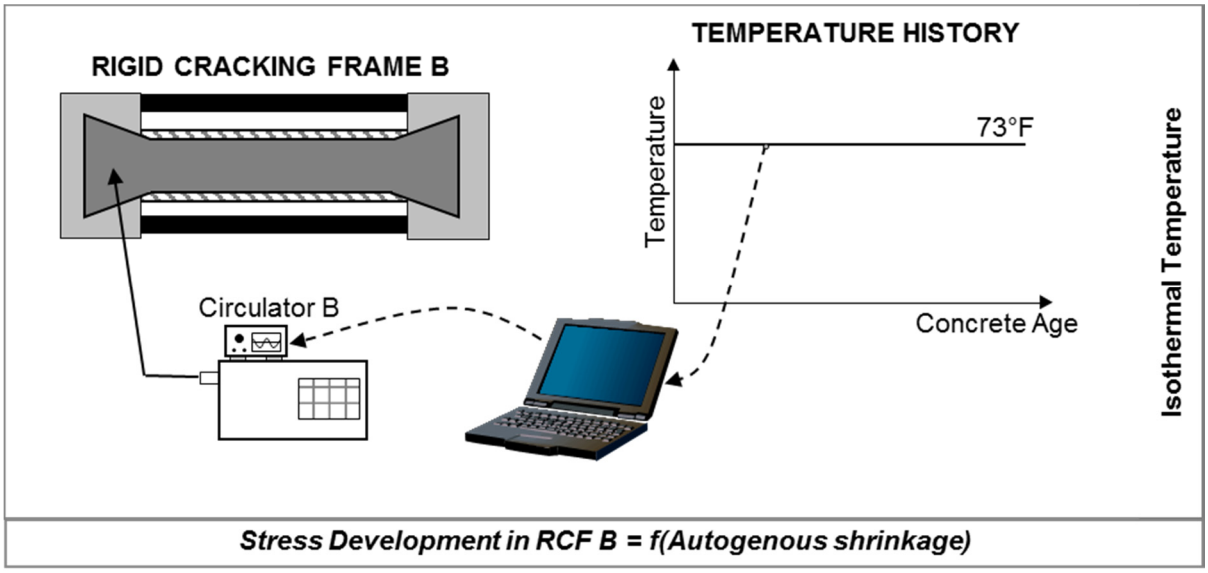

Figure 3-2: Isothermal curing test setup

3.2 LIGHTWEIGHT AGGREGATES

3.2.1 Source

Expanded shale was used in the production of all concretes containing lightweight aggregates. The type and source of the LWA is shown in Table 3-1. One fine and one coarse gradation of LWA was shipped directly from the supplier in super sacks to Auburn University's Concrete Materials Laboratory.

Table 3-1: Lightweight aggregate source, type, and properties

Item	Shale Lightweight Aggregate	
Source	Norlite Aggregates (Albany, NY)	
Type of LWA	Fine Aggregate	Coarse Aggregate
Particle size	0 to #4	#4 to ¾ in.
Relative density (SD§)	1.67	1.35
Pre-wetted absorption *	20%	18%
Fineness modulus	3.3	NA

Note: * Measured water absorption after soaking in water for 7 days.

§ Relative density at surface-dry state after 7 days of soaking in water.

3.2.2 Properties

The LWAs were sampled upon arrival and their gradations obtained by sieve analysis as per ASTM C136 (2014). The specific gravity and moisture content were obtained in accordance with ASTM C127 (2014) and ASTM C128 (2014). The samples were prewetted for a period of 7 days. In order to obtain the absorption of pre-wetted LWA, the lightweight aggregates were sampled as per ASTM C1761 (2015). This method is usually known as the "paper towel method" and utilizes commercial grade paper towels to determine the surface-dry condition of the LWAs. The particle size, relative density, pre-wetted absorption, and fineness modulus results are shown in Table 3-1. The gradations are provided in Appendix A.

3.2.3 Lightweight Aggregate Preconditioning

The lightweight aggregates (LWA) were placed in water-filled 55-gallon plastic barrels for moisture preconditioning. The LWAs were submerged in plastic barrels for a period of 7 days, as shown in Figure 3-3. The presence of valves at the bottom of the barrel aided in draining the water. A 6 in. thick filter layer of normalweight aggregates were placed at the bottom of one of the barrels for filtering fine LWA. This layer facilitated draining of water without any clogging occurring in the valve. Water was slowly drained after prewetting to reduce the amount of fine LWA lost. Oval-shaped steel tanks with a design similar to the barrels were also used. After soaking for 7 days, the excess water was drained and the lightweight coarse and fine aggregate separately placed on a plastic sheet. The excess surface moisture was allowed to evaporate until the surface-dry condition was achieved. Following which, they were placed in sealed

five- gallon buckets for batching. Prior to mixing the concrete, aggregate samples were sampled to determine their moisture content, which was used to make moisture corrections on the concrete proportions. The laboratory environment was maintained at a constant temperature of 73°F; hence no temperature preconditioning was required.

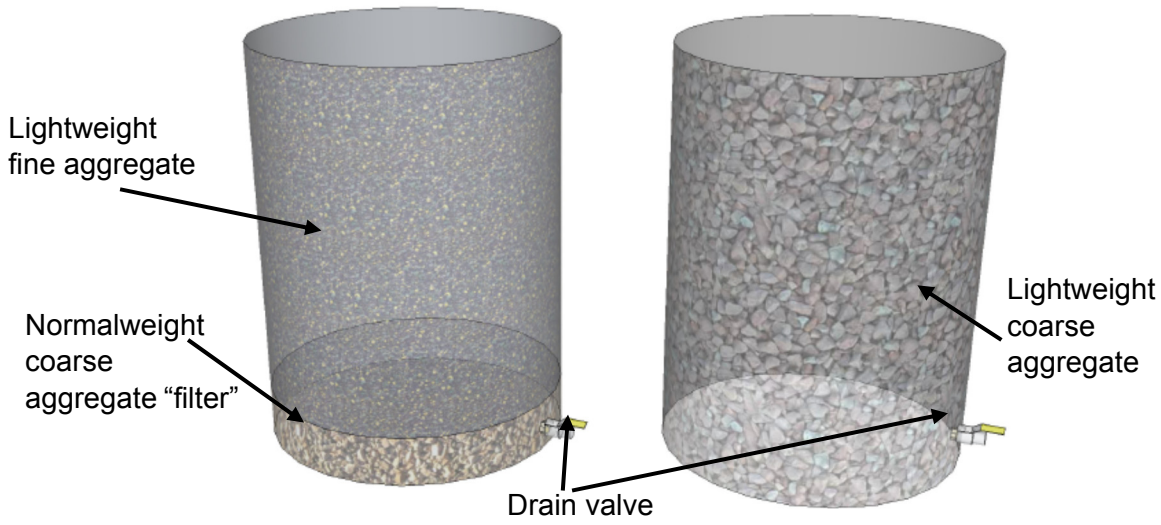

Figure 3-3: Illustration of barrel setup used for lightweight aggregate preconditioning (Byard and Schindler 2010)

3.3 MIXTURE PROPORTIONS

Five types of concrete mixtures were assessed at two different *w/cm*. They consisted of a reference normalweight concrete (REF), internally cured (IC) concrete, sand-lightweight (SLW) concrete, inverse sand-lightweight (ISLW) concrete, and all-lightweight (ALW) concrete.

For clarity, a mixture identification system is used in this report to refer to a specific concrete mixture containing a specific amount of LWA and *w/cm*. The identification system is as follows:

Mixture Type		and	***w/cm***
REF	= Reference concrete		0.45
ICC	= Internally cured concrete		0.38
ISLWC	= Inverse sand-lightweight concrete		
SLWC	= Sand-lightweight concrete		
ALWC	= All-lightweight concrete		

Example: **ALWC 0.45,** represents the all-lightweight concrete with a *w/cm* of 0.45.

The mixture proportions for the two groups of concretes made at *w/cm* of 0.45 and 0.38 are shown in Tables 3-2 and Tables 3-3, respectively. LWAs may never reach a state of 100 percent saturation, hence the term saturated-surface dry is not used for them, and instead the term pre-wetted surface dry is used for LWAs. Therefore, the LWA batch weights are for pre-wetted surface-dry (SD) conditions.

Table 3-2: Proportions and properties for all *w/cm* = 0.45 mixtures

Item	REF 0.45	ICC 0.45	ISLWC 0.45	SLWC 0.45	ALWC 0.45
Water Content (lb/yd^3)	263	263	263	263	263
Cement Content (lb/yd^3)	410	410	410	410	410
Class F Fly Ash Content (lb/yd^3)	175	175	175	175	175
SSD Normalweight Coarse Aggregate (lb/yd^3)	1740	1740	1425	0	0
SD Lightweight Coarse Aggregate (lb/yd^3)	0	0	0	910	857
SSD Normalweight Fine Aggregate (lb/yd^3)	1220	1000	0	1190	0
SD Lightweight Fine Aggregate (lb/yd^3)	0	140	975	0	820
Water-Reducing Admixture (oz/yd^3)	16.0	14.0	11.0	0.0	0.0
Mid-Range Water-Reducing Admixture (oz/yd^3)	0.0	0.0	3.0	22.0	18.0
Rheology-Controlling Admixture (oz/yd^3)	0.0	0.0	10.0	0.0	32.0
Air-Entraining Admixture (oz/yd^3)	1.0	1.0	1.0	3.5	3.5
Target Total Air Content (%)	5.0	5.0	5.0	5.0	5.0
Water-to-Cementitious Materials Ratio (*w/cm*)	0.45	0.45	0.45	0.45	0.45

Table 3-3: Proportions and properties for all *w/cm* = 0.38 mixtures

Item	REF 0.38	ICC 0.38	ISLWC 0.38	SLWC 0.38	ALWC 0.38
Water Content (lb/yd^3)	243	243	243	243	243
Cement Content (lb/yd^3)	435	435	435	435	435
Class F Fly Ash Content (lb/yd^3)	195	195	195	195	195
SSD Normalweight Coarse Aggregate (lb/yd^3)	1740	1740	1425	0	0
SD Lightweight Coarse Aggregate (lb/yd^3)	0	0	0	910	857
SSD Normalweight Fine Aggregate (lb/yd^3)	1220	1000	0	1190	0
SD Lightweight Fine Aggregate (lb/yd^3)	0	140	975	0	820
Water-Reducing Admixture (oz/yd^3)	20.0	20.0	0.0	0.0	0.0
Mid-Range Water-Reducing Admixture (oz/yd^3)	0.0	0.0	22.0	28.0	26.0
Rheology-Controlling Admixture (oz/yd^3)	0.0	0.0	12.0	0.0	34.0
Air-Entraining Admixture (oz/yd^3)	1.0	1.0	1.0	3.5	3.5
Target Total Air Content (%)	5.0	5.0	5.0	5.0	5.0
Water-to-Cementitious Materials Ratio (*w/cm*)	0.38	0.38	0.38	0.38	0.38

The reference mixture as explained in previous sections was proportioned to represent mass concrete mixtures commonly used in the state of Alabama and meets the requirements of the Alabama Department of Transportation. In this study the ICC was proportioned to meet the requirements of

normalweight concrete as per AASHTO LRFD Bridge Design Specifications (2016). Hence the amount of LWA was calculated so that the equilibrium density of the mixture was 135 pcf or greater. Therefore, the ICC mixtures contained less LWA than that required by the Bentz formula (Bentz et al. 2005).

The SLWC contained coarse LWA and normalweight fine aggregate, the ISLWC contained coarse normalweight aggregates and fine LWA, while ALWC contained both coarse and fine LWA. A slump of 4 ± 1 in. and total air content of 5.0 ±1.5% was targeted. The measured densities were to be within ± 1 pcf of the calculated density for each concrete mixture. These values represent typical fresh concrete properties used in mass concrete production.

The amount of internal curing water required by the Bentz formula and the amount of internal curing water provided by each concrete, is presented in Table 3-4. The absorption values and the desorption coefficients were computed from values presented from Equation 2-9 (Bentz et al. 2005). As can be seen, the amount of internal curing water supplied by the LWA is less than the amount required by the Bentz formula. During the internal-curing process, it is assumed that the normalweight aggregate does not contribute to the process of internal curing, owing to its low absorption capacity in comparison to LWA. The data in Table 3-4 indicate that for ICC mixtures having *w/cm* of 0.45 and 0.38, the amount of internal curing water provided is 33 and 38 percent, respectively, less than the amount of water required by the Bentz formula. All SLW, ISLW, and ALW concretes supply more water than that required by the Bentz formula.

Table 3-4: Total absorbed water available from LWA and water required by Equation 2-9

Concrete Type	Internal Curing Water Available from LWA (lb/yd^3)		Water Required by Equation 2-9 (lb/yd^3)	
	***w/cm* = 0.45**	***w/cm* = 0.38**	***w/cm* = 0.45**	***w/cm* = 0.38**
Internally cured concrete	27	27	41	44
Inverse sand-lightweight concrete	195	195	41	44
Sand-lightweight concrete	180	180	41	44
All-lightweight concrete	318	318	41	44

3.4 TEST METHODS

3.4.1 Heat of Hydration Characterization

The hydration reaction of portland cement and fly ash with water is an exothermic reaction, resulting in a temperature rise of the concrete specimen. Knowledge of this temperature rise during the hydration process helps in predicting the early-age temperature history of a concrete structure (Morabito 1998). The temperature rise over a period of time is unique for every concrete mixture proportion (Schindler and Folliard 2005). Semi-adiabatic calorimetry is employed in this study to characterize the temperature rise of each concrete.

Adiabatic calorimetry refers to a test method wherein a specimen is placed in an insulated chamber and no heat exchange (loss or gain) occurs with the surroundings. Semi-adiabatic calorimetry (SAC) is the condition in which, the rate of heat exchange is controlled from the concrete specimen with the help of insulating material and no external sources of heat are employed (Morabito 1998). Calibration of the SAC ensures that the heat loss is known and accounted for. This setup is convenient and provides accurate means of measuring the heat released during the hydration process (RILEM 119-TCE 1998).

In this study, a QDrum (iQuadrel) illustrated in Figure 3-4, was used as SAC. The laboratory equipment for performing the test was supplied by Digital Site Systems, Pittsburg, PA. No standard ASTM test procedure is available, therefore a draft RILEM procedure was used (RILEM 119-TCE 1998). The SAC setup comprised of an insulated 55-gallon drum, instrumented with sensors to measure the concrete temperature, ambient temperature, and the amount of heat lost through the calorimeter wall.

Prior to testing the heat of hydration of concrete, a calibration test must be performed to calculate the thermal losses of the SAC. Water of a known temperature was placed inside and the thermal losses of the calorimeter computed (Schindler and Folliard 2005). The thermal loss is a function of the insulating components and the differences between the sample and ambient temperature.

Trial batches were performed to establish whether the total air content, slump, and other fresh concrete properties met the required project mixture design parameters. Following which, fresh concrete was consolidated in a 6×12 in. cylinder mold, that was weighed before being placed in the calorimeter. A temperature probe was fitted into the mold and the drum was sealed. Data was recorded for a period of 5 days. The hydration parameters were then computed using the SAC data (Schindler and Folliard 2005).

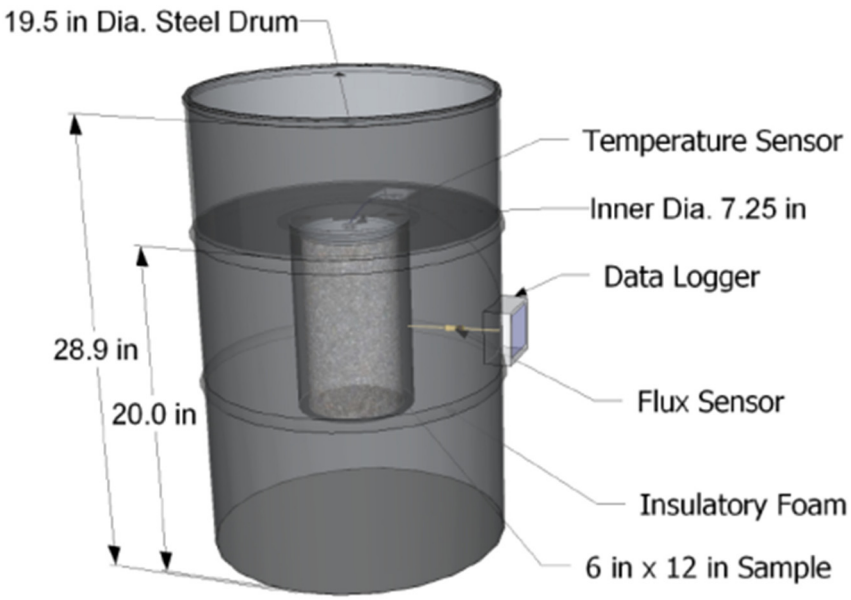

Figure 3-4: Semi-adiabatic calorimeter (adapted from Weakley 2009)

3.4.2 Thermal Diffusivity Evaluation

To assess the specific heat of the lightweight aggregates, the thermal diffusivity of the concrete was back-calculated using the SAC test apparatus. After casting, a 6×12 in. cylinder was moist cured for a period of 7 days. After 7 days, the concrete cylinder was sealed and heated to approximately 160˚F and then sealed in the SAC. The thermal decay was measured for a period of 5 days and the thermal diffusivity was back-calculated to fit the measured thermal decay curve. This allows one to determine the specific heat of the coarse LWA in the SLW concrete, since the specific heat of the remaining aggregates are established from published values, shown in Table 3-5 (Xu and Chung 2000; Robertson 1988). The same procedure was repeated for the ALW concrete and the specific heat of the fine LWA was determined.

Table 3-5: Specific heat of concrete materials from published data

Concrete Raw Material	Specific heat (Btu/lb per °F)
Portland cement	0.17
Fly ash	0.17
River gravel coarse aggregate	0.20
Natural river fine aggregate	0.20
Water	1.00

With knowledge of the thermal and hydration parameters of the concrete, a temperature profile for mass concrete placement during fall season (placement temperature ~73˚F) was determined using the ConcreteWorks program (Poole et al. 2006). ConcreteWorks allows one to simulate the environmental conditions such as wind, temperature, humidity, etc. and other factors such as formwork, concrete placement time, etc. The temperature modeling conditions and other parameters used for the ConcreteWorks analysis are covered in detail in Section 3.5.

3.4.3 Restrained Stress Development

The rigid cracking frame (RCF) was initially developed by Dr. Springenschmidt in Germany in the 1970s for evaluating thermal stresses in concrete pavements (Springenschmidt et al. 1994). It comprises of a 6 × 6 × 49 in. prismatic specimen with dogbone-shaped ends held in two mild-steel cross-heads as shown in Figure 3-5(a). The dogbone-shaped ends have steel teeth to help firmly grip the concrete. The specimen is restrained by two Invar side bars extending along both sides as shown in Figure 3-5(b). Strain gauges are mounted on the Invar bars that measure strains continuously during the test. The insulated and temperature controlled formwork is completely lined with plastic sheeting and is firmly supported by the Invar bars. The plastic sheeting prevents any moisture loss and reduces friction between the form surface and the concrete. The temperature profile simulated was for an 8 × 8 ft column placed in fall conditions. The temperature profile development is discussed in Section 3.5. After a period of 96 hours, if no cracking is observed in the concrete, it is cooled at a rate of 0.9˚F/hr until cracking occurs. The stress response was

measured every five minutes with the help of a data acquisition system. In order to test autogenous stress development, the concrete was subjected to isothermal conditions (73˚F) and the stress response recorded.

a)

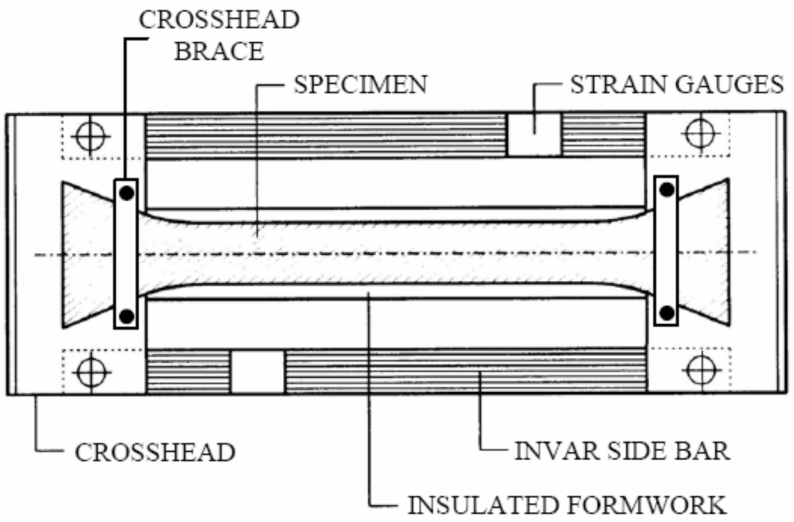

b)

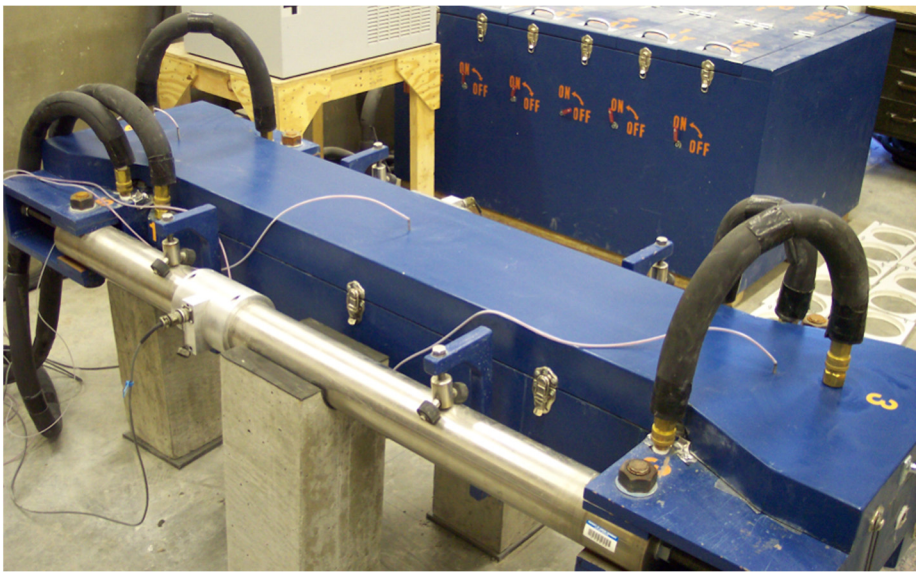

Figure 3-5: Rigid cracking frame test setup: a) Schematic of test setup (Mangold 1998) and b) Actual equipment used (Meadows 2007)

Fresh concrete is placed in two lifts and consolidated in the formwork using a needle vibrator. After finishing, a plastic sheet is placed on top of the concrete surface and taped to the formwork to prevent any moisture loss. Thus, drying shrinkage effects are not considered in this study. The formwork is closed from the top and connected via hoses to a circulator that circulates a mixture of water and ethylene glycol (50:50 ratio, by mass) through the formwork. The formwork contains 0.5 in. diameter copper tubes, which enables subjecting the concrete to any target temperature profile.

After final set, stresses start to develop due to autogenous and thermal shrinkage. The Invar bars provide restraint to the movement of the concrete, which results in the development of concrete stresses. Consequently, the strain gauges on the Invar bars record the strains, which are converted to stresses using a computer-aided software program. Thermocouples are also inserted in the ends and center of the specimen to record the concrete temperature.

The stress observed at the time of cracking is less than the splitting tensile strength measured from match-cured concrete cylinders. This is because of differences in the loading rate, test specimen size, and type of loading of the concrete specimen (Riding et al. 2014). The rate of loading is lower in the case of the RCF and a lower rate of loading produces lower apparent strengths (Neville 1995). The splitting tensile strength specimens were loaded to failure in less than five minutes, whereas the duration of the RCF tests cover a period of approximately 4 to 6 days (Meadows 2007; Byard 2011). The tensile stresses are spread over a larger area (6 × 6 × 49 in.) in the RCF than in the cylinders (12 × 6 in.), hence there is a higher probability of finding flaws in the larger specimen, which makes it more susceptible to fail at a lower apparent strength (also known as size effects). In addition, the concrete cylinders undergo a splitting tension test, which is an *indirect* tensile strength test, whereas the concrete in the RCF is subjected to direct tension. The ratio of cracking frame stress at failure to the splitting tensile strength at the same time is generally between 40 and 80 percent (Riding et al. 2014).

3.4.4 Unrestrained Free Shrinkage

Free-shrinkage strain refers to the unrestrained uniaxial strain of the concrete. A free-shrinkage frame (FSF) was initially designed by Bjøntegaard (1999) in Norway to study autogenous shrinkage strains in concrete. A similar frame developed at Auburn University was used in this project and is shown in Figure 3-6(c).

The FSF used has dimensions of 6×6×24 in. and comprises of temperature-control formwork with two movable steel plates at its sides, with the whole setup supported on an Invar frame. The formwork has 0.5 in. copper tubes contained inside and is sealed to prevent any moisture loss. Two small holes on the top of the lid are present, which allow for temperature readings with the aid of thermocouples. The movable steel plates have openings at their center, which allow for the insertion of an Invar rod at each end. One end of each Invar rod remains embedded in the concrete, while the other end is connected to a linear variable differential transformer (LVDT), which measures the expansion and contraction of the concrete. The formwork is connected via hoses to a circulator, which allows for the system to cure the concrete specimen to any desirable temperature profile. The formwork is lined with two layers of plastic sheeting, which prevents any adhesion between the frame and the concrete. A layer of oil lubrication separates the two plastic sheets, which allows for reduced friction and free movement of concrete. Fresh concrete is placed in the formwork, consolidated, and is sealed from the top with plastic to prevent any drying from taking place. Therefore, the effect of drying shrinkage is not considered in this test.

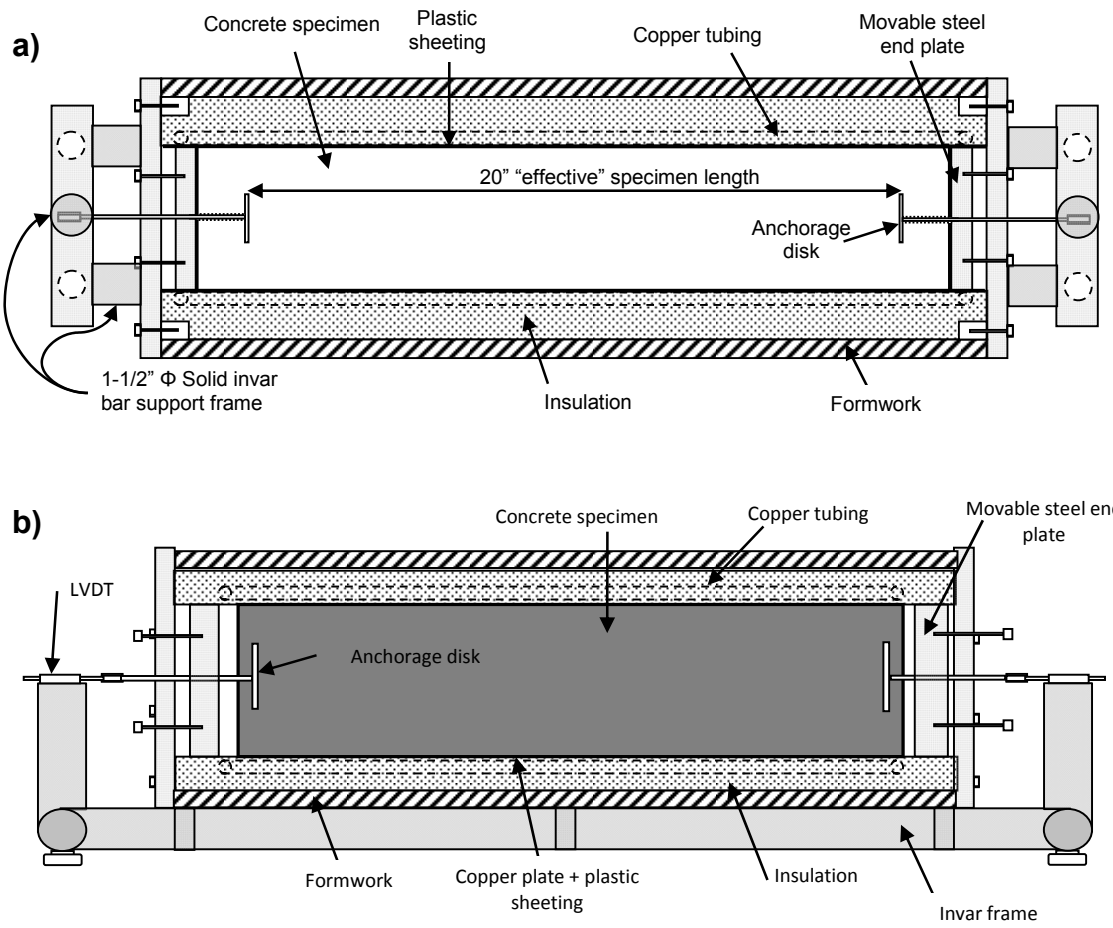

Figure 3-6: Free-shrinkage frame setup: a) Plan view schematic of test equipment, b) Section view schematic (Rao 2008), and c) Actual equipment used (Byard 2011)

The movable steel plates initially support the concrete ends; however, following initial set, the plates are moved back, which allows the concrete to move freely. Figures 3-6(a) and 3-6(b) indicate the position

of the movable steel plates before and after initial set, respectively. Initial set is determined from penetration resistance as per ASTM C403 (2014), as discussed in Section 3.4.7. The unrestrained free shrinkage was recorded for all the concrete mixtures for a duration of 5 to 7 days. The temperature profile was match-cured to that of the RCF.

3.4.5 Concrete Mechanical Properties

The concrete mechanical properties were determined at 0.5, 1, 2, 3, 7, and 28 days by performing compressive, splitting tensile, and modulus of elasticity as per ASTM C39 (2014), ASTM C496 (2014), and ASTM C469 (2014), respectively.

A match-curing system was used to evaluate the mechanical properties and is shown in Figure 3-7. It comprises of a wooden box that can hold 24 6×12 in. cylinders, and is connected via hoses to a temperature control circulator. A mixture of water and ethylene glycol is circulated through a series of copper tubes running around each cylinder in the box, which allows the concrete cylinders to be simultaneously match-cured to the specimens in the RCF and FSF.

Figure 3-7: Cylinder match-curing system: a) Wooden box containing cylinders and b) A unit with two cylinders (Rao 2008)

3.4.6 Coefficient of Thermal Expansion

The coefficient of thermal expansion (CTE) of concrete is tested as per AASHTO T336 (2009). A 6×7 in. concrete cylinder is placed in a frame, shown in Figure 3-8, that is submerged in water. Mounted on the frame is a spring-loaded LVDT which is placed in contact with the concrete cylinder. The temperature of the water bath is varied between 50˚F to 122˚F, and the ensuing change in length of the concrete cylinder is measured. From the resulting displacements over the temperature changes, the coefficient of thermal expansion of the concrete can be calculated.

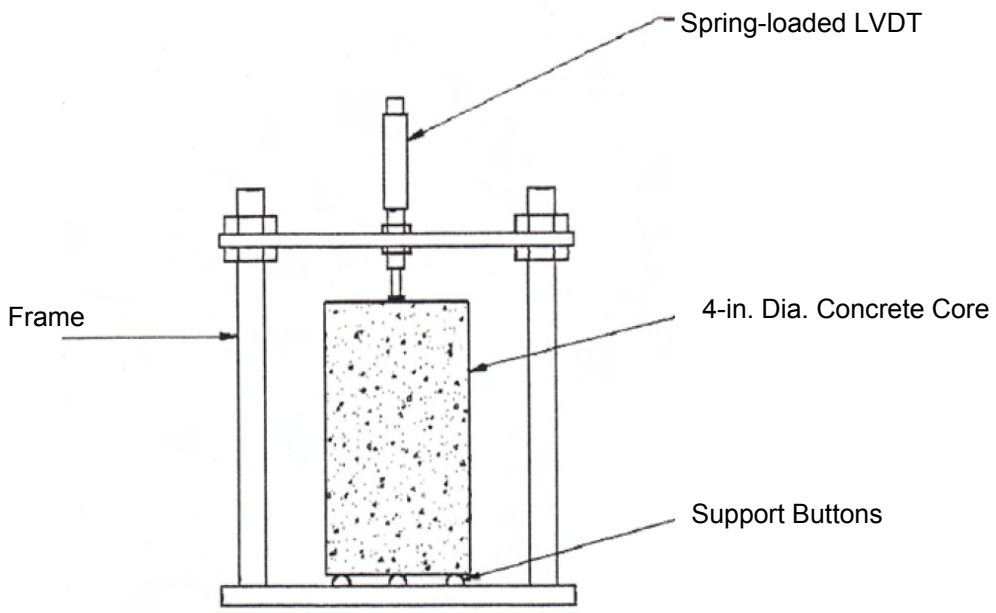

Figure 3-8: Schematic of the thermal expansion test setup (AASHTO T 336 2009)

For every concrete mixture, two 6 × 7 in. cylinders were cast and cured for a period of 28 days. Following which, they were tested in the CTE apparatus shown in Figure 3-9 as per AASHTO T336 (2009). Certain modifications were made to improve the repeatability of this test (Byard 2011). Specifically, ceramic inserts were added between the concrete specimen and the LVDT to mitigate any effects that temperature changes might have on the LVDT readings. Additionally, a small ceramic disk was used under the tip of the LVDT, along with a ceramic collar which was used to mount the LVDT onto the frame. The use of the ceramic collar was to ensure that temperature transfer was prevented from interfering with the LVDT through the mounting crossbar. Since the water levels in the temperature-controlled bath would fluctuate from time to time, an Invar spacer was employed and was placed on top of the concrete specimen. This provided additional height and ensured that the water fluctuations did not interfere with the LVDT readings. The ceramic collar, disks, and other Invar spacer were present during the calibration procedure involving standard 6×7 in. steel specimens. Thus, the presence of these additions was accounted for in the calibration procedure and computations of the CTE.

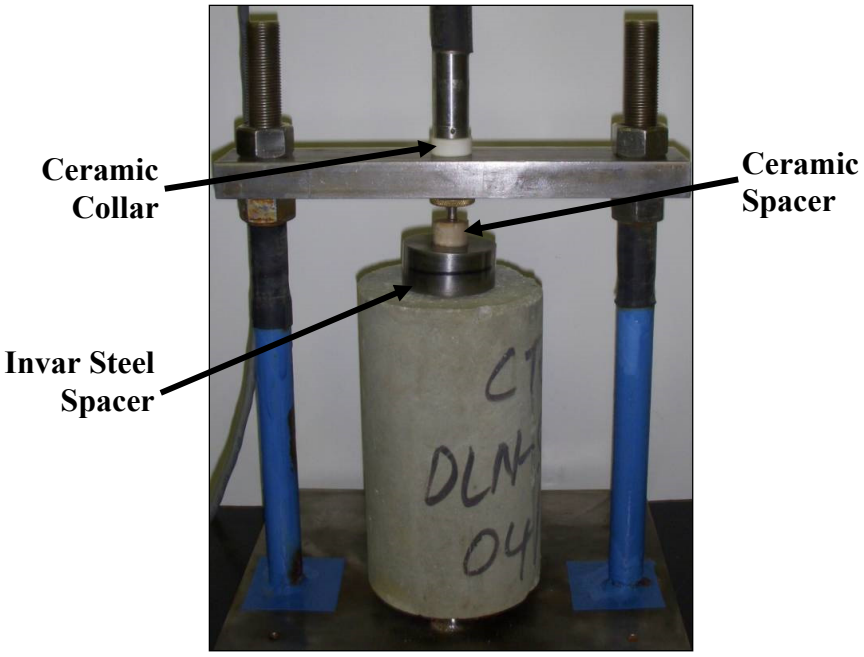

Figure 3-9: Modified AASHTO T336 setup used for CTE testing (Byard 2011)

3.4.7 Setting Test

The time of initial set is the time at which stresses in the concrete are discernable and can be recorded (Neville 2011). Initial set of concrete is established when the concrete reaches a penetration resistance of 500 psi, and final set is achieved when the penetration resistance reaches 4000 psi (ASTM C403 2014). To determine the time of initial set, each concrete mixture was sieved through a No. 4 sieve and the mortar was cast in a 6 × 8 in. cylindrical container and match-cured to the temperature in the RCF and FSF tests. Penetration resistance tests were performed on the specimens as per ASTM C403 (2014).

3.4.8 Other Fresh Quality Control Tests

The concrete was mixed as per ASTM C192 (2014) under standard laboratory conditions. The slump, temperature, and the density were measured as per ASTM C143 (2014), ASTM C1064 (2014), and ASTM C138 (2014), respectively for every batch of concrete. The total air content was determined using the pressure method as per ASTM C231 (2014) for normalweight concretes. The volumetric method as per ASTM C173 (2014) was used to determine the total air content for concretes incorporating lightweight aggregates.

3.5 CONCRETE TEMPERATURE MODELING

The temperature modeling for the concrete mixtures was performed with the help of a software program called ConcreteWorks. It was developed at UT Austin and is utilized by TXDOT and some other states (Poole et al. 2006). ConcreteWorks can model the temperature history of a mass concrete element considering the geometry of the elements, type of aggregates used, chemical composition of cementitious

materials, concrete mixture proportions, placement temperature, weather conditions (including humidity, solar radiations, and wind speeds), and type of formwork employed.

Initially semi-adiabatic calorimetry was performed on the concrete mixtures and the hydration parameters were determined (Schindler and Folliard 2005). Preliminary investigations were performed with ConcreteWorks to identify the appropriate mass concrete element size for temperature modeling. The ALWC with a *w/cm* of 0.38, 30 percent Class F fly ash (substitution by mass), and Type I cement were chosen for preliminary modeling purposes, since it was expected that this mixture would experience the highest maximum concrete temperature (Byard and Schindler 2010). Three different mass concrete element sizes—4×4 ft, 8×8 ft, and 12×12 ft—were chosen for modeling purposes. These sizes are representative mass concrete element sizes for many transportation substructure components. The inputs used for modeling the temperature profile in ConcreteWorks were the hydration parameters along with the mixture proportion values and other factors including the placement date, type of formwork, etc. The results from ConcreteWorks include the maximum core and edge temperatures and are presented for the three mass concrete element sizes in Figures 3-10 and 3-11, respectively.

From Figures 3-10 and 3-11, it can be observed that the maximum core and edge temperatures for ALWC 0.38 are the highest for a 12×12 ft column. However, the differences between the maximum temperatures for 8×8 ft and 12×12 ft size column is minimal. Also, the maximum temperatures are below the critical DEF limit of 185°F (ACI 301 2016). Therefore, a 8×8 ft size column was chosen. From previous research (Tankasala et al. 2017), it was determined that thermal cracking is expected at the edge of cross-section when compared to the core, especially at early ages. All constituent materials were kept at room temperature (73˚F) prior to mixing. In order to ensure that all RCF tests are completed within a reasonable time frame, a duration of seven days was selected for temperature modeling and early-age concrete testing.

In this study, ConcreteWorks was used to model the edge temperature profile for a duration of four days (96 hours) for of 8 × 8 ft concrete column placed under fall placement conditions in Montgomery, Alabama on construction date of September 15th. The temperature profiles were modeled for both groups of *w/cm* concretes. After a period of four days (96 hours) if cracking has not occurred, the concrete was artificially cooled at a rate of 0.9˚F/hr until the onset of cracking. This approach is similar to the practice adopted by Breitenbucher and Mangold (1994) and Byard and Schindler (2010), except the cooling rate was halved. This gradual cooling rate ensured all the concrete specimens would fail within one week.

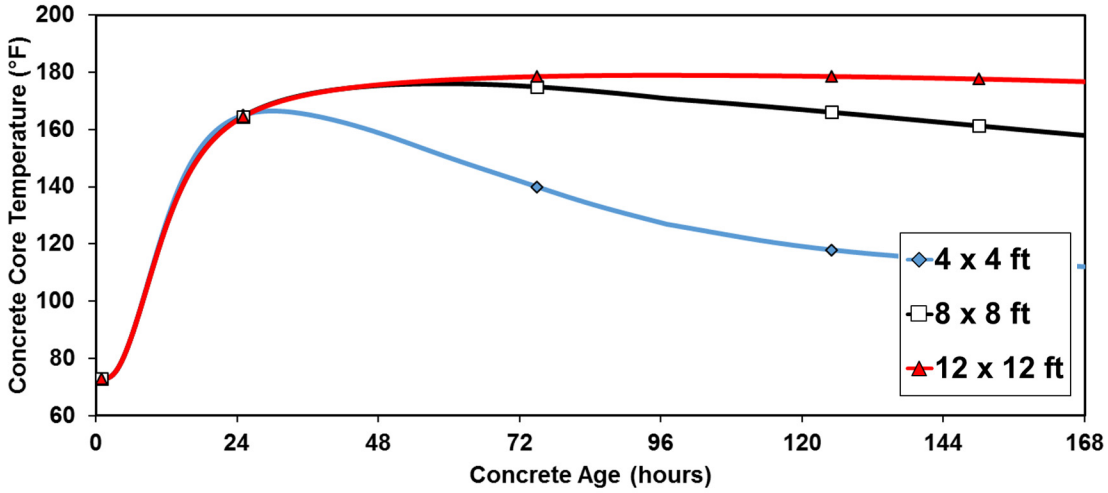

Figure 3-10: Concrete core temperature for various cross-section sizes (ALWC 0.38)

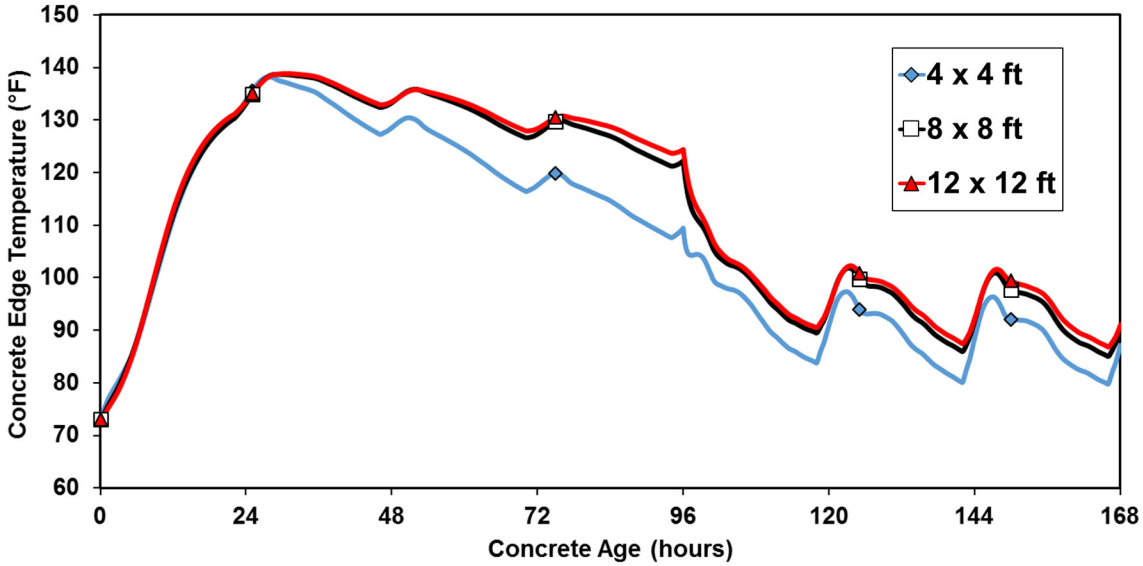

Figure 3-11: Concrete edge temperature for various cross-section sizes (ALWC 0.38)

3.6 OTHER RAW CONCRETE MATERIALS

3.6.1 Portland Cement

Type I cement was used in all concretes made in this study. The chemical composition and fineness of this cement are as shown in Table 3-6.

Table 3-6: Portland cement chemical composition and fineness

C_3S	C_2S	C_3A	C_4AF	Free CaO	SO_3	MgO	Blaine Fineness
60.3 %	18.2 %	5.4 %	11.3 %	0.9 %	2.6 %	1.3 %	351 (m^2/kg)

3.6.2 Fly Ash

The fly ash used for this study was Class F fly ash and was obtained from Boral Material Technologies. The chemical composition of this fly ash is listed in Table 3-7.

Table 3-7: Fly ash chemical composition

SiO_2	Al_2O_3	Fe_2O_3	CaO	MgO	SO_3	K_2O	Na_2O	Total Alkalis
55.7 %	27.9%	6.5 %	1.2 %	0.7 %	0.1 %	2.5%	0.3 %	2.0%

3.6.3 Normalweight Coarse and Fine Aggregates

The coarse aggregates used in this study were ASTM C33 (2014) No. 67 siliceous river gravel. The fine aggregate used was siliceous river sand. Both the aggregates were obtained from a concrete plant located in Auburn, Alabama which had stockpiles of the above aggregates. Sieve analysis was performed on sampled aggregates according to ASTM C136 (2014) and their gradations are shown in Appendix A. The specific gravity and absorption capacities of the aggregates were tested in accordance with ASTM C127 (2014) and ASTM C128 (2014), respectively. The properties of the normalweight aggregates are shown in Table 3-8.

Table 3-8: Properties of normalweight coarse and fine aggregate

Property	Coarse Aggregate	Fine Aggregate
Absorption Capacity (%)	0.16	0.34
Specific gravity	2.63	2.64
Fineness modulus	-	3.00

3.6.4 Chemical Admixtures

Chemical admixtures were used to obtain the desired slump and total air content for each concrete mixture. All chemical admixtures were supplied by the BASF Corporation. The dosages of all admixtures are provided in Tables 3-2 and 3-3.

MB AE90 was used as the air-entraining admixture (AEA) and it meets all the requirements of ASTM C260 (2014). The AEA dosage for each concrete mixture was determined with trial batches until the desired total air content was achieved.

The water-reducing admixture used was Pozzolith 322 N. A mid-range water-reducing admixture, (Polyheed 1025) was also used to achieve the desired slump for lower *w/cm* mixtures. Both these admixtures met all the requirements of ASTM C494 (2014). The dosages of the water-reducing admixtures were also determined using trial batches for each concrete mixture.

Due to the harsher nature and workability issues encountered for the ISLWC and ALWC, a rheology-controlling admixture (Navitas 33) was used. The rheology-controlling admixture helped to reduce the harshness of both the ISLWC and the ALWC and improve their workability. The rheology-controlling admixture met the requirements of ASTM C494 (2014) as a Type S Admixture.

Chapter 4

Experimental Results

The results from the experimental work performed for this study are presented in this chapter. Discussions and analysis of results are presented in Chapter 5. The results contain herein include:

- Combined mixture gradations,
- Fresh concrete properties,
- Thermal properties,
- Concrete temperature histories,
- Restrained stress development,
- Unrestrained strain development, and
- Time-dependent development of mechanical properties.

4.1 CONCRETES WITH W/CM = 0.45

4.1.1 Combined Mixture Gradations

Five concrete mixtures with a *w/cm* of 0.45 and with four of them containing lightweight aggregates were produced and tested. The mixture proportions for these five concretes are presented in Table 3-2. In order to assess the impact of using lightweight aggregates on the fresh concrete properties, the combined gradations of these concretes are plotted on a 0.45-power curve and their workability factor determined. The 0.45-power curve in Figure 4-1 presents the particle packing of the combined aggregate gradation (Young, Mindess and Darwin 2002). The workability factors (Shilstone 1990) for all 0.45 *w/cm* concretes are also presented in Figure 4-2.

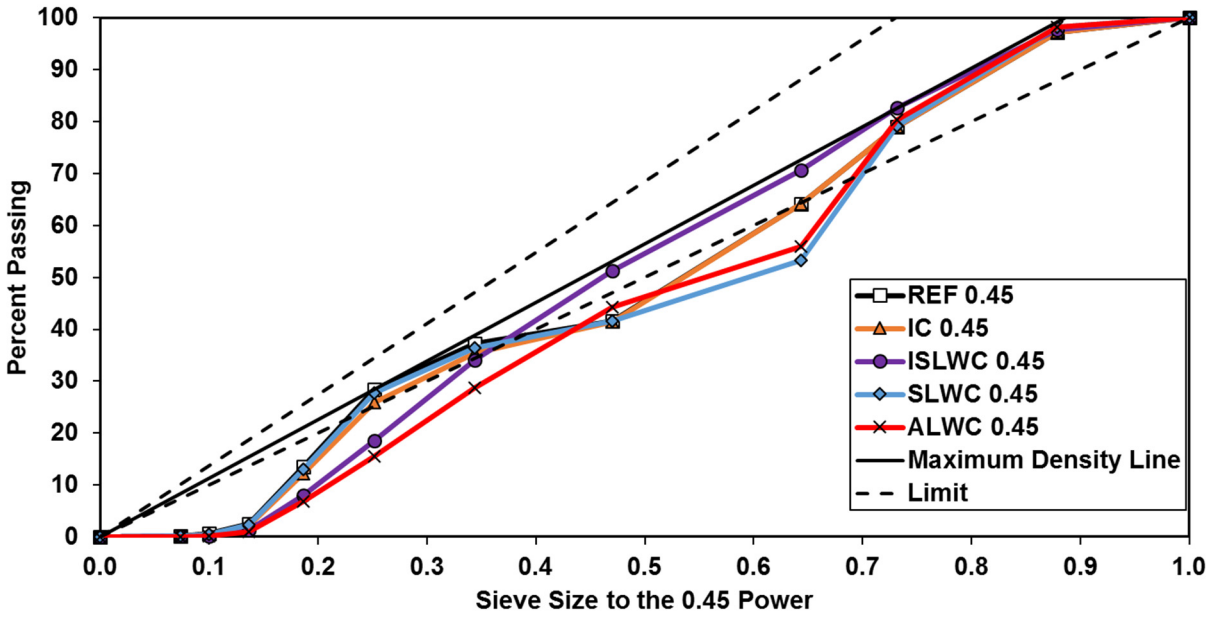

Figure 4-1: Combined gradation of all 0.45 *w/cm* concretes on the 0.45 power curve

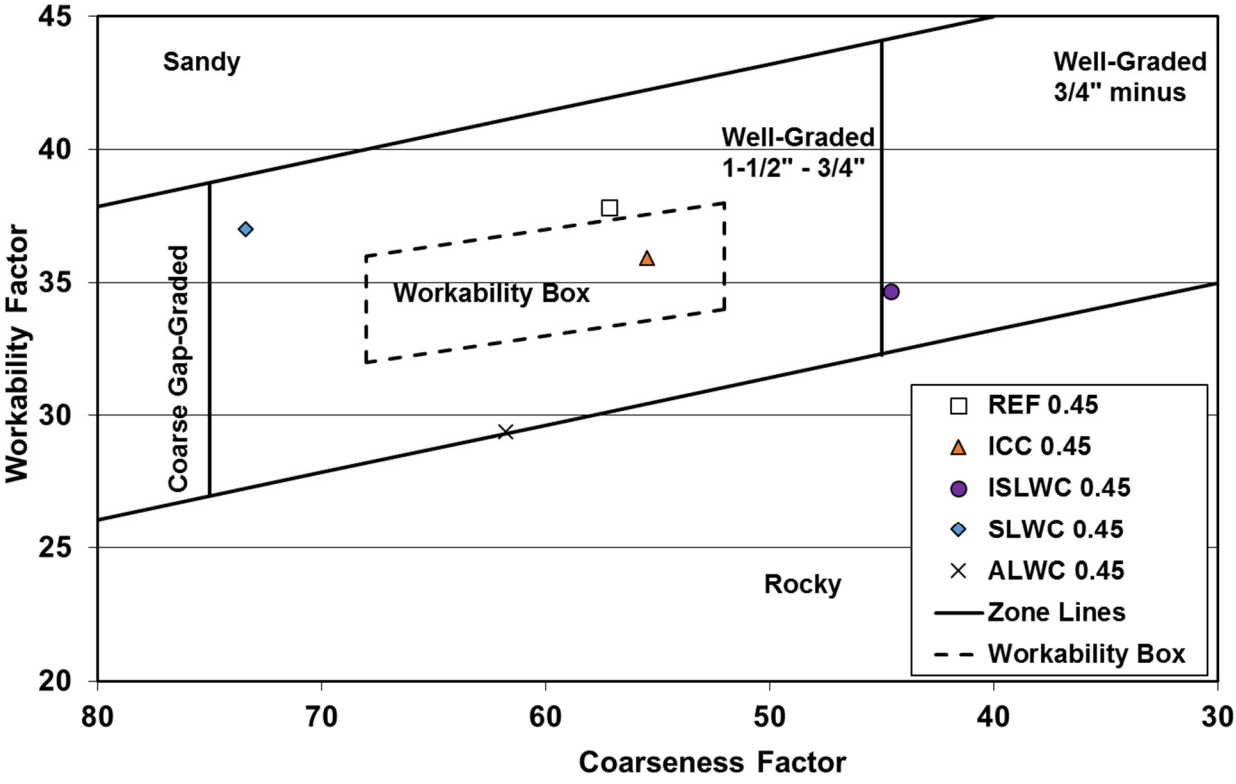

Figure 4-2: Workability factor versus coarseness factor for all 0.45 *w/cm* concretes

4.1.2 Fresh Concrete Properties

Trial batches were performed for each mixture until the desired slump and total air content were achieved. Following this, two batches of concrete were produced, with one batch being tested for mechanical properties of concrete and the other batch for RCF and FSF testing. The fresh properties of each mixture and batch are presented in Table 4-1. The "Δ density" column in Table 4-1 is the difference between the measured and designed densities after performing the corrections for measured total air content. A positive sign indicates that the measured density was higher than the calculated density and vice versa. The calculated equilibrium densities in accordance with ASTM C567 (2014) are also shown in Table 4-1. Only the slump of ISLWC 0.45 (Batch 1) was 0.5 in. below the target slump range of 3 to 5 in.; however, the workability of this mixture was sufficient to allow it to be effectively consolidated.

Table 4-1: Measured fresh concrete properties for all 0.45 *w/cm* concretes

Concrete Mixture	Batch No.	Fresh Concrete Test Results				Calculated
		Slump (in.)	Temp. (°F)	Total Air (%)	Density (lb/ft^3)	Δ Density (lb/ft^3)
REF 0.45	1	3.5	74	5.0	141.5	0.5
	2	4.5	73	5.5	141.9	0.9
ICC 0.45	1	4.0	73	5.5	140.8	-0.7
	2	3.5	75	5.0	139.6	-1.0
ISLWC 0.45	1	2.5	73	4.0	120.6	0.1
	2	3.0	75	4.5	120.1	-0.4
SLWC 0.45	1	3.5	74	4.5	114.1	0.9
	2	3.5	73	5.0	114.2	1.0
ALWC 0.45	1	5.0	71	5.0	101.5	-0.6
	2	4.5	72	5.5	101.3	-0.8

4.1.3 Thermal Properties

The calculated equilibrium density, coefficient of thermal expansion, and thermal diffusivity are summarized in Table 4-2.

Table 4-2: Miscellaneous properties of all 0.45 *w/cm* concretes

Property	REF 0.45	ICC 0.45	ISLWC 0.45	SLWC 0.45	ALWC 0.45
Calculated Equilibrium Density (lb/ft^3)	139.0	135.5	115.4	110.6	95.6
Coefficient of Thermal Expansion (με/°F)	5.8	5.7	5.2	5.1	4.1
Thermal Diffusivity (ft^2/hr)	0.039	0.037	0.035	0.022	0.019

4.1.4 Peak Temperatures

The time-dependent development of temperatures at the core of an 8×8 ft column calculated from ConcreteWorks for the concretes with a *w/cm* of 0.45 are presented in Figure 4-3. The edge temperatures computed using ConcreteWorks were simulated in the rigid cracking frame, as mentioned in Section 3.5.

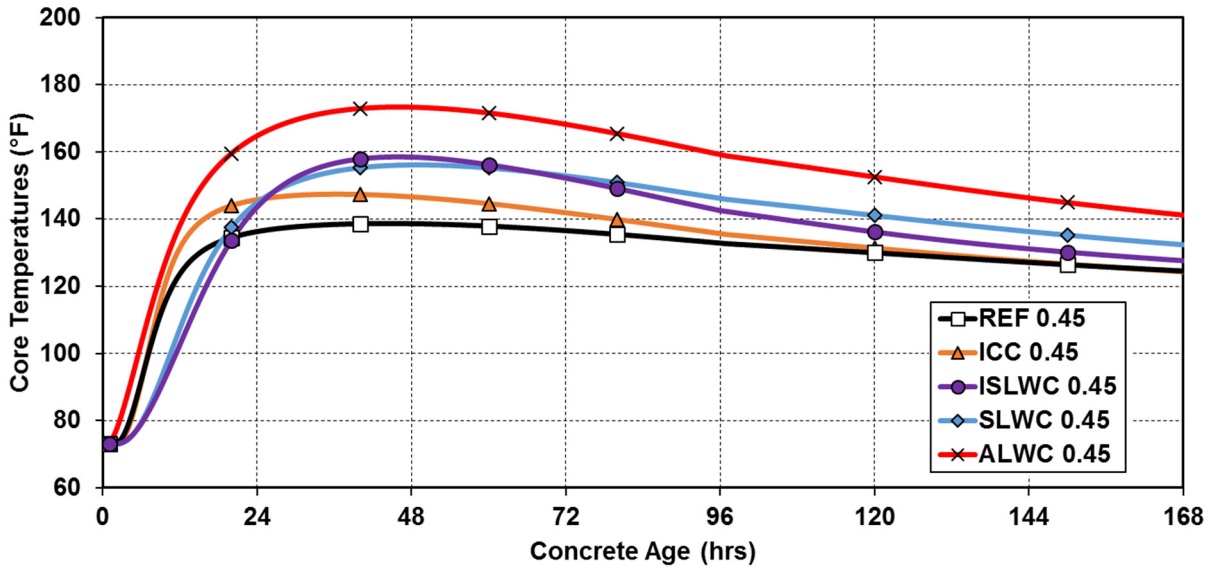

Figure 4-3: Temperature development in a 8×8 ft column for all 0.45 *w/cm* concretes

4.1.5 Restrained Stress Development

The restrained stress development measured with the RCF for all five concretes with *w/cm* of 0.45 and their curing temperatures are shown in Figures 4-4 and 4-5. The stresses are shown until the time of cracking, which is indicated by a sudden drop in stress. Isothermal stress development was not measured for any of the concretes with *w/cm* of 0.45, because their autogenous shrinkage is expected to be negligible (Weiss and Bentz 2010; Lura et al. 2003).

4.1.6 Unrestrained Strain Development

The unrestrained strain measurement measured with the FSF for all concrete specimens with a *w/cm* of 0.45 are shown in Figure 4-6. The concrete specimens were match-cured using the modeled temperature profiles of the RCF.

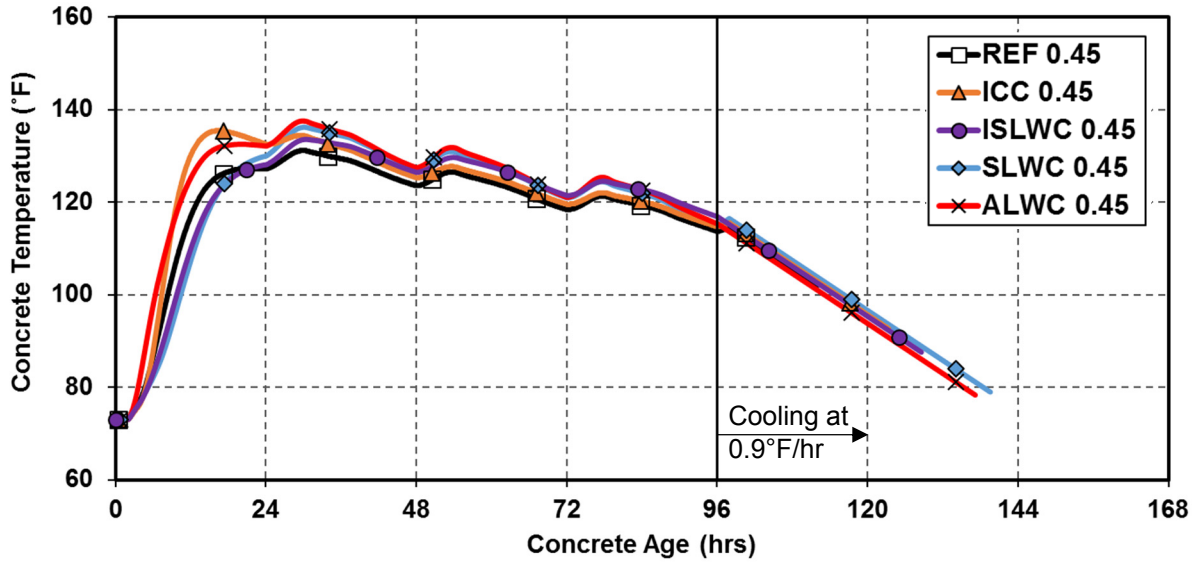

Figure 4-4: Concrete temperature profile for all 0.45 *w/cm* concretes

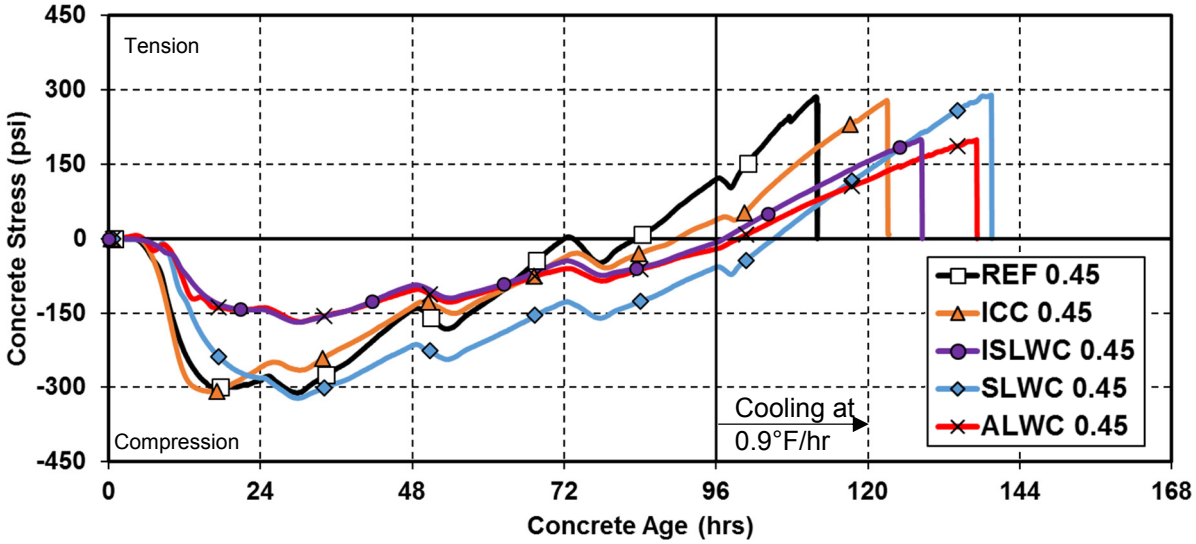

Figure 4-5: Restrained stress development for all 0.45 *w/cm* concretes

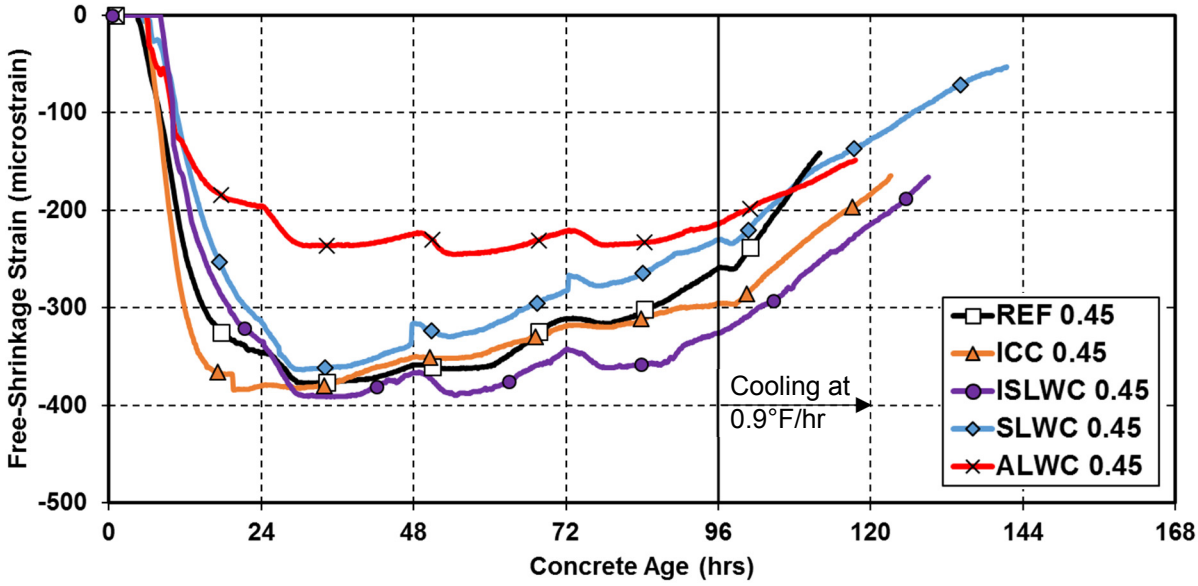

Figure 4-6: Unrestrained strain development for all 0.45 *w/cm* concretes

4.1.7 Summary of Rigid Cracking Frame Test Results

The maximum RCF temperature, time of cracking in the RCF, and the stresses at cracking are shown in Table 4-3 for all the concretes with *w/cm* of 0.45.

Table 4-3: Summary of RCF results for concrete with *w/cm* of 0.45

Item	*w/cm* = 0.45				
	REF 0.45	ICC 0.45	ISLWC 0.45	SLWC 0.45	ALWC 0.45
Maximum RCF temperatures (°F)	130	135	135	136	139
Time of cracking (hrs)	110	123	128	139	137
Stress at cracking (psi)	290	290	200	290	200

4.1.8 Time-Dependent Development of Mechanical Properties

The time-dependent development of compressive strength, splitting tensile strength, and modulus of elasticity were tested for each concrete mixture. The measured values were averaged for two cylinders and are presented in Appendix B. Twenty-four cylinders were match-cured along with the RCF and FSF and were tested at varying ages. A regression analysis was performed according to ASTM C1074 (2014), which recommends the use of an exponential function. Best-fit curves were determined for the measured values and are plotted in Figures 4-7 to 4-9.

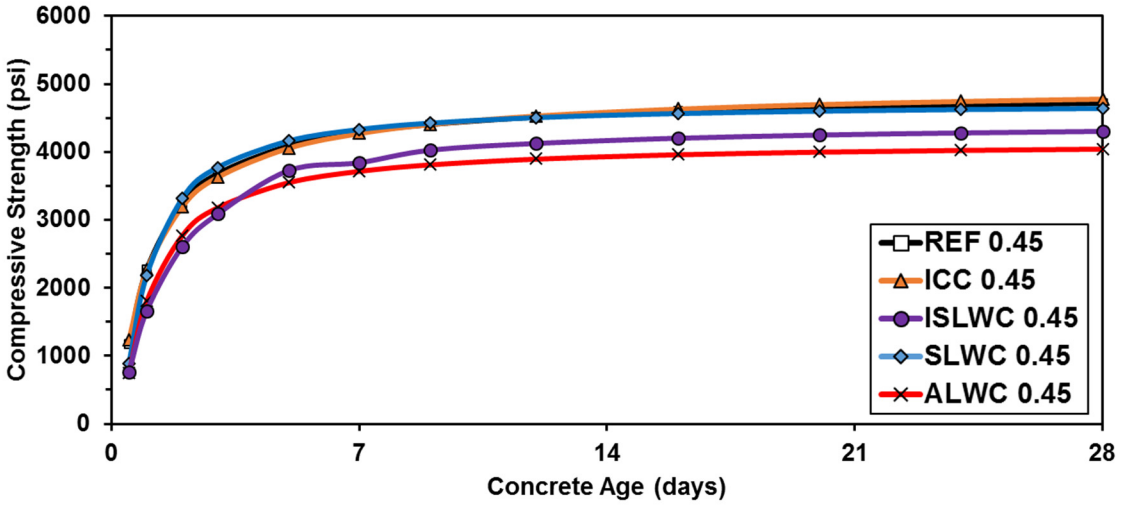

Figure 4-7: Compressive strength development for all 0.45 *w/cm* concretes

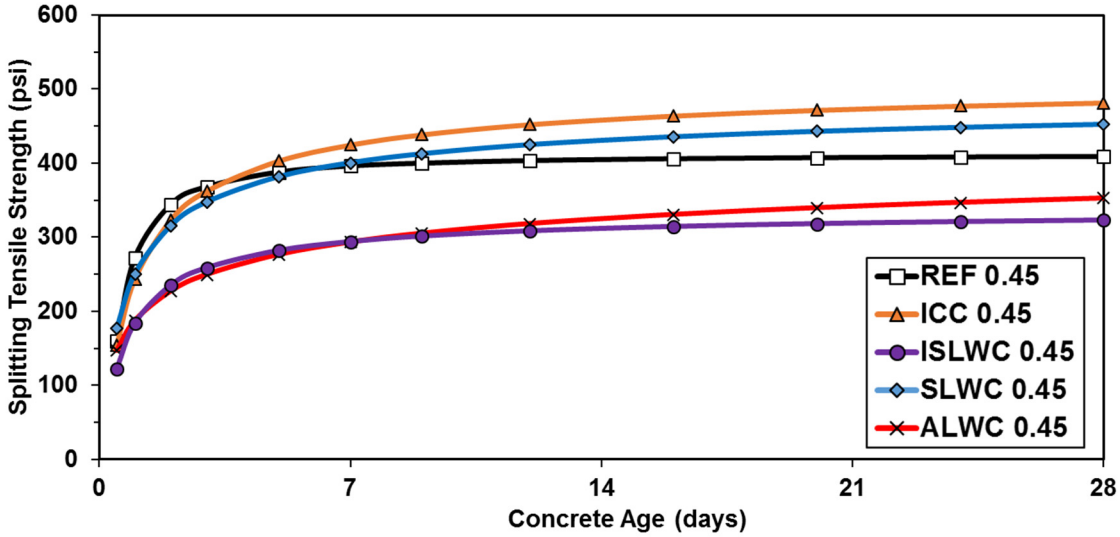

Figure 4-8: Splitting tensile strength development for all 0.45 *w/cm* concretes

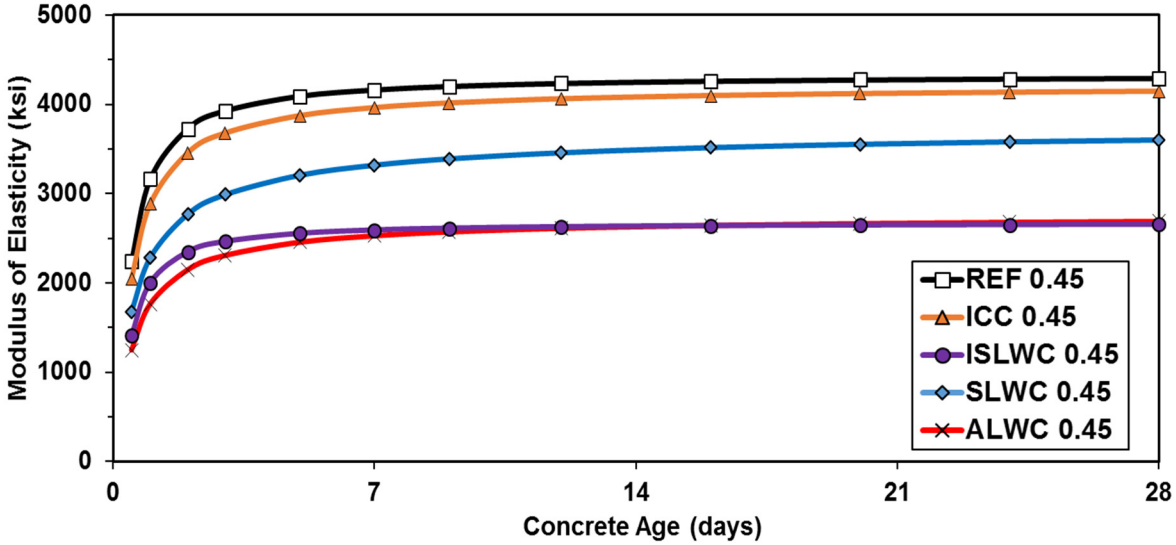

Figure 4-9: Modulus of elasticity development for all 0.45 *w/cm* concretes

4.2 CONCRETES WITH W/CM = 0.38

4.2.1 Combined Mixture Gradations

Five concrete mixtures with a *w/cm* of 0.38 and with four of them containing lightweight aggregates were produced and tested for fall conditions. The mixture proportions are, for these fine concretes are presented in Table 3-3. In order to assess the impact of using lightweight aggregates on the fresh concrete properties, the combined gradations of the concrete are plotted on a 0.45-power curve and their workability factor determined. The 0.45-power curve presented in Figure 4-10 presents the particle packing of the blended aggregate gradation (Young, Mindess and Darwin 2002). The workability factors (Shilstone 1990) for all 0.38 *w/cm* concretes are also presented in Figure 4-11.

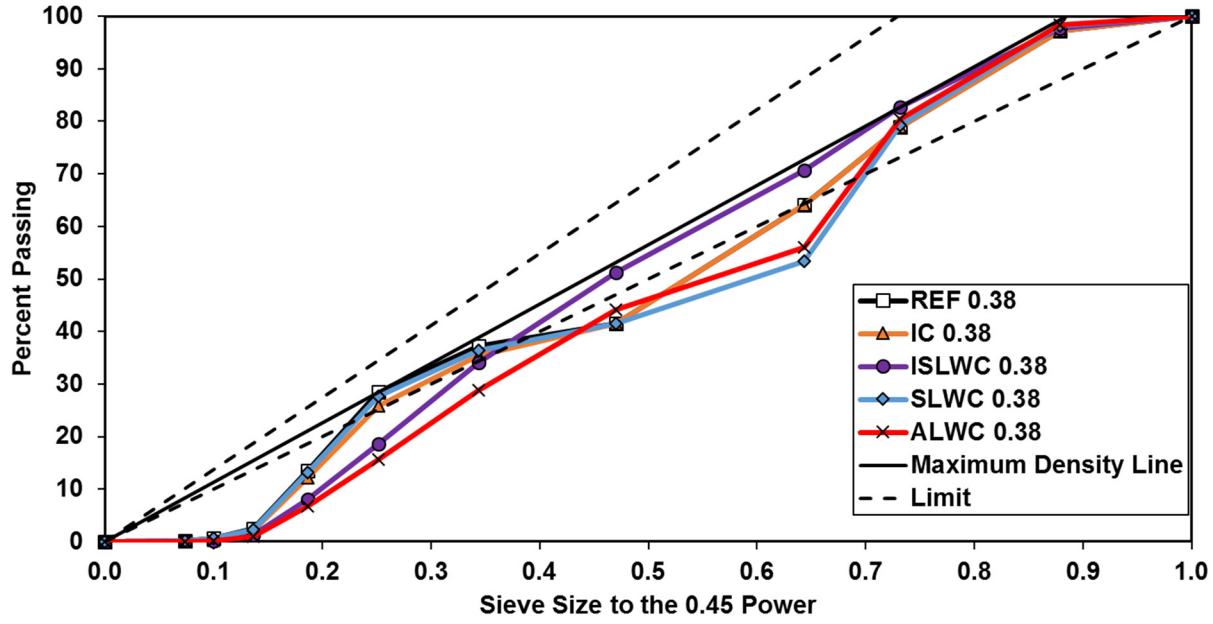

Figure 4-10: Combined gradation of all 0.38 *w/cm* concretes on the 0.45 power curve

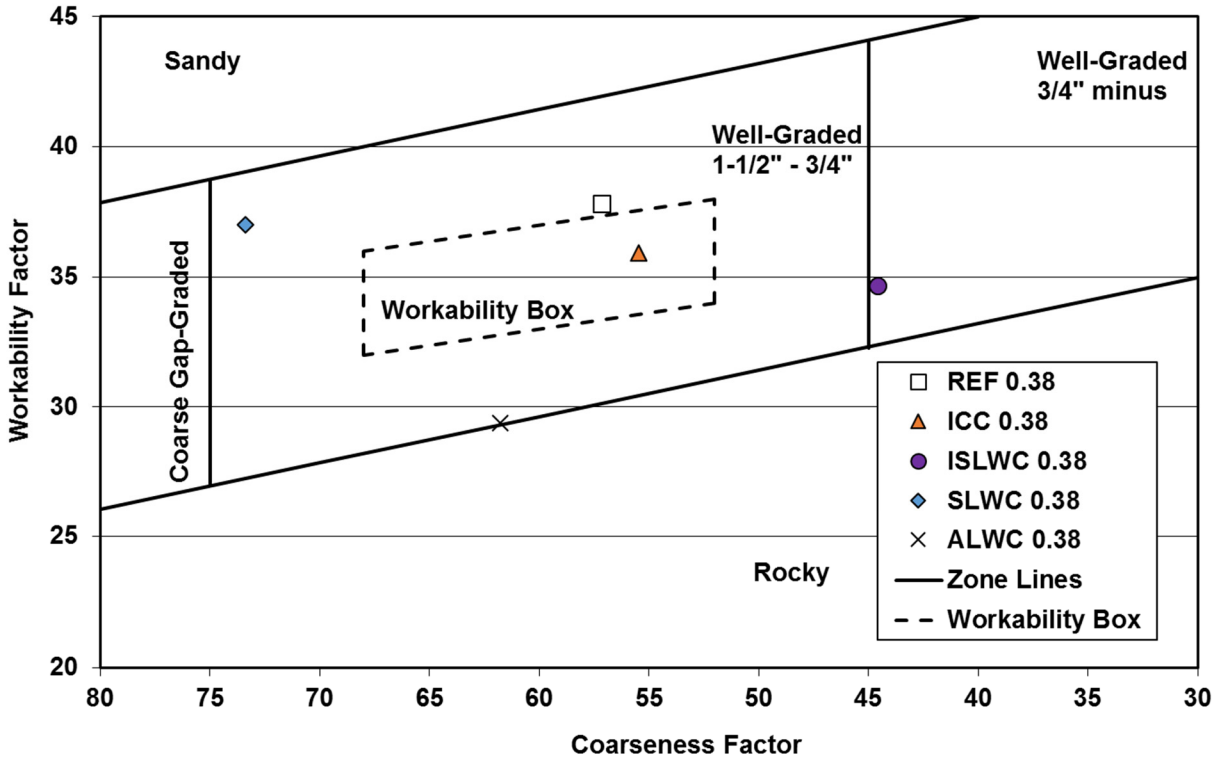

Figure 4-11: Workability factor versus coarseness factor for all 0.38 *w/cm* concretes

4.2.2 Fresh Concrete Properties

Trial batches were performed for each mixture until the desired slump and total air content were achieved. Following this, two batches of concrete were produced, with one batch being tested for mechanical properties of concrete and the other batch for RCF and FSF testing. The fresh properties of each mixture and batch are presented in Table 4-4. The "Δ density" column in Table 4-4 is the difference between the measured and designed densities after performing the corrections for measured total air content. A positive sign indicates that the measured density was higher than the calculated density and vice versa. The calculated equilibrium densities in accordance to ASTM C567 (2014) are also shown in Table 4-4. The slumps of SLWC 0.38 (Batch 1) and ALWC 0.38 (Batch 1) were 0.5 in. outside the target slump range of 3 to 5 in.; however, the workability of these concretes were sufficient to allow them to be effectively consolidated without any signs of segregation.

Table 4-4: Measured Fresh properties for all 0.38 *w/cm* concretes

Concrete Mixture	Batch No.	Fresh Concrete Test Results				Calculated
		Slump (in.)	Temp. (°F)	Total Air (%)	Density (lb/ft^3)	Δ Density (lb/ft^3)
REF 0.38	1	4.0	73	5.5	141.6	0.4
	2	3.0	73	5.0	141.9	0.7
ICC 0.38	1	3.5	72	4.5	141.2	0.6
	2	3.5	75	5.5	140.1	-0.5
ISLWC 0.38	1	3.5	73	4.0	120.8	0.3
	2	4.0	74	4.0	121.2	0.7
SLWC 0.38	1	2.5	73	5.5	115.0	1.2
	2	4.0	71	6.0	114.6	0.8
ALWC 0.38	1	5.5	74	6.0	101.3	-0.8
	2	4.0	73	5.5	101.8	-0.3

4.2.3 Thermal Properties

The calculated equilibrium density, coefficient of thermal expansion, and thermal diffusivity are summarized in Table 4-5.

Table 4-5: Miscellaneous properties of all 0.38 *w/cm* concretes

Property	REF 0.38	ICC 0.38	ISLWC 0.38	SLWC 0.38	ALWC 0.38
Calculated Equilibrium Density (lb/ft^3)	139.2	135.5	115.8	110.2	95.2
Coefficient of Thermal Expansion (με/°F)	6.1	5.9	5.3	5.3	4.1
Thermal Diffusivity (ft^2/hr)	0.039	0.038	0.037	0.021	0.014

4.2.4 Peak Temperatures

The time-dependent development of temperatures at the core of an 8×8 ft column calculated from ConcreteWorks for the concretes with a *w/cm* of 0.38 are presented in Figure 4-12. The edge temperatures computed using ConcreteWorks were simulated in the rigid cracking frame, as mentioned in Section 3.5.

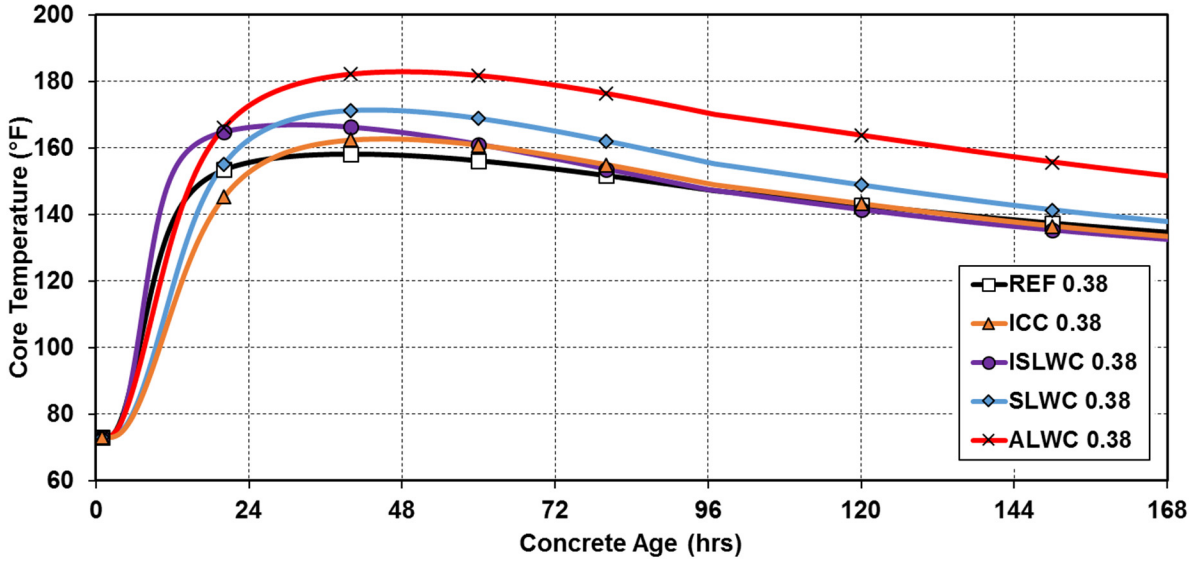

Figure 4-12: Temperature development in a 8×8 ft column for all 0.38 *w/cm* concretes

4.2.5 Restrained Stress Development

The restrained stress development measured with the RCF for all five concretes with *w/cm* of 0.38 and their curing temperature profiles are shown in Figures 4-13 and 4-14. The stresses are shown until the time of cracking, which is indicated by a sudden drop in stress.

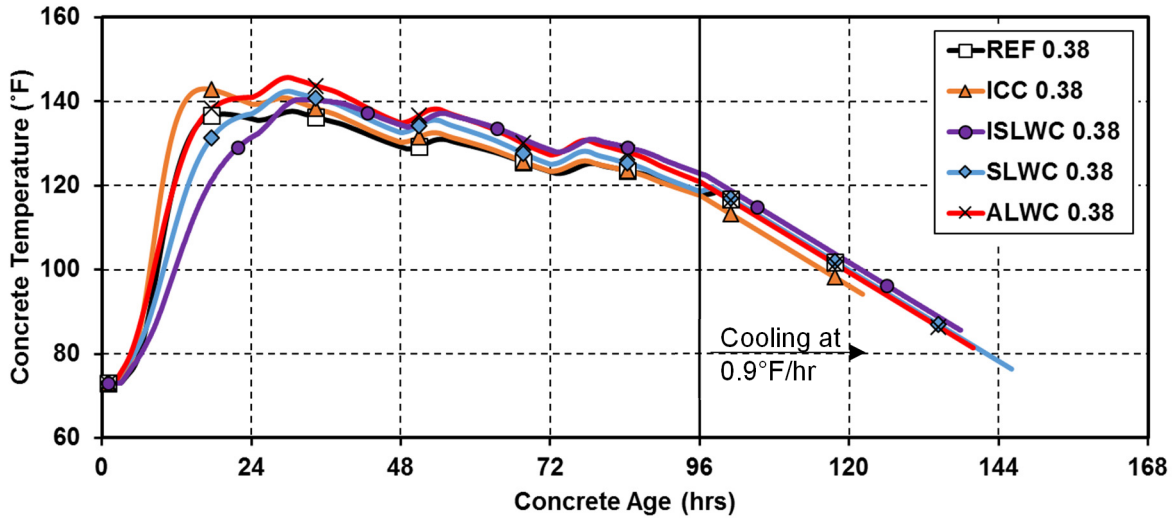

Figure 4-13: Concrete temperature profile for all 0.38 *w/cm* concretes

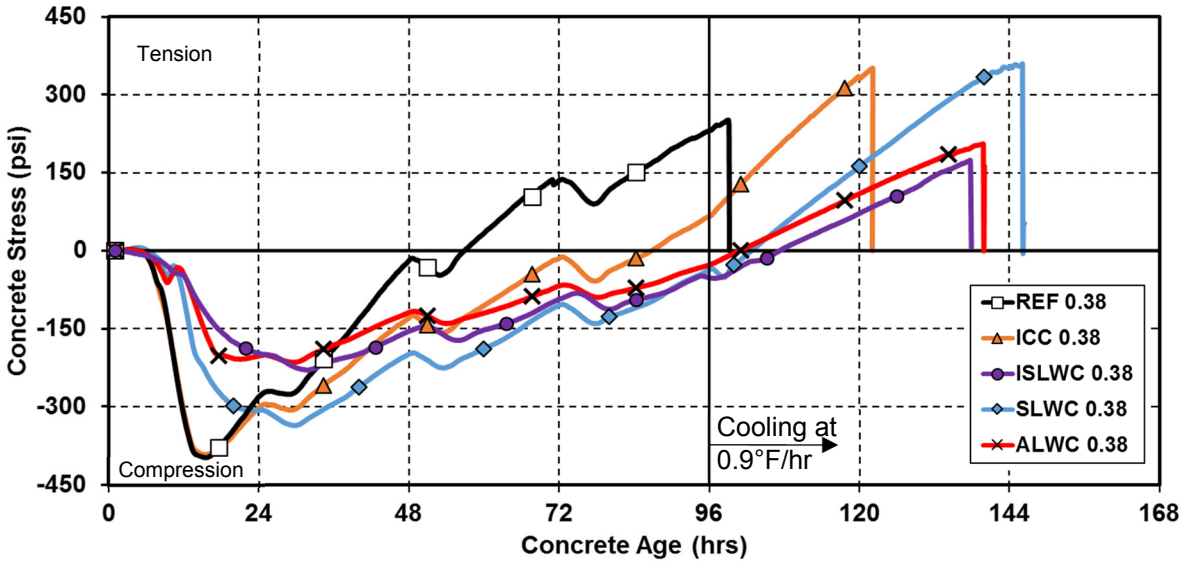

Figure 4-14: Restrained stress development for all 0.38 *w/cm* concretes

4.2.6 Unrestrained Strain Development

The unrestrained strain measurement measured with the FSF for all the concrete specimens with *w/cm* of 0.38 are shown in Figure 4-15. The concrete specimens were match-cured using the modeled temperature profiles of the RCF.

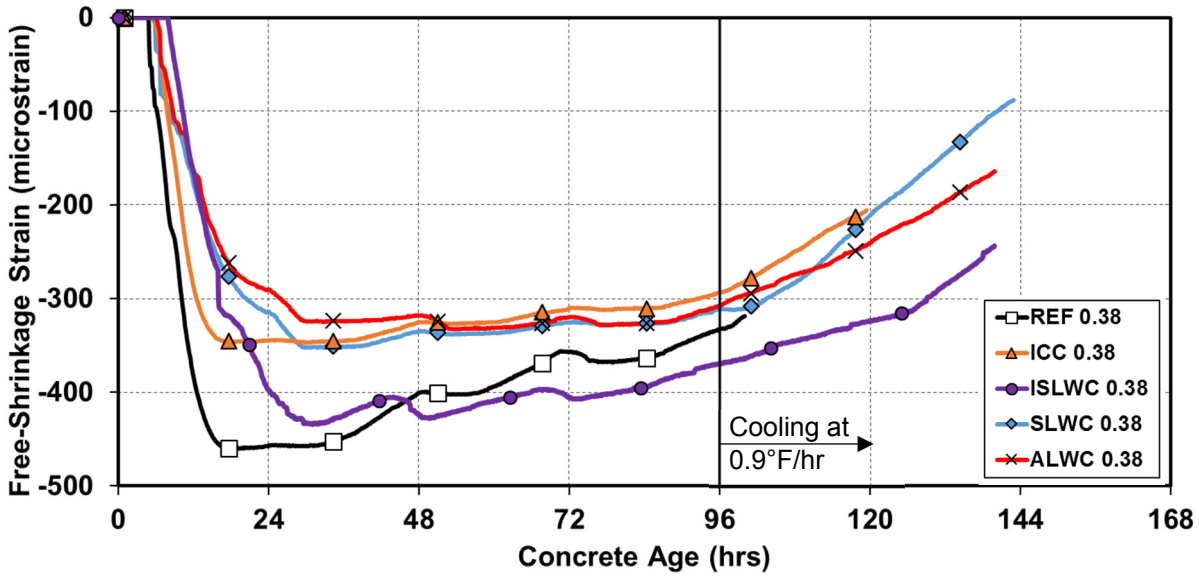

Figure 4-15: Unrestrained strain development for all 0.38 *w/cm* concretes

4.2.7 Isothermal Stress Development

The isothermal stress development measured with the RCF for all five low *w/cm* concretes are shown in Figure 4-16. The isothermal stresses refer to the concrete stresses when the specimen is subjected to a uniform temperature of 73°F, so in this setup these stresses only develop due to autogenous shrinkage.

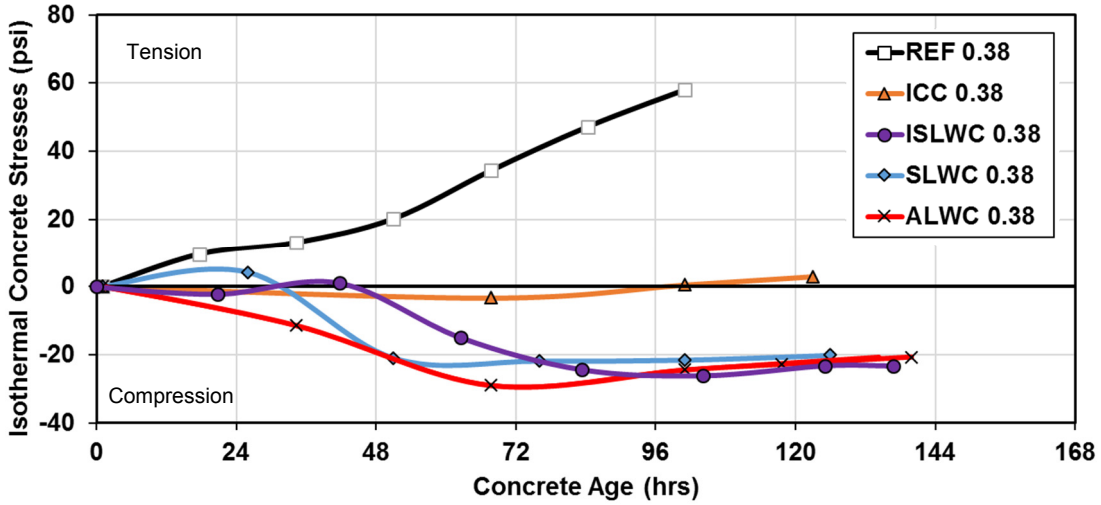

Figure 4-16: Isothermal stress development for all 0.38 *w/cm* concretes

4.2.8 Summary of Rigid Cracking Frame Test Results

The maximum RCF temperature, time of cracking in the RCF, and the stress at cracking are shown in Table 4-6 for all concrete with *w/cm* of 0.38.

Table 4-6: Summary of RCF results for concrete with *w/cm* of 0.38

Item	*w/cm* = 0.38				
	REF 0.38	**ICC 0.38**	**ISLWC 0.38**	**SLWC 0.38**	**ALWC 0.38**
Maximum RCF temperatures (°F)	136	140	141	142	146
Time of cracking (hrs)	99	123	138	146	142
Stress at cracking (psi)	260	345	190	355	205
Maximum isothermal tensile stress (psi)	60	0	0	5	0

4.2.9 Time-Dependent Development of Mechanical Properties

The time-dependent development of compressive strength, splitting tensile strength, and modulus of elasticity were tested for each concrete mixture. Twenty-four cylinders were match-cured along with the RCF and FSF were tested at varying ages. The measured values were averaged for two cylinders and are presented in Appendix B. A regression analysis was performed as per ASTM C1074 (2014), which recommends the use of an exponential function. Best-fit curves were determined for the measured values and are plotted in Figures 4-17 to 4-19.

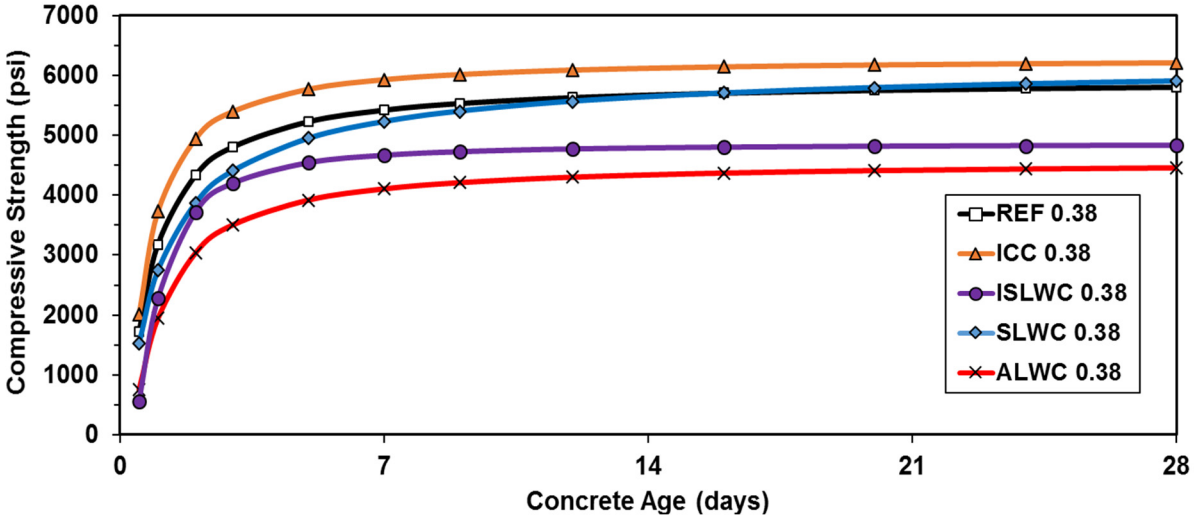

Figure 4-17: Compressive strength development for all 0.38 *w/cm* concretes

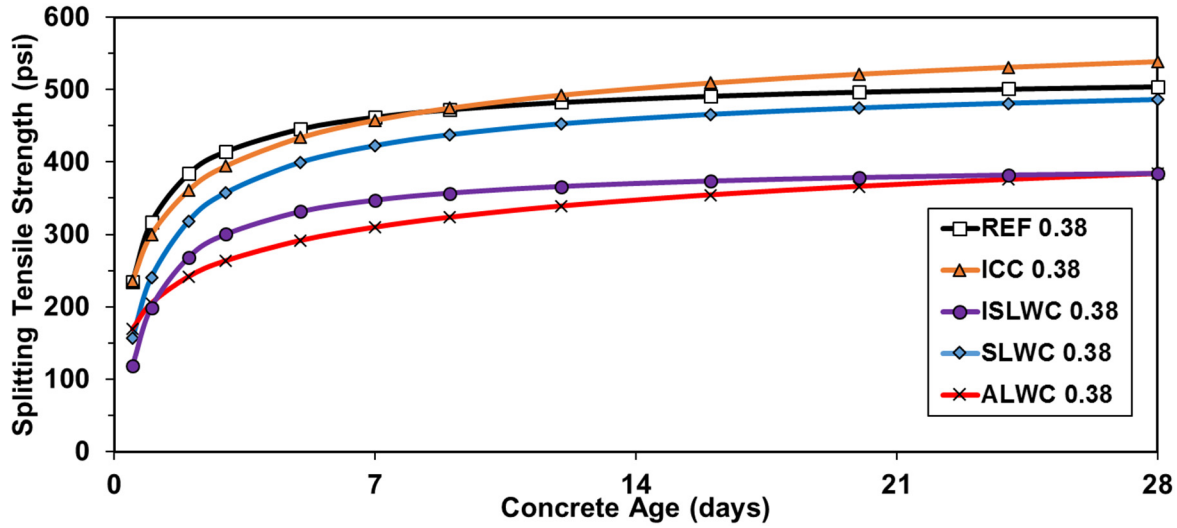

Figure 4-18: Splitting tensile strength development for all 0.38 *w/cm* concretes

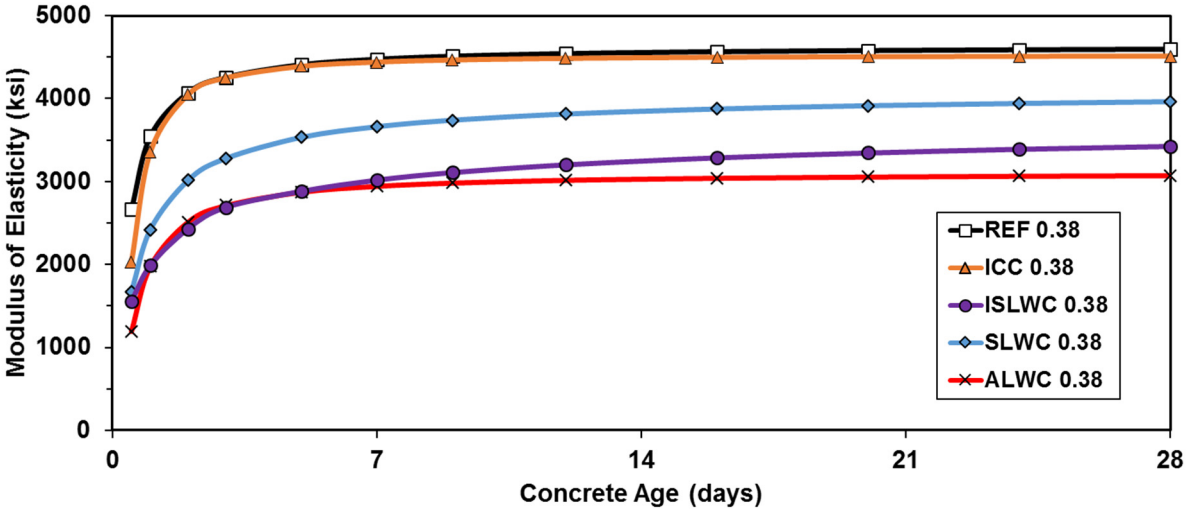

Figure 4-19: Modulus of elasticity development for all 0.38 *w/cm* concretes

Chapter 5

Discussion of Results

A discussion of the collected results is presented in this chapter. The change in concrete properties due to the use of lightweight aggregates is assessed in Section 5.1. In Section 5.2, the effect of internal curing on autogenous stress development is covered. Next, the effects of lightweight aggregates on early-age concrete stresses are evaluated in Section 5.3. The cracking tendency, time to cracking, and peak hydration temperatures for all concretes are also compared and the reason for the observed behavior is discussed. Finally, the modulus of elasticity and splitting tensile strength results are compared to predictions from various expressions at the end of this chapter.

5.1 EFFECT OF LIGHTWEIGHT AGGREGATE ON CONCRETE PROPERTIES

5.1.1 Compressive Strength

Compressive strength developments for all concretes are presented in Figures 4-7 and 4-17. The 28-day design compressive strength for the reference concrete was 4,000 psi, and the experimental results indicate that the compressive strengths exceeded the design strength. When considering the with-in test variability, the compressive strength development for the reference, IC, and SLW concretes are similar for both groups of *w/cm* concretes. Similarly, ALW and ISLW concretes had approximately 10 % to 15 % lower compressive strengths compared to the reference concretes for both groups of *w/cm* concretes. This is most likely due to the use of large amount of fine LWA in both the ISLW and ALW concretes. It was unexpected that the ISLW concrete had a strength much lower than the SLW concrete; however, the use of high volume of fine LWA could explain this result. When comparing the strengths achieved in Figures 4-7 and 4-17, it can be seen that both ISLW and ALW concretes are capable of higher strengths, if low *w/cm* concrete mixtures are used.

5.1.2 Splitting Tensile Strength

The splitting tensile strength developments for all concretes are presented in Figures 4-8 and 4-18. When considering the with-in test variability, the splitting tensile strength development for the reference, IC, and SLW concretes are similar for both groups of *w/cm* concretes. Whereas the ISLW and ALW concretes had approximately 20 % to 30 % lower splitting tensile strengths, when compared to the reference concretes for both groups of *w/cm* concretes. The most likely reasons for this result could be due to the higher proportion of fine LWA, poor particle packing of the ALW concretes, and the low coarseness factor of the ISLW concretes (Shilstone and Shilstone 1989) when compared to the reference concrete as shown in Figure 4-2 and 4-11.

5.1.3 Modulus of Elasticity

The modulus of elasticity development results for all concretes are presented in Figures 4-9 and 4-19. When considering the with-in test variability, the modulus of elasticity development for the reference and IC concretes are similar for both groups of *w/cm* concretes. The average modulus of elasticity values are lower by 12 %, 33 %, and 33 % for SLW, ISLW, and ALW concretes, respectively, when compared to the reference concretes for both groups of *w/cm* concretes. The primary factors contributing to this result are the lower stiffness of LWA and the reduced density of LWA concretes when compared to normalweight concretes. An unexpected result is the reduced modulus of elasticity of the ISLW concrete when compared to SLW concrete. The SLW concrete has a slightly lower density (approximately 6 lb/ft^3) than ISLW concrete, but has a higher modulus of elasticity in comparison. A possible reason could be due to the much-reduced compressive strength of both ISLW concretes, as discussed in Section 5.1.1. Based on either Equation 2-7 or 2-8, a large decrease in strength will lead to a large decrease in modulus of elasticity. However, this large decrease in modulus of elasticity may be beneficial to reduce early-age concrete stresses.

5.1.4 Coefficient of Thermal Expansion

The coefficient of thermal expansion (CTE) values for all concretes are presented in Tables 4-2 and 4-5. As shown in Figure 5-1, the CTE values for both the *w/cm* concretes indicate that the concretes with an increasing amount of LWAs exhibit reduced CTE values, with an average CTE reduction of 5 % for IC, 10 % for ISLW, 10 % for SLW, and 30 % for ALW concretes when compared to the two reference concretes. The reduction in concrete CTE of concrete containing LWA is attributed to the lower CTE of LWA (Neville 2011). In accordance with Equation 2-1, a reduction in concrete CTE will result in a decrease in concrete thermal stress, which will lead to an improvement in resistance to thermal cracking.

5.1.5 Thermal Diffusivity

The thermal diffusivity for all the concretes are summarized in Tables 4-2 and 4-5. As shown in Figure 5-2, the thermal diffusivity values for both the *w/cm* concretes indicate that the concretes with increasing amount of LWAs exhibit reduced thermal diffusivity values, with an average thermal diffusivity reduction of 5 % for IC, 10 % for ISLW, 30 % for SLW, and 50 % for ALW concretes when compared to the two reference concretes. The lower diffusivity for concrete containing lightweight aggregates is due to its lower thermal conductivity and a lower density. The lower thermal diffusivity indicates that lightweight aggregate concretes will dissipate heat more slowly, which will lead to higher peak temperatures in mass concrete applications when compared to normalweight concrete.

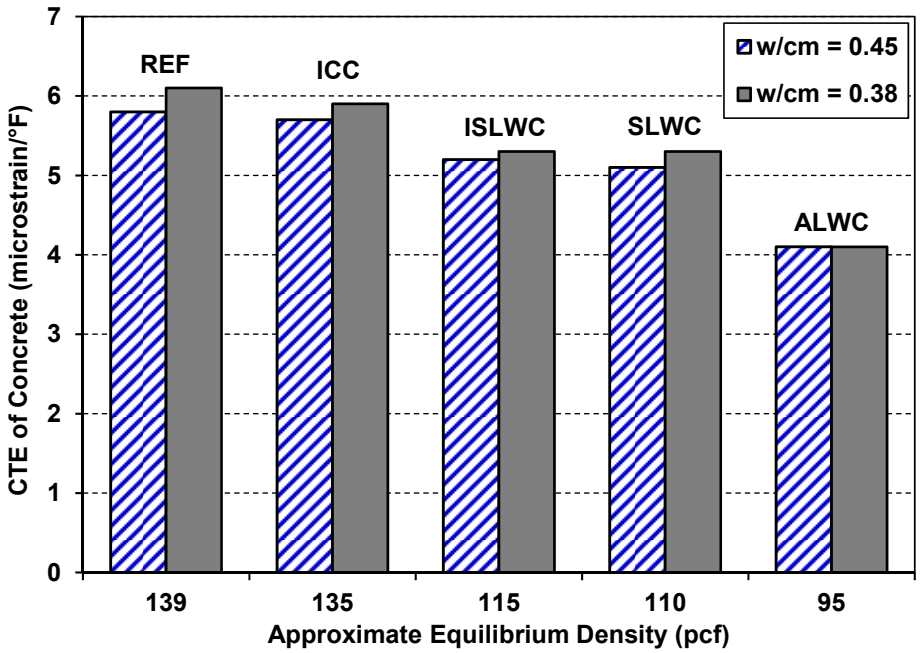

Figure 5-1: Measured CTE values for all concretes

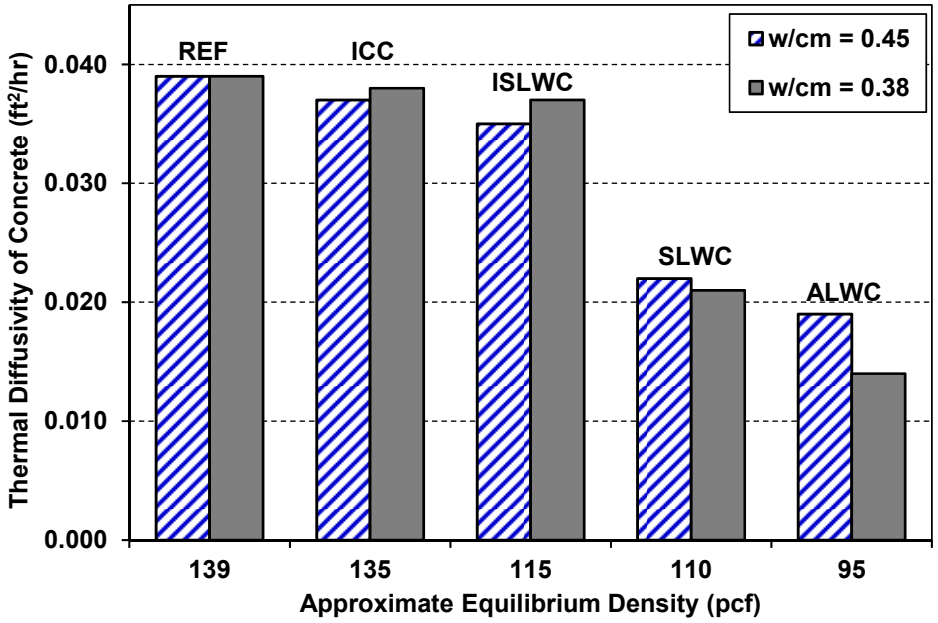

Figure 5-2: Measured thermal diffusivity values for all concretes

5.1.6 Peak Temperature

The development of peak temperatures at the core of an 8 × 8 ft cross-sectional mass concrete column are presented in Figures 4-3 and 4-12. These concrete temperatures were determined by using the ConcreteWorks software with the measured semi-adiabatic calorimeter and thermal diffusivity values for all

concretes. As the *w/cm* of the concrete decreases, the peak concrete temperatures increase, which is due to the presence of more cementitious material in low *w/cm* concretes (Schindler and Folliard 2005).

It can be observed that the peak concrete temperatures are the highest for the ALW concretes, followed by the SLW and ISLW concretes that are higher than the peak temperatures of the IC and reference concretes. The reference concrete has the lowest maximum concrete temperature for all the concretes followed by the IC concrete. The major reason can be attributed to the systematically lower thermal diffusivity observed in these lightweight aggregate concretes as compared to the normalweight concrete, as shown in Figure 5-2. The decrease in thermal diffusivity tends to have an insulating effect on the structure leading to a higher buildup of peak temperatures in concrete containing lightweight aggregates (Maggenti 2007; Byard and Schindler 2010). Another reason is due to the higher degree of hydration in lightweight aggregate concretes, due to internal curing provided by the pre-wetted LWAs in the concrete (Bentz and Weiss 2011). Since the maximum in-place concrete temperatures increased as more LWAs were used in the mixture, care should be taken when using LWA concrete in mass concrete to make sure not to exceed the in-place concrete temperature threshold for DEF.

5.2 EFFECT OF INTERNAL CURING ON AUTOGENOUS STRESS DEVELOPMENT

The internal curing water provided by lightweight aggregates for each concrete type is presented in Table 3-4. The availability of internal curing water is the highest in the ALW concrete, followed by SLW, ISLW, and IC concretes, because concrete containing higher proportion of the same LWA contains more internal curing water. The autogenous shrinkage stress development for all 0.38 *w/cm* concretes is presented in Figure 4-16. The autogenous shrinkage stresses are greatly reduced in all concretes containing LWA when compared to the reference concrete. The stress due to autogenous shrinkage is for all practical purposes zero in all concretes incorporating LWA. This decrease in autogenous shrinkage stresses has been documented in several research studies (Byard and Schindler 2010; Bentz and Weiss 2011; RILEM TC 196 2007). The internal curing water acts as internal water reservoirs, thus increasing the internal relative humidity inside the concrete, and resulting in no autogenous shrinkage related stresses (RILEM TC 196 2007). This reduction or elimination of autogenous shrinkage related stresses point out that enough internal curing water is available to mitigate the effects of autogenous shrinkage.

It can be seen in Figure 4-5 and 4-14 that when compared to the reference concrete, the use of lightweight aggregates delays the occurrence of cracking in all concretes incorporating LWA. The lower *w/cm* reference concrete cracks at an earlier time when compared to the higher *w/cm* reference concrete. Although the 0.38 *w/cm* reference concrete has an increased splitting tensile strength, the earlier time to cracking in the 0.38 *w/cm* reference concrete is partly due to its higher modulus of elasticity and the contribution of autogenous shrinkage stresses which becomes more prominent at lower *w/cm*. The use of LWA in concrete with low *w/cm* will thus be more beneficial, because this is when the autogenous shrinkage will be at its highest, and the LWA will help to lower the modulus of elasticity of the low *w/cm* concrete.

5.3 EVALUATION OF THE BEHAVIOR OF VARIOUS TYPES OF LIGHTWEIGHT AGGREGATE CONCRETES

The early-age behavior of the concretes incorporating lightweight aggregates are compared with the behavior of the two reference concretes in this section.

5.3.1 Behavior of Internally Cured Concretes

The concrete temperature profiles and restrained stress development for the internally cured concretes for both *w/cm* concretes are compared to the response of the two reference concretes in Figures 5-3 and 5-4. For comparison, the modulus of elasticity and splitting tensile strength development of all IC concretes and reference concretes are plotted in Figures 5-5 and 5-6. The concrete temperatures of the IC concretes are higher than their reference concrete counterparts. This is due to the increased availability of internal curing water and the reduced thermal diffusivity of the IC concretes.

The 0.45 *w/cm* IC concrete exhibit an increase in time to cracking, when compared to its reference concrete. This is mostly attributed to the reduced coefficient of thermal expansion observed in the 0.45 *w/cm* IC concrete, when compared its reference concrete, as discussed in Section 5.1.

For the low *w/cm* concrete mixture, a 30 % increase in stress at cracking and a 24-hour delay in time to cracking are observed in the IC concrete, when compared to the reference concrete. The improvement in cracking behavior of internally cured concretes of 0.38 *w/cm* is attributed to a combination of reduced coefficient of thermal expansion and autogenous shrinkage stress when compared to the reference concrete.

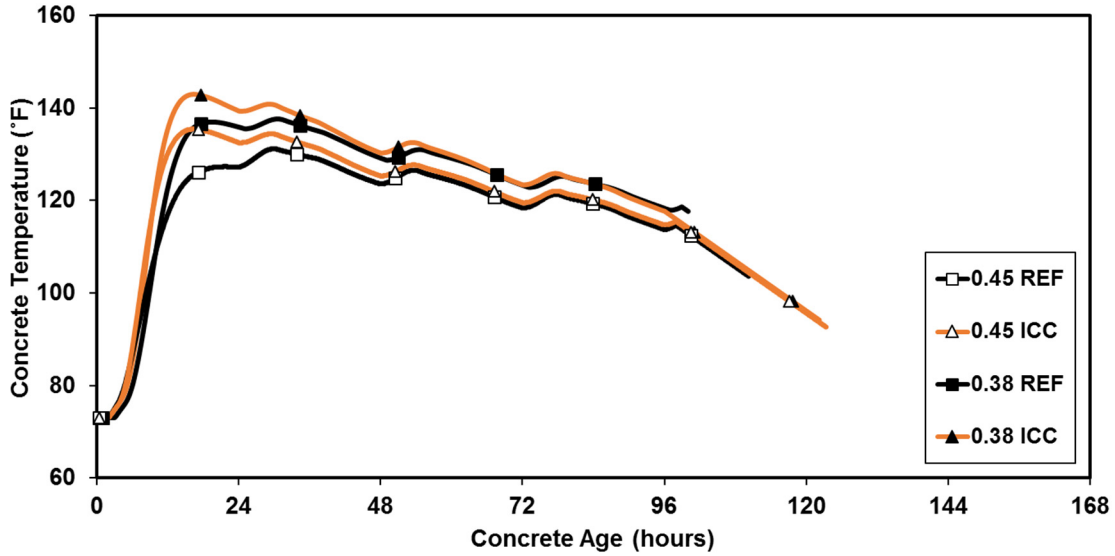

Figure 5-3: Concrete temperature profile of IC and reference concretes

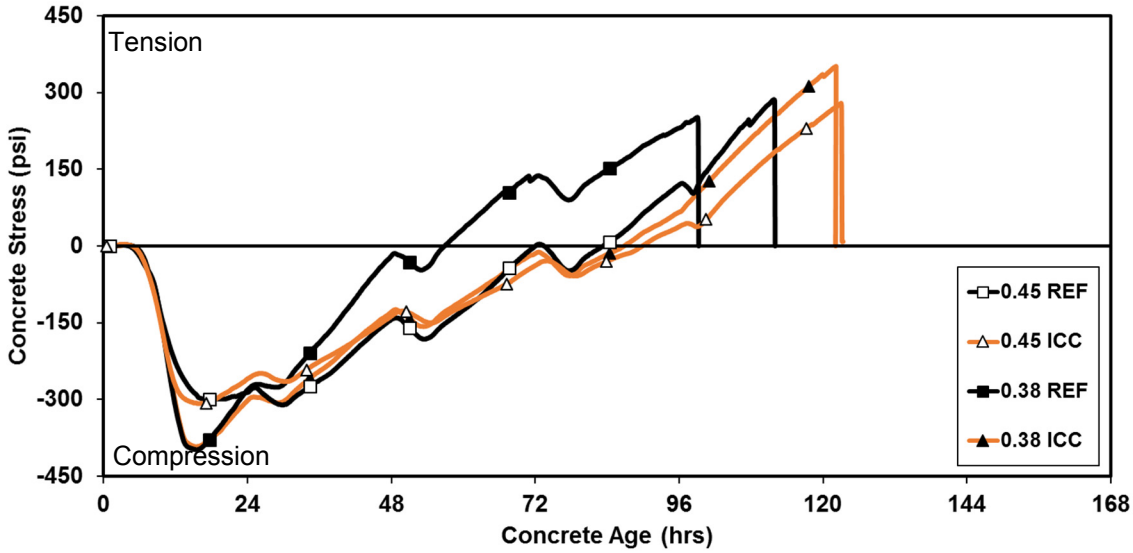

Figure 5-4: Measured restrained stress development of IC and reference concretes

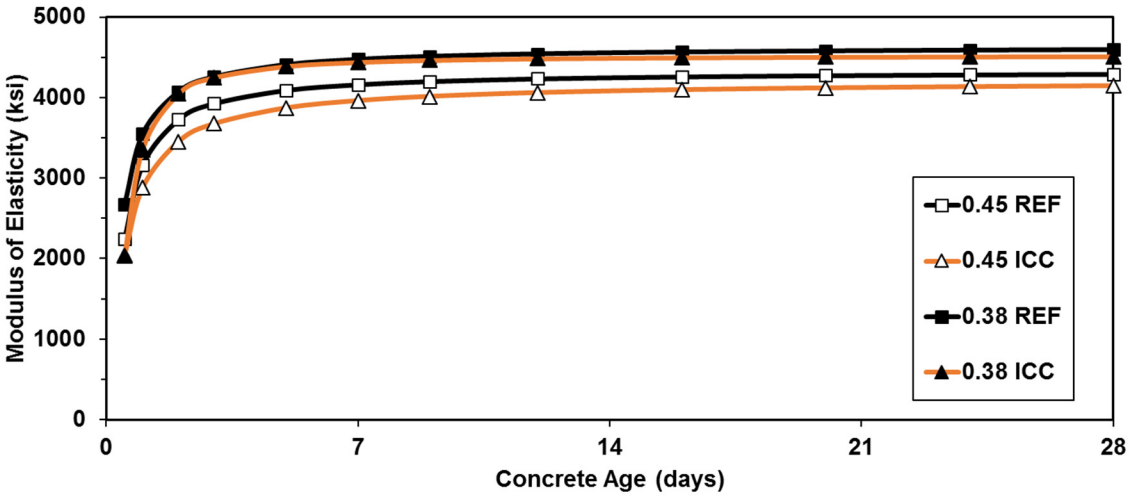

Figure 5-5: Measured modulus of elasticity of IC and reference concretes

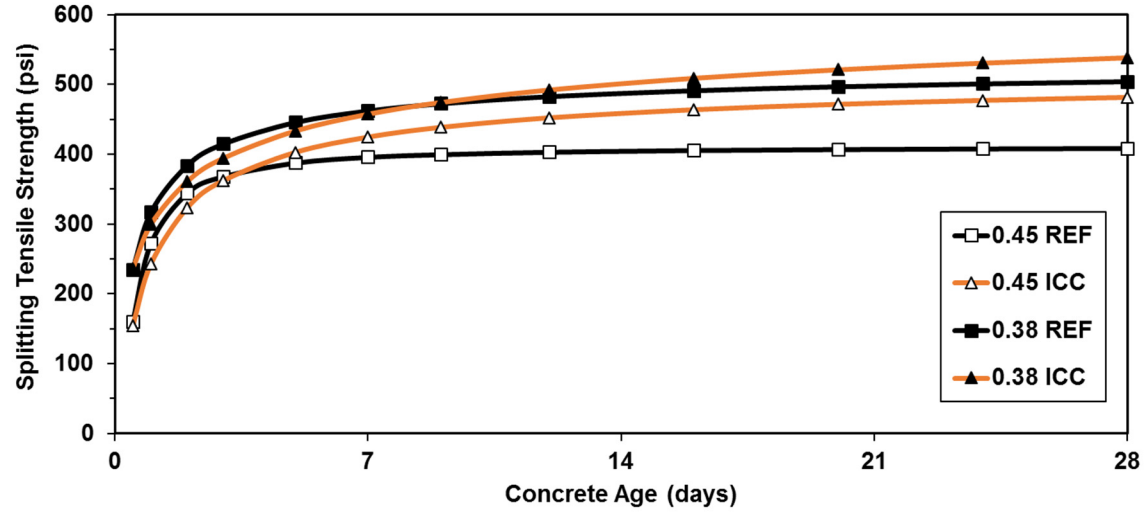

Figure 5-6: Measured splitting tensile strengths of IC and reference concretes

5.3.2 Behavior of Inverse Sand-Lightweight Concretes

The concrete temperature profiles and restrained stress development for the ISLW concretes for both *w/cm* concretes are compared to the response of the two reference concretes in Figures 5-7 and 5-8. For comparison, the modulus of elasticity and splitting tensile strength development of both ISLW and reference concretes are plotted in Figures 5-9 and 5-10.

The concrete temperatures of the ISLW concretes are higher than the reference concretes for both the *w/cm* concrete mixtures, due to a higher proportion of lightweight aggregates. This result is because of the decreased thermal diffusivity and increased heat of hydration due to internal curing, which causes higher temperatures in the ISLW concretes.

The time of cracking for ISLW concretes is increased by 18 and 39 hours for *w/cm* = 0.45 and *w/cm* = 0.38, respectively, in comparison to the reference concretes. Although the ISLW concretes had much lower splitting tensile strengths when compared to the reference concretes (as shown in Figure 5-10), it still had an improved cracking tendency when compared to the reference concretes. An average reduction of 33% in modulus of elasticity for both *w/cm* concretes (as shown in Figure 5-9), complete elimination of autogenous shrinkage related stresses for the 0.38 *w/cm* ISLW concrete, and a lower coefficient of thermal expansion, all combine to delay the time to cracking for ISLW concretes when compared to the reference concretes.

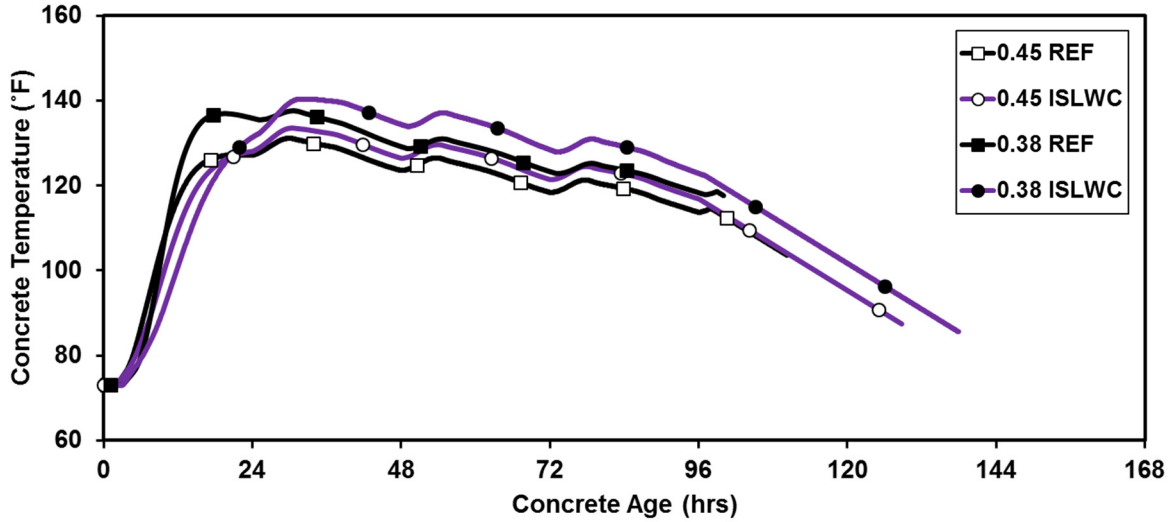

Figure 5-7: Concrete temperature profile of ISLW and reference concretes

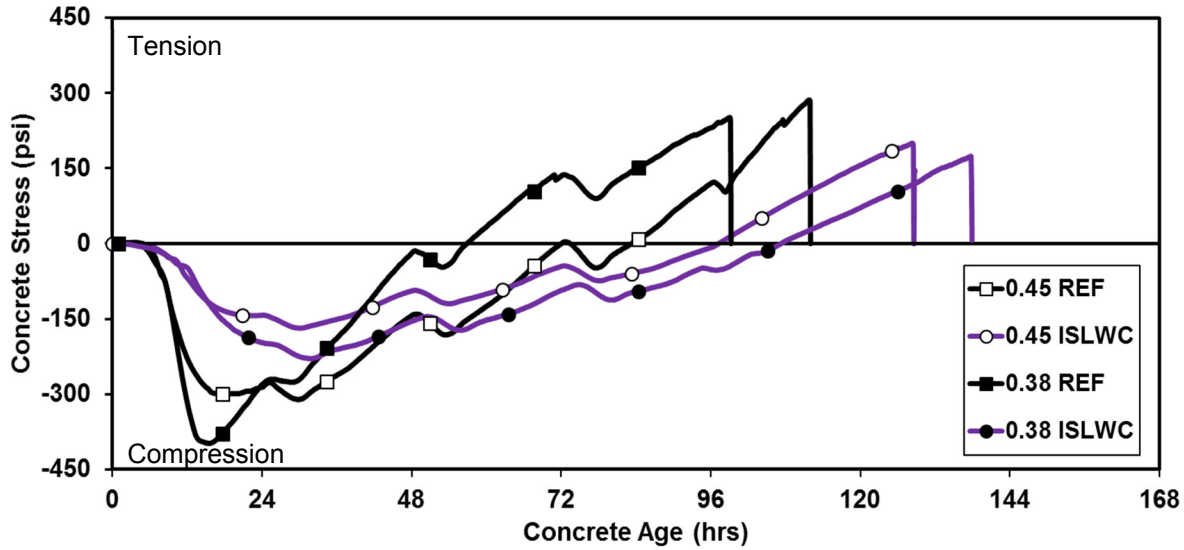

Figure 5-8: Measured restrained stress of ISLW and reference concretes

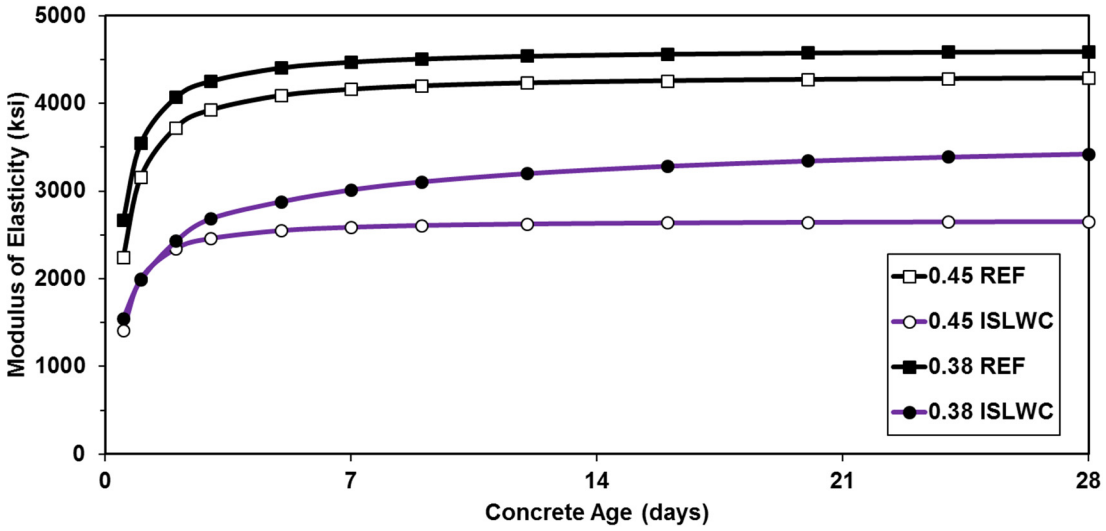

Figure 5-9: Measured modulus of elasticity of ISLW and reference concretes

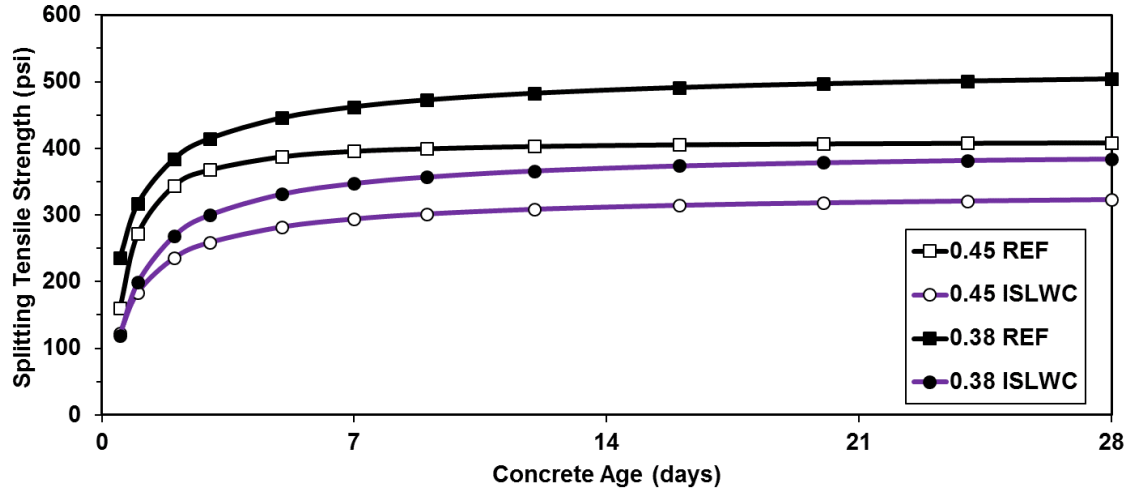

Figure 5-10: Measured splitting tensile strengths of ISLW and reference concretes

5.3.3 Behavior of Sand-Lightweight Concretes

The concrete temperature profiles and restrained stress development for the SLW concretes for both *w/cm* concretes are compared to the response of the two reference concretes in Figures 5-11 and 5-12. For comparison, the modulus of elasticity and splitting tensile strength development of both SLW and reference concretes are plotted in Figures 5-13 and 5-14.

The concrete temperatures of the SLW concretes are higher than the reference concretes, due to an increased proportion of lightweight aggregates. This result is because of the decreased thermal diffusivity and increased heat of hydration due to internal curing, which causes higher temperatures in the SLW concretes.

The time of cracking is increased by 24 hours (*w/cm* = 0.45) and 48 hours (*w/cm* =0.38) for the SLW concretes in comparison to the reference concretes. An average reduction of 12% in modulus of elasticity for both the *w/cm* concrete mixtures, (as shown in Figure 5-13), elimination of autogenous shrinkage related stresses for the 0.38 *w/cm* SLW concretes, and a lower coefficient of thermal expansion, all combine to delay the time to cracking for SLW concretes when compared to reference concretes.

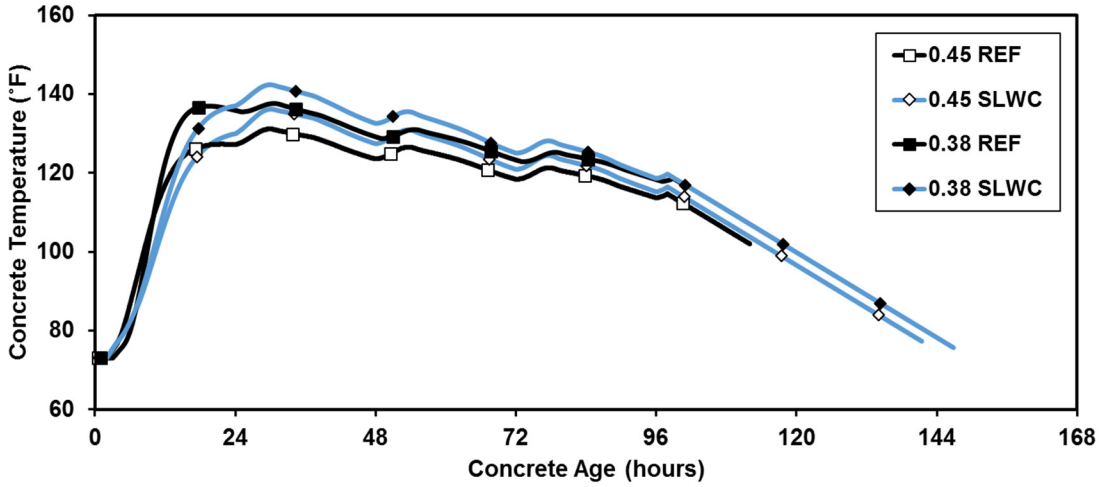

Figure 5-11: Concrete temperature profile of SLW and reference concretes

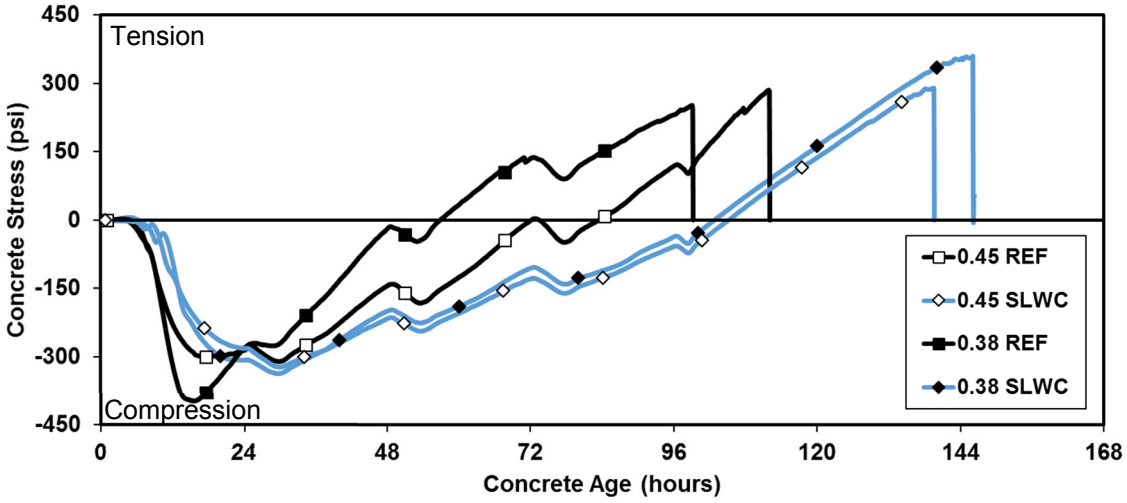

Figure 5-12: Measured restrained stress development of SLW and reference concretes

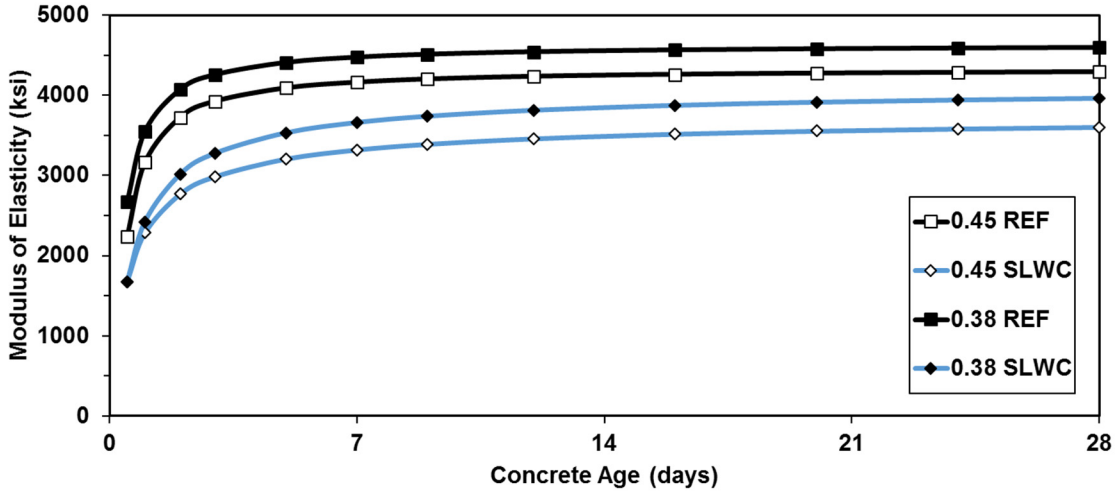

Figure 5-13: Measured modulus of elasticity of SLW and reference concretes

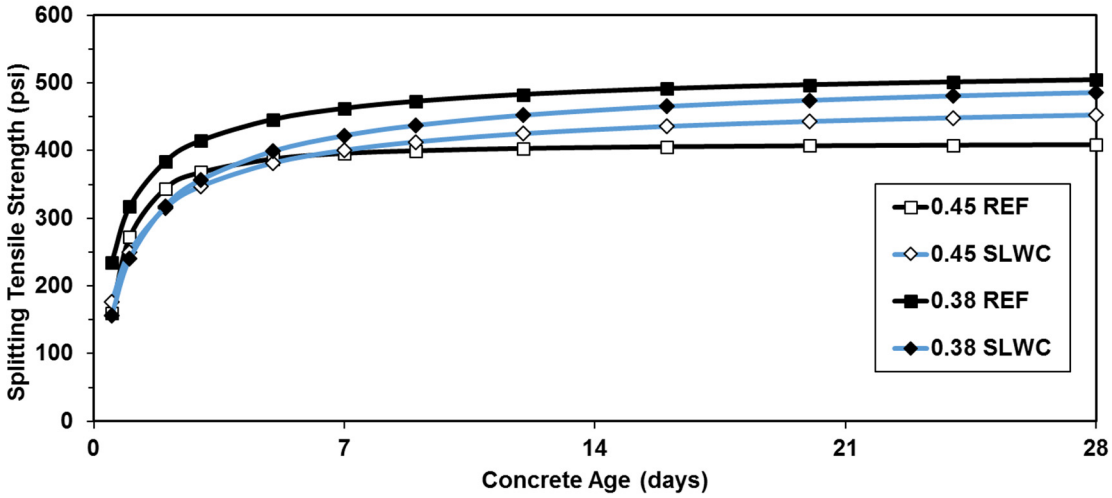

Figure 5-14: Measured splitting tensile strengths of SLW and reference concretes

5.3.4 Behavior of All-Lightweight Concretes

The concrete temperature profiles and restrained stress development for the ALW concretes for both *w/cm* concretes are compared to the response of reference concretes in Figures 5-15 and 5-16. For comparison, the modulus of elasticity and splitting tensile strength development of both ALW and reference concretes are plotted in Figures 5-17 and 5-18.

The concrete temperatures of the ALW concrete are higher than the reference concretes by 5% and 8%, for *w/cm* = 0.45 and *w/cm* = 0.38, respectively, since all the aggregate particles are lightweight aggregates. The reduced thermal diffusivity and increased heat of hydration due to internal curing, which causes higher temperatures in ALW concretes.

The time of cracking for ALW concretes is delayed by 22 and 43 hours for *w/cm* = 0.45 and *w/cm* = 0.38, respectively, in comparison to the reference concretes. Although the ALW concretes had much

lower splitting tensile strengths when compared to the reference concretes (as shown in Figure 5-18), they still had a much improved cracking tendency when compared to the reference concretes. An average reduction of 33 % in modulus of elasticity for both the *w/cm* concretes (as shown in Figure 5-17), the elimination of autogenous shrinkage related stresses for the 0.38 *w/cm* ALW concrete, and a lower coefficient of thermal expansion, all combine to delay the time to cracking for the ALW concretes when compared to reference concretes.

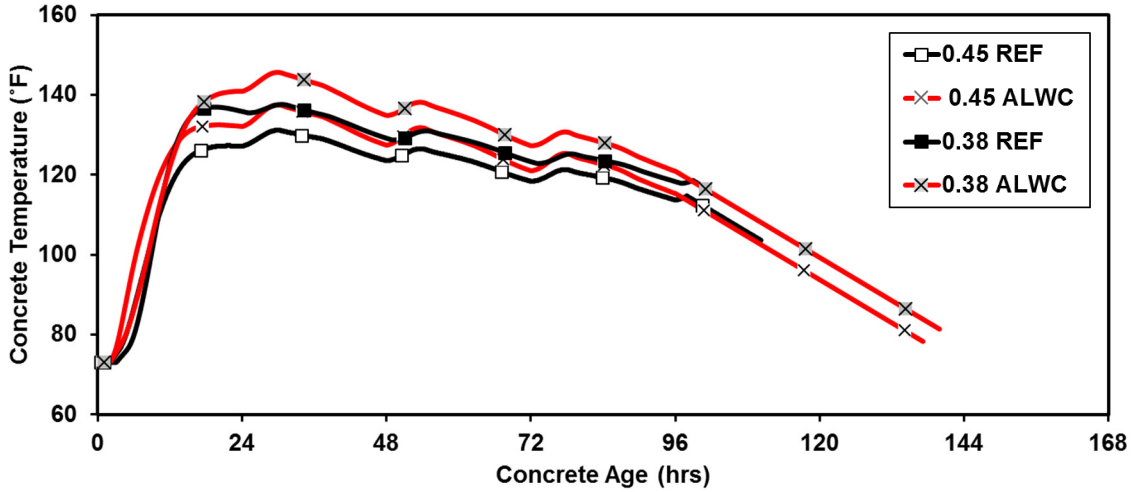

Figure 5-15: Concrete temperature profile of ALW and reference concretes

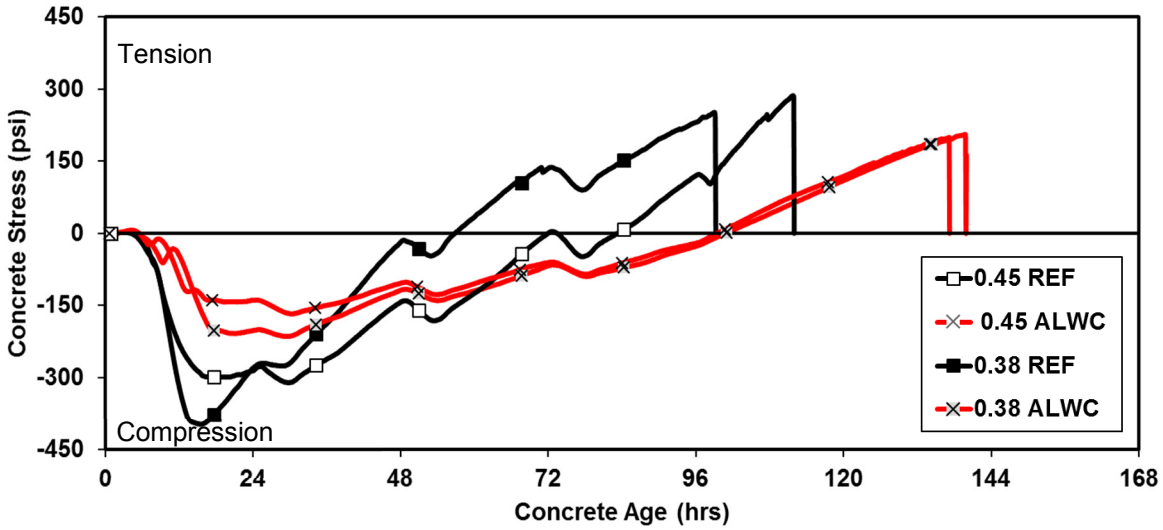

Figure 5-16: Measured restrained stress development of ALW and reference concretes

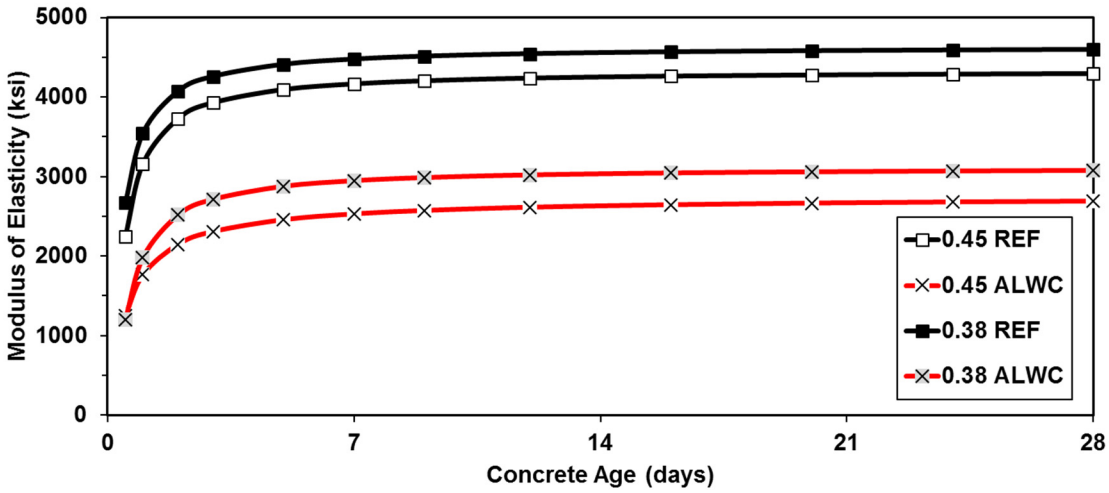

Figure 5-17: Measured modulus of elasticity of ALW and reference concretes

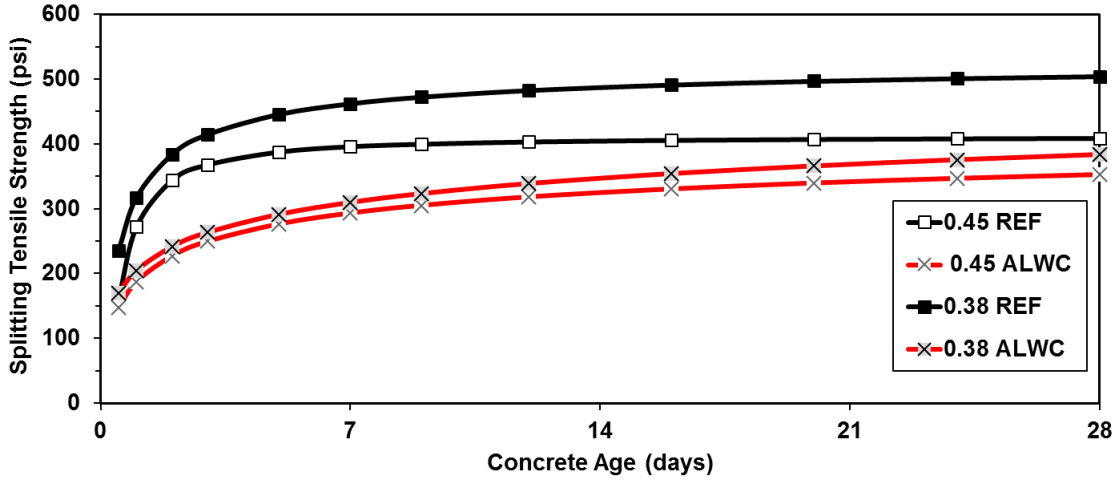

Figure 5-18: Measured splitting tensile strengths of ALW and reference concretes

5.4 EFFECT OF LIGHTWEIGHT AGGREGATE CONCRETES ON EARLY-AGE CONCRETE STRESS DEVELOPMENT

The restrained stress development and concrete temperature profiles for all concretes tested were discussed in the previous section. The maximum concrete temperature, denoted as T_{max}, reached in the rigid cracking frame for each concrete type is plotted in Figure 5-19(a) versus the approximate equilibrium density of each concrete. Similarly, in Figure 5-19(b), the time of cracking, denoted as t_c, for each concrete type as tested in the rigid cracking frame is plotted versus the approximate equilibrium density of concrete. As can be seen in Figure 5-19(a), ALW concrete has the highest maximum concrete temperature followed in order of decreasing maximum concrete temperature by the SLW, ISLW, IC, and reference concretes. The addition of LWA to concrete systematically lowers the thermal diffusivity, as shown in Figure 5-2, and subsequently increases the maximum concrete temperature. It can be observed from Figure 5-19 that

despite an increase in the maximum concrete temperatures for LWA concretes in comparison to the reference concretes, all concretes made with LWA exhibit an improved crack resistance. The presence of LWA in concrete delays the time to cracking with SLWC having tcthe latest time to cracking followed in order of decreasing time to cracking by ALW, ISLW, IC, and reference concretes.

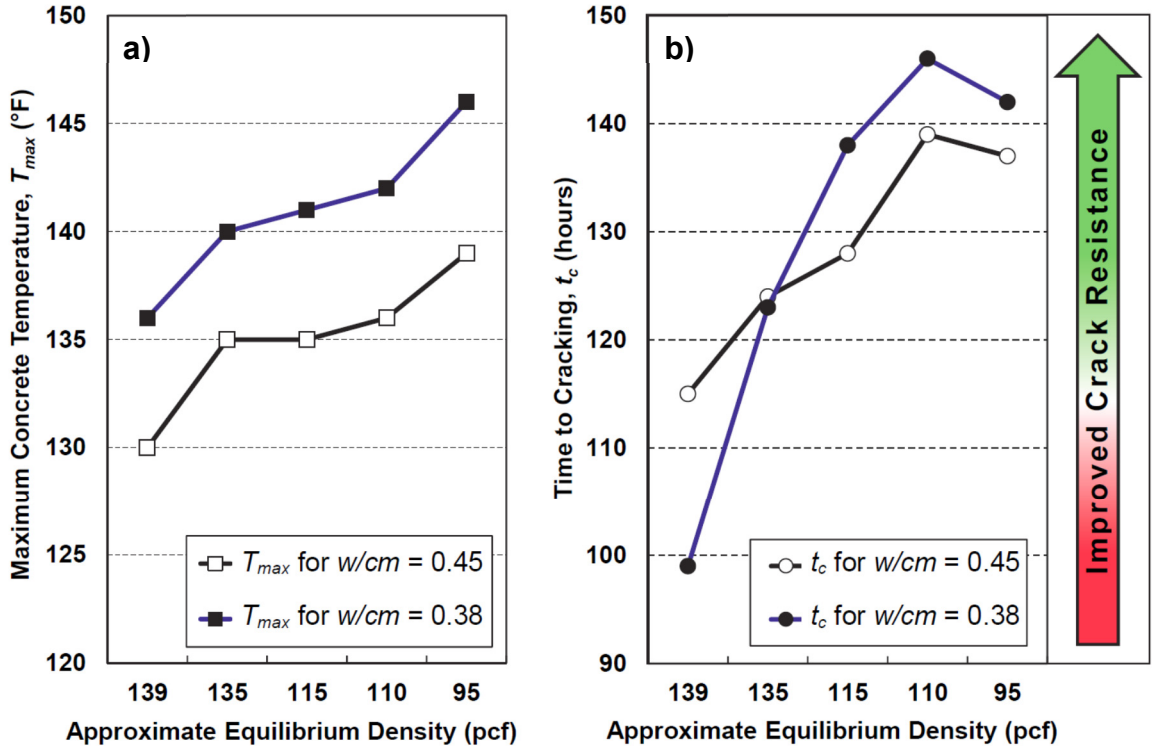

Figure 5-19: Summary of cracking tendency test results versus concrete density: a) Maximum concrete temperature and b) Time to cracking

Increasing the amount of pre-wetted LWA in concrete systematically decreases the density and subsequently the modulus of elasticity of the concrete. The only exception being ISLWC, which had a very low modulus of elasticity and this, is attributed to a lower compressive strength observed in both groups of ISLW concrete specimens. In addition, for both groups of concrete, the CTE decreases with an increasing proportion of pre-wetted LWA, as shown in Figure 5-1. Furthermore, autogenous shrinkage related stresses are eliminated in the 0.38 *w/cm* lightweight aggregate concretes, due to internal curing provided by the pre-wetted LWAs. Similar decrease in autogenous shrinkage related stresses have been reported by others (Byard and Schindler 2010; Lura et al. 2003).

It can thus be concluded that although an increasing amount of LWA in concrete will increase the maximum concrete temperature, the increasing use of LWA will reduce the modulus of elasticity, reduce the coefficient of thermal expansion, and eliminate autogenous shrinkage effects, which all result in an overall improvement in resistance to early-age cracking. As shown in Figure 5-19, sand-lightweight

concrete provided the best overall resistance to early-age cracking. The all-lightweight concrete did not perform as well as the sand-lightweight concrete, and this is attributed to its reduced splitting tensile strength when compared to the sand-lightweight concrete.

5.5 MEASURED MODULUS OF ELASTICITY COMPARED TO ACI 318 and AASHTO LRFD ESTIMATES

Equation 2-7 (ACI 318 2014) and 2-8 (AASHTO LRFD 2016) can be used to estimate the concrete modulus of elasticity using a known compressive strength. The concrete equilibrium density was used to estimate the modulus of elasticity for both ACI 318 (2014) and AASHTO LRFD (2016). The estimated modulus of elasticity according to ACI 318 (2014) and AASHTO LRFD (2016) is compared with the measured modulus of elasticity at 0.5, 1, 2, 3, 7, and 28 days in Figure 5-20 and 5-21, respectively.

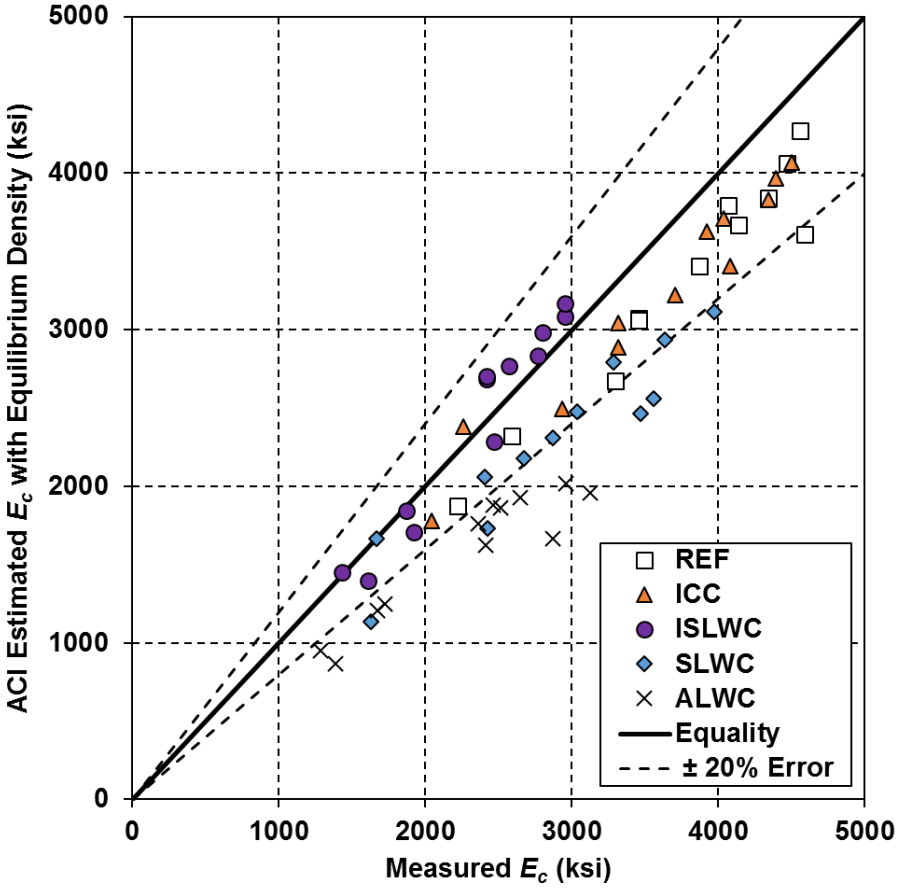

Figure 5-20: Measured versus ACI 318 (2014) predicted modulus of elasticity

From Figure 5-20, it can be observed that the ACI 318 (2014) modulus of elasticity formulation provides accurate results for the reference, IC, and ISLW concretes, because most of the data points fall within the ± 20 % error zone. However, many of the results for the SLW and ALW concretes fall below the

– 20 % error line; therefore, ACI 318 (2014) tends to underestimate the modulus of elasticity for the SLW and ALW concretes tested in this project.

From Figure 5-21, it can be observed that the AASHTO LRFD (2016) modulus of elasticity formulation provides accurate results for the reference, IC, and ISLW concretes, because most of the data fall within the ± 20 % error zone. However, many of the results for the SLW and ALW concretes fall below the – 20 % error line; therefore, AASHTO LRFD (2016) tends to underestimate the modulus of elasticity for the SLW and ALW concretes tested in this project.

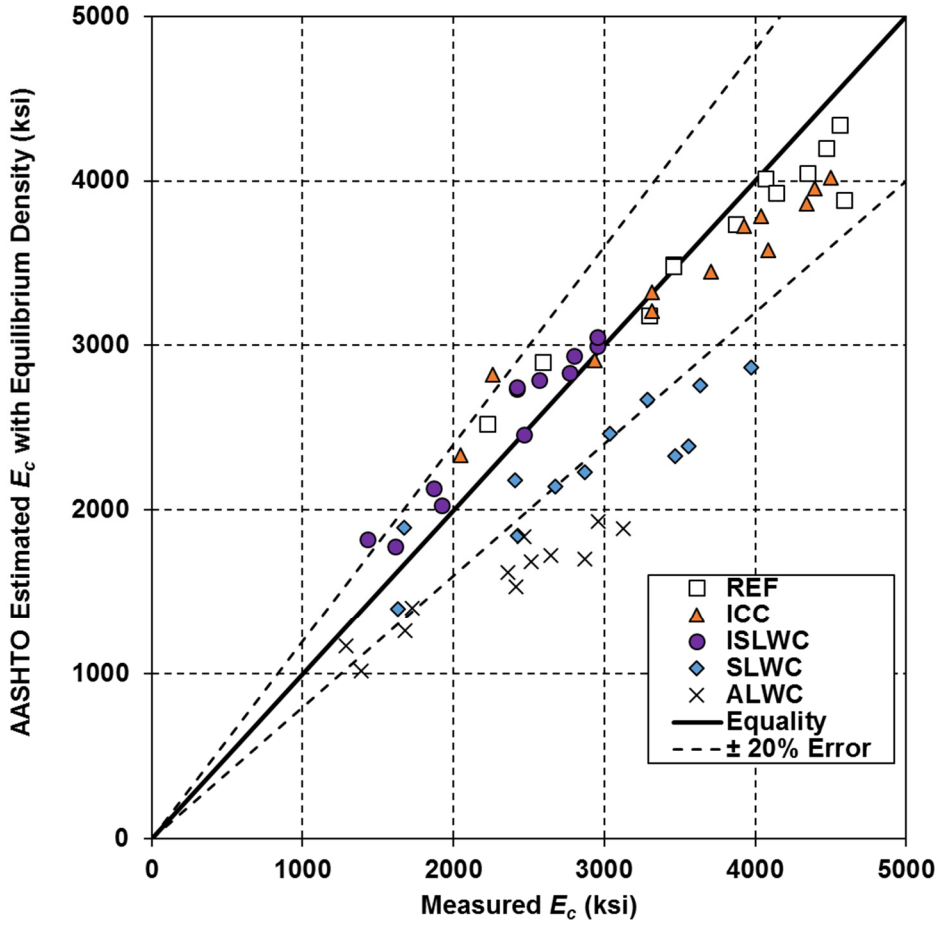

Figure 5-21: Measured versus AASHTO LRFD (2016) predicted modulus of elasticity

The unbiased estimate of the standard deviation of the absolute error, S_j, can be determined as shown in Equation 5-1 (Ayyub and McCuen 2011). The average unbiased estimate of the standard deviation of the absolute error for the modulus of elasticity when using the ACI 318 (2014) and AASHTO LRFD (2016) equations is presented in Table 5-1. It can be seen from the results shown in Table 5-1 that the ACI 318 and AASHTO LRFD expressions predict the modulus of elasticity well for high-density concretes (i.e. REF, ICC, and ISLWC), but produce a high S_j for concretes having lower densities (i.e. SLW and ALW concretes). Based on the average S_j values reported in Table 5-1, it can be concluded that

the ACI 318 (2014) and AASHTO LRFD (2016) expressions predict the modulus of elasticity with similar accuracy.

$$S_j = \sqrt{\frac{1}{n-1}\sum_{i}^{n}\Delta_i^2} \quad \text{..... (Equation 5-1)}$$

Where,

S_j = unbiased estimate of the standard deviation (units of property),

n = number of data points (unitless), and

Δ = absolute error (units of property).

Table 5-1: Unbiased estimate of standard deviation of absolute error for the modulus of elasticity estimation models

Modulus of Elasticity Estimation Model	S_j for E_c Estimate (ksi)					
	REF	**ICC**	**ISLWC**	**SLWC**	**ALWC**	**Average**
ACI 318: Equation 2-7	525	450	205	715	815	545
AASHTO LRFD: Equation 2-8	310	380	235	805	870	520

5.6 SPLITTING TENSILE STRENGTH BEHAVIOR COMPARED TO ACI ESTIMATES

The ACI 207.2R (2007) and ACI 207.1R (2012) splitting tensile strength equations were used to estimate the measured splitting tensile strength from measured compressive strength test results. The measured splitting tensile strengths at various ages are compared to the estimates obtained from the ACI 207.2R (2007) and ACI 207.1R (2012) equations in Figures 5-22 and 5-23, respectively.

From Figure 5-22, it can be observed that ACI 207.2R (2007) provides reasonably accurate estimates of the splitting tensile strength for the reference and IC concretes, because most of the data points fall within the ± 20 % error zone. However, many of the results for the ISLW, SLW and ALW concretes fall above the + 20 % error line; therefore, ACI 207.2R (2007) tends to overestimate the splitting tensile strength for the ISLW, SLW and ALW concretes tested in this project.

From Figure 5-23 it can be observed that ACI 207.1R (2012) provides reasonably accurate estimates of the splitting tensile strength for the reference and IC concretes, because most of the data points fall within the ± 20 % error zone. However, the majority of the results for the ISLW, SLW, and ALW concretes fall above the + 20 % error line; therefore, ACI 207.1R (2012) overestimates the splitting tensile strength for the ISLW, SLW, and ALW concretes tested in this project.

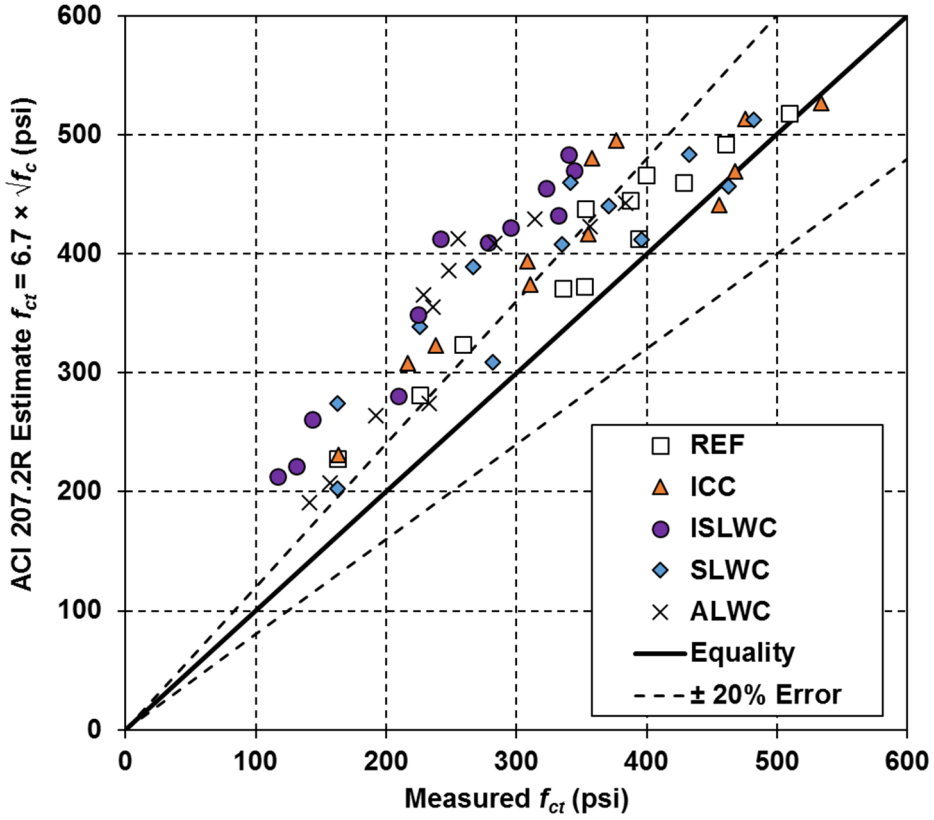

Figure 5-22: Measured versus ACI 207.2R (2007) predicted splitting tensile strength

The unbiased estimate of the standard deviation of absolute error, S_j, for the splitting tensile strength when using the ACI 207.2R (2007) and ACI 207.1R (2012) equations is presented in Table 5-2. It can be seen from the results shown in Table 5-2 that both ACI 207.2R (2007) and ACI 207.1R (2012) equations provide similar estimates of the splitting tensile strengths of the concretes.

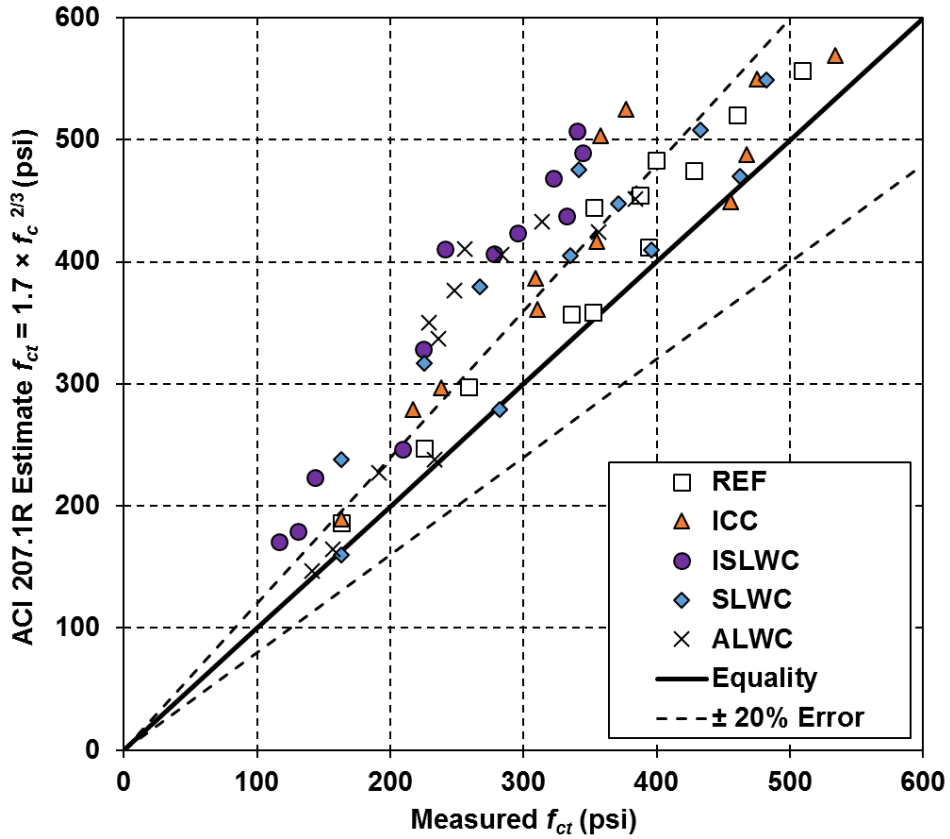

Figure 5-23: Measured versus ACI 207.1R (2012) predicted splitting tensile strength

Table 5-2: Unbiased estimate of standard deviation of absolute error for the splitting tensile strength estimation models

Splitting Tensile Strength Estimation Model	S_j for f_{ct} Estimate (psi)					
	REF	ICC	ISLWC	SLWC	ALWC	Average
ACI 207.2R: Equation 2-3	55	80	135	80	110	90
ACI 207.1R: Equation 2-4	55	80	130	80	105	90

5.7 EVALUATION OF MEASURED LIGHTWEIGHT MODIFICATION FACTORS FOR SPLITTING TENSILE STRENGTH

Green and Graybeal (2013) recommended the use of lightweight modification (λ) factor to estimate the splitting tensile strength as discussed in Section 2.1.4.2. This λ-factor can be computed in two ways (Green and Graybeal 2013):

1. If the splitting tensile strength is known, the λ-factor can be computed using Equation 5-2.

$$\lambda = \frac{4.7 \times f_{ct}^{"}}{\sqrt{f_c^{"}}} \leq 1.0 \quad \text{..... (Equation 5-2)}$$

Where,

λ = lightweight modification factor,

f_{ct}'' = splitting tensile strength (ksi), and

f'_c = compressive strength (ksi).

2. If splitting tensile strength is unknown, then the λ-factor can be computed with Equation 5-3.

$$0.75 \leq \lambda = 7.5 \times w_c'' \leq 1.0 \quad \text{..... (Equation 5-3)}$$

Where,

w''_c = concrete equilibrium density (kcf).

The average λ-factors obtained using Equations 5-2 and 5-3 for SLW, ISLW, and ALW concretes are presented in Table 5-3. Since the equilibrium density of the reference and IC concretes are 135 pcf or greater, they are considered normalweight concretes and are thus not included in Table 5-3. It can be observed that for SLW and ALW concretes, the λ-factor calculated by using the measured compressive and splitting tensile strengths (Equation 5-2) are similar to those obtained by using equilibrium densities (Equation 5-3). However, the λ-factor obtained from Equation 5-3 for ISLW concrete is much higher than the value obtained from using the measured compressive and splitting tensile strengths. This is partly due to the unexpected lower compressive and splitting tensile strengths observed in the ISLW concretes. Based on these observations, it can be concluded that the λ-factor calculated by using equilibrium density as shown in Equation 5-3, can be used to accurately estimate the splitting tensile strength of the SLW and ALW concretes tested in this project.

Table 5-3: Average lightweight modification factor (λ-value) by mixture type

Calculation Method	Lightweight Modification Factor		
	ISLWC	SLWC	ALWC
λ-factor from Equation 5-2	0.65	0.82	0.74
λ-factor from Equation 5-3	0.90	0.83	0.75

Chapter 6

Conclusions and Recommendations

6.1 SUMMARY

In this study, the effect of using lightweight aggregate on the early-age cracking tendency of mass concrete was evaluated. Two groups of concrete mixtures with a water-to-cementitious materials ratio (*w/cm*) of 0.38 and 0.45 were tested. Each group of concretes contained five mixtures: a reference normalweight concrete, internally cured (IC) concrete, inverse sand-lightweight (ISLW) concrete, sand-lightweight (SLW) concrete, and all-lightweight (ALW) concrete. Ten concretes were thus produced under laboratory conditions and evaluated in this study. The IC concrete is similar to normalweight concrete, except that a portion of fine aggregates was replaced with lightweight fine aggregates. The amount of lightweight aggregate was determined to ensure that the autogenous shrinkage was eliminated and the equilibrium density was greater than 135 pcf, which classifies the IC concrete as normalweight concrete according to AASHTO LRFD (2016). ISLW concrete contained normalweight coarse aggregates and lightweight fine aggregates, whereas the SLW concrete contained normalweight fine aggregate and lightweight coarse aggregate. The ALW concrete contained lightweight fine and coarse aggregates. In order to be representative of mass concrete, Class F fly ash at a 30% (by mass) cement replacement level was used in all mixtures.

The cracking tendency of the concretes were measured in a rigid cracking frame (RCF), using a unique temperature profile to simulate mass concrete placement under fall environmental conditions. For the lower *w/cm* concrete mixtures, the development of stress due to autogenous shrinkage were recorded under isothermal conditions. A free-shrinkage frame (FSF) was used to assess the unrestrained free shrinkage of the concretes. The time-depended development of mechanical properties was determined by performing compressive, splitting tensile, and modulus of elasticity tests at 0.5, 1, 2, 3, 7, and 28 days. The cylinders used to test the time-depended development of mechanical properties were match cured to the temperature of the RCF specimens. Semi-adiabatic calorimetry was used to characterize the release of heat of hydration from each mixture. The thermal diffusivity of each concrete was also tested to characterize the impact of lightweight aggregate on the development of concrete temperatures. The coefficient of thermal expansion of the hardened concrete was also assessed with a test setup similar to that required by AASHTO T 336 (2009).

6.2 CONCLUSIONS

6.2.1 Effect of Using Lightweight Aggregates on Concrete Properties

From this research, the following conclusions can be made regarding the effects of lightweight aggregate on concrete properties:

1. The compressive strength development for the reference, IC, and SLW concretes were similar. However, the compressive strengths of the ALW and ISLW concretes were approximately 10 to 15 % lower when compared to the reference concretes.
2. The splitting tensile strength development for the reference, IC, and SLW concretes were similar. However, the splitting tensile strengths of the ISLW and ALW concretes were approximately 20 to 30 % lower when compared to the reference concretes.
3. Increasing the amount of lightweight aggregate systematically decreased the concrete density, thereby also reducing the modulus of elasticity of concrete. When considering the with-in test variability, the modulus of elasticity development for the reference and IC concretes were similar. The modulus of elasticity values were lower on average by 12 %, 33 %, and 33 % for SLW, ISLW, and ALW concretes, respectively, when compared to the reference concretes.
4. Increasing the amount of lightweight aggregate in concrete systematically decreased the concrete coefficient of thermal expansion (CTE). The average CTE values were reduced by 5 %, 10 %, 10 %, and 30 % for IC, ISLW, SLW, and ALW concretes, respectively when compared to the reference concretes.
5. Concretes with increasing proportion of LWAs exhibit lower thermal diffusivity values, with an average thermal diffusivity reduction of 5 %, 10 %, 30 %, and 50 % for IC, ISLW, SLW, ALW concretes, respectively when compared to the reference concretes.
6. The ACI 318 (2014) and AASHTO LRFD (2016) modulus of elasticity formulations provide accurate estimates for the reference, IC, and ISLW concretes tested in this project. However, both ACI 318 (2014) and AASHTO LRFD (2016) tend to underestimate the modulus of elasticity for the SLW and ALW concretes tested in this project.
7. The ACI 207.2R (2007) and ACI 207.1R (2012) splitting tensile strength formulations provide reasonably accurate estimates for the reference and IC concretes tested in this project. However, both ACI 207.2R (2007) and ACI 207.1R (2012) tend to overestimate the splitting tensile strength for the ISLW, SLW, and ALW concretes tested in this project.
8. The lightweight modification factor (λ-factor), calculated by using the equilibrium density as proposed by Green and Graybeal (2013), can be used to accurately estimate the splitting tensile strength of the SLW and ALW concretes tested in this project.

6.2.2 Early-Age Concrete Behavior

From this research, the following conclusions can be made about the effect of using lightweight aggregate on the effect of cracking tendency and autogenous shrinkage of concrete:

1. Concretes containing an increased proportion of LWAs experienced higher concrete temperatures when compared to the reference concretes. ALW concrete had the highest maximum concrete temperature followed in order of decreasing maximum concrete temperature by the SLW, ISLW, IC, and reference concretes. This behavior is attributed to the lower thermal diffusivity and increased heat of hydration present in concretes containing LWAs. Care should be taken when using LWA concrete in mass concrete to make sure that the threshold for DEF to occur is not exceeded.
2. As the *w/cm* of the concrete decreased, the peak concrete temperatures increased, which is due to the presence of more cementitious material in low *w/cm* concretes.
3. The presence of LWA in concrete delayed the time to cracking, with SLW concrete providing the best overall resistance to early-age cracking. The time to cracking for all concretes containing pre-wetted lightweight aggregates was greater than the time to cracking of the normalweight concretes.
4. For the concretes with *w/cm* = 0.38, the presence of pre-wetted lightweight aggregate eliminated autogenous shrinkage and its related stresses. The use of lightweight aggregates in concrete with low *w/cm* is beneficial to control early-age cracking, because it helps to mitigate autogenous shrinkage and lower the modulus of elasticity of the higher strength concrete.
5. Although an increasing amount of LWA in the concrete will increase the maximum concrete temperature in mass concrete applications, the increasing use of LWA will reduce the modulus of elasticity, reduce the coefficient of thermal expansion, and eliminate autogenous shrinkage effects, which all contribute to improve the resistance to early-age cracking.

6.3 RECOMMENDATIONS FOR FUTURE WORK

The following recommendations are offered for future research:

1. The compressive strength, splitting tensile strength, and modulus of elasticity results of the ISLW concrete were lower in comparison to SLW concrete, despite their densities being reasonably similar. This may be related to the specific fine lightweight aggregates, particle packing, or the combined gradation of aggregates used in this project. However, since this result was unexpected, it is recommended to determine how to proportion ISLW and SLW concrete with the same *w/cm* to achieve similar mechanical properties.
2. Due to the resources available, the thermal properties of the lightweight aggregates were back calculated from semi-adiabatic calorimetry and were not directly measured. When modeling the temperature development in mass concrete elements, it is recommended that the thermal properties of the concrete be determined using standardized ASTM test methods.

3. The effect of lightweight aggregate on drying shrinkage was not evaluated in this study. Study of drying shrinkage will aid in the evaluation of long-term effects of lightweight aggregate on drying shrinkage.
4. The early-age and long-term performance of similar full-scale mass concrete elements constructed with normalweight and sand-lightweight concrete should be collected and compared.

REFERENCES

AASHTO. 2016. AASHTO *LRFD Bridge Design Specifications, 7th Edition with 2016 Interim Revisions*. American Association of State Highway and Transportation Officials, Washington, D.C.

AASHTO T336. 2009. *Standard Method of Test for Coefficient of Thermal Expansion of Hydraulic Cement Concrete.* American Association of State Highway and Transportation Officials, Washington, D.C.

ACI Committee 207.1R. 2012. *Guide to Mass Concrete*. American Concrete Institute, Farmington Hills, MI.

ACI Committee 207.2R. 2007. *Report on Thermal and Volume Change Effects on Cracking of Mass Concrete*. American Concrete Institute, Farmington Hills, MI.

ACI Committee 213. 2013. *Guide for Structural Lightweight-Aggregate Concrete*. American Concrete Institute, Farmington Hills, MI.

ACI Committee 301. 2016. *Specifications for Structural Concrete*. American Concrete Institute, Farmington Hills, MI.

ACI Committee 318. 2014. *Building Code Requirements for Structural Concrete and Commentary.* American Concrete Institute. Farmington Hills, MI.

ACI CT-16. 2016. *Concrete Terminology- An ACI Standard*. American Concrete Institute, Farmington Hills, MI.

Atrushi, D. 2003. *Tensile and Compressive Creep of Early Age Concrete: Testing and Modelling*. Doctoral Dissertation, NTNU Trondheim, Norway.

Ayyub, B.M. and R.H. McCuen. 2011. *Probability, Statistics, and Reliability for Engineers and Scientists*. CRC Press, 3rd Edition, Boca Rotan, FL.

Bamforth, P.B. 1981. *Large Pours*. Letters to the editor, Concrete, Concrete and Cement Association, London.

Bažant, Z.P. 1982. *Mathematical Models for Creep and Shrinkage of Concrete Structures*. Creep and Shrinkage in Concrete Structures (ed. Bažant and Wittmann), John Wiley & Sons, New York, NY, pp. 163-256.

Bentz, D.P., and W.J. Weiss. 2011. *Internal Curing: A 2010 State-of-the- Art Review*. Publication NISTIR 7765. National Institute of Standards and Technology, Gaithersburg, MD.

Bentz, D.P., P. Lura, and J.W. Roberts. 2005. *Mixture proportioning for internal curing*. Concrete International, Vol. 27, No. 2, pp. 35-40.

Bjøntegaard, Ø. 1999. *Thermal Dilation and Autogenous Deformation as Driving Forces to Self-Induced Stresses in High Performance Concrete*. Doctoral Thesis. Norwegian University of Science and Technology, Division of Structural Engineering, Norway.

Bremner, T., and J. Ries. 2009. *Stephen J. Hayde: Father of the Lightweight Concrete Industry*. Concrete International, Vol.31, No. 8, pp. 35-38.

Byard B.E., A.K. Schindler, and R.W. Barnes. 2012. Early-Age Cracking Tendency and Ultimate Degree of Hydration of Internally Cured Concrete. *ASCE Journal of Materials in Civil Engineering*, Vol. 24, No. 8, pp. 1025-1033.

Byard B.E. 2011. *Early-age Properties of Lightweight Aggregate Concrete*. Doctoral Dissertation. Auburn University, Auburn, AL.

Carino, N.J. 1991. The Maturity Method. *Handbook on Non-Destructive Testing of Concrete* (Ed.by V.M. Malhotra and N.J. Carino), C.R.C. Press, Boca Rotan, FL, pp. 101-147

Castro, J., L. Keiser., M. Golias., and W. Weiss. 2011. Absorption and Desorption of Fine Lightweight Aggregate for Applications to Internally Cured Concrete Mixtures. *Cement and Concrete Composites*, Vol. 33, No. 10, pp. 1001-08.

Chandra, S., and L. Berntsson. 2002. *Lightweight Aggregate Concrete*. 1st Edition, William Andrew, NY.

Clarke, J.L. 1993. *Structural Lightweight Aggregate Concrete*. CRC Press, Boca Rotan, FL.

Delatte, N., D. Crowl., E. Mack., and J. Cleary. 2008. Evaluating High Absorptive Materials to Improve Internal Curing of Concrete. In ACI Special Publication 256, *Internal Curing of High-Performance Concretes*, (ed. D. Bentz and B. Mohr), Farmington Hills, MI.

Emborg, M. 1989. *Thermal Stresses in Concrete at Early Ages*. Doctoral Dissertation. Luleå University of Technology, Luleå, Sweden.

Emborg, M., and S. Bernander. 1994. Thermal Stresses Computed by a Method for Manual Calculations. *In RILEM Proceedings 25, Thermal Cracking in Concrete at Early Age*, (ed.by R. Springenschmid) E&FN Spon, London, pp. 321–328.

FitzGibbon, M.E. 1976. *Large pours for reinforced concrete structures*. Concrete, Concrete and Cement Association, Vol 10, No. 3, pp. 41, London.

Folliard, K.J., R. Barborak., T. Drimalas., L. Du., S. Garber., J. Ideker., T. Ley., S. Williams., M.G. Juenger., B. Fournier., and M.D.A. Thomas. 2006. *Preventing ASR/DEF in New Concrete: Final Report.* Center for Transportation Research, University of Texas at Austin.

Freieslben Hansen, P., and E. J. Pederson. 1977. *Maturity Computer for Controlling Curing and Hardening of Concrete.* Nordisk Betong, Vol. 1, No. 19, pp. 21-25.

Gajda, J., and M.G. VanGeem. 2002. Controlling Temperatures in Mass Concrete. *Concrete International*, Vol. 24, No. 1, pp. 58-62.

Gajda, J. 2007. *Mass Concrete for Buildings and Bridges*. Portland Cement Association, Skokie, IL.

Greene, G., and B.A. Graybeal. 2012. Synthesis and Evaluation of Lightweight Concrete Research Relevant to the AASHTO LRFD Bridge Design Specifications: Potential Revisions for Definition and Mechanical Properties. *Publication FHWA –HRT-13-030*. FHWA, U.S Department of Transportation.

Hedlund, H. 2000. *Hardening Concrete Modelling of Non Elastic Deformations and Related Properties*. Doctoral Dissertation, Luleå University of Technology, Sweden.

Henkensiefken, R., D.P. Bentz., T. Nantung., and W.J. Weiss. 2009. Volume Change and Cracking in Internally Cured Mixtures Made with Saturated Lightweight Aggregates under Sealed and Unsealed Conditions. *Cement and Concrete Composites*, Vol. 31, No. 7, pp. 426-437.

Henkensiefken, R., T. Nantung., and W.J. Weiss. 2011. Saturated Lightweight Aggregate for Internal Curing in Low w/c Mixtures: Monitoring Water Movement Using X-ray Absorption. *Strain*, Vol 47, Issue 1, pp.1-10.

Holm, T.A. and J. Ries. 2007. *ESCSI's Reference Manual for the Properties and Applications of Expanded Shale, Clay and Slate Lightweight Aggregate.* ESCSI, Salt Lake City, UT.

Holt, E. *Early Age Autogenous Shrinkage of Concrete*. 2001. Doctoral Thesis. The University of Washington, Seattle, WA.

Jahren, T.C., J.L. Li., J.J. Shaw, and K. Wang. 2014. *Iowa Mass Concrete for Bridge Foundations Study – Phase II.* Publication Iowa DOT In-Trans Project 10-384. Institute for Transportation, Ames, IA.

Klieger, P. 1957. Early High Strength Concrete for Prestressing. *Proceedings World Conference on Prestressed Concrete*, San Francisco, pp. A5-1 to A5-14.

Larson, M. 2003. *Thermal Crack Estimation in Early Age Concrete: Models and Methods for Practical Application*. Doctoral Dissertation, Luleå University of Technology, Sweden.

Livingston, R.A., C. Ormsby., A.M. Made., M.S. Ceary., N. McMorris., and P.G. Finnerty. 2006. *Field Survey of Delayed Ettringite Formation-Related Damage in Concrete Bridges in the State of Maryland*. American Concrete Journal, Special Publication 234, pp. 251-268.

Lura, P., O.M. Jensen., and K. Breugel. 2003. Autogenous Shrinkage in High-Performance Cement Paste: An Evaluation of Basic Mechanisms. *Cement and Concrete Research*, Vol. 33, Issue 2, pp. 223-232.

Maggenti, R. 2007. From Passive to Active Thermal Control. *Concrete International*, Vol. 29, No. 11, pp. 24-30.

Mangold, M. 1998. Methods for Experimental Determination of Thermal Stresses and Crack Sensitivity in the Laboratory. In RILEM Report 15, *Prevention of Thermal Cracking in Concrete at Early Ages* (ed. R. Springenschmidt), London, E & FN Spon, pp. 26-40.

Meadows, J.L. 2007. *Early-Age Cracking of Mass Concrete Structures*. Master of Science Thesis, Auburn University, AL.

Mehta, P.K., and P.J.M. Monteiro. 2013. *Concrete: Microstructure, Properties and Materials*. McGraw-Hill Education, Inc., New York, NY.

Mindess, S., J.F. Young, and D. Darwin. 2002. *Concrete*. 2nd Edition, Prentice Hall, Saddle River, NJ.

Morabito, P. 1998. Methods to Determine the Heat of Hydration of Concrete. In RILEM Report 15, *Prevention of Thermal Cracking in Concrete at Early ages*, (ed. R. Springenschmidt) E&FN Spon, London, pp. 1-25.

Neville, A.M. 2011. *Properties of Concrete*. 5th Edition, Pearson Education, Inc., Essex, England.

Poole, J.L, K.A. Riding, R.A. Browne, and A.K. Schindler. 2006. Temperature Management of Mass Concrete Structures. *Concrete Construction Magazine*.

Rao, A. 2008. *Evaluation of Early-Age Cracking Sensitivity in Bridge Deck Concrete*. Master of Science Thesis, Auburn University, AL.

Raoufi, K. 2011. *Restrained Shrinkage Cracking of Concrete: The Influence of Damage Localization*. Doctoral Dissertation, Purdue University, IN.

Raphael, J.M. 1984. *Tensile Strength of Mass Concrete*. American Concrete Institute, Vol. 81, No. 17, pp. 158-165.

Riding, K.A. 2007. *Early Age Concrete Thermal Stress Measurement and Modeling*. Doctoral Dissertation. University of Texas, Austin, TX.

Riding, K., J. Poole, A.K. Schindler, M.G. Juenger, and K.J. Folliard 2014. Statistical Determination of Cracking Probability for Mass Concrete. *ASCE Journal of Materials in Civil Engineering*, Vol. 26, No. 9.

RILEM Technical Committee 119-TCE. 1998. Testing of the Cracking Tendency of Concrete at Early Ages in the Cracking Frame Test. *In RILEM Report 15, Prevention of Thermal Cracking in Concrete at Early Ages*, (ed. R. Springenschmidt), E & FN Spon, London, pp. 315-339.

RILEM Technical Committee 196-ICC. 2007. Mechanisms of Internal Water Curing. *In RILEM Report 41*. *Internal Curing of Concrete* (Ed. by Kovler and Jensen). RILEM publications, Bagneux, France.

Robertson, E.C. 1988. *Thermal Properties of Rocks*. USGS Open File Report 88-441. United States Geological Survey, Reston, VA. 106 p.

Rostasy, F.E., T. Tanabe., and M. Laube. 1998. *Assessment of External Restraint*. In RILEM Report 15, *Prevention of Thermal Cracking in Concrete at Early Ages*, (ed. R. Springenschmidt), E&FN Spon, London, pp. 149-168.

Schindler, A.K., and B.F. McCullough. 2002. The Importance of Concrete Temperature Control during Concrete Pavement Construction in Hot Weather Conditions. *Journal of the Transportation Research Board*, No. 1813, Washington, D.C., pp 3-10.

Schindler, A.K., and K.J. Folliard. 2005. Heat of Hydration Models for Cementitious Materials. *ACI Materials Journal*, Vol. 102, No. 1, pp. 24-33.

Shilstone, J.M. and J.M. Shilstone, Jr. 1989. *Concrete Mixtures and Construction Needs*. Concrete International Vol. 11, No. 12, pp. 53-57.

Shilstone Sr., J.M. 1990. Concrete Mixture Optimization. *Concrete International*, Vol. 12, No. 6, pp 33-39.

Springenschmidt, R., R. Breitenbucher., and M. Mangold. 1994. Development of the Cracking Frame and Temperature-Stress Testing Machine. In RILEM Proceedings 25, *Thermal Cracking in Concrete at Early Ages*, (ed. R. Springenschmidt), London, E & FN Spon, pp. 137-45.

Sylla, H.M. 1988. Reactions in Hardened Cement Paste Caused by Heat Treatment, *Beton*, Vol. 38, pp. 488–493

Tankasala, A., A.K. Schindler, K.A. Riding. 2017. Thermal Cracking Risk of Using Lightweight Aggregate in Mass Concrete. *Journal of the Transportation Research Board*, TRR No. 2629.

Taylor, H.F.W., C. Famy, and K.L. Scrivener. 2001. Delayed Ettringite Formation. *Journal of Cement and Concrete Research*, Vol. 31, Issue 5, pp. 683-693.

Tazawa, E. 1998. Autogenous Shrinkage and Its mechanism. *Autogenous Shrinkage of Concrete* (ed. E. Tazawa), E&FN Spon, London.

Thomas, M.D.A., K. Folliard, T. Drimalas, and T. Ramlochan. *2008.* Diagnosing Delayed Ettringite Formation in Concrete Structures. *Cement and Concrete Research*, Vol. 38*,* No. 6, pp. 841-847*.*

Umehara, H., T. Uehara., T. Hsaka., and A. Sugiyama. 1994. Effect of Creep in Concrete at Early Ages on Thermal Stress. *In RILEM Proceedings 25, Thermal Cracking in Concrete at Early Ages*, (Ed. By R. Springinschmidt), E&FN Spon, London, pp. 79-87.

Weakley, R.W. 2009. *Evaluation of Semi-Adiabatic Calorimetry to Quantify Concrete Setting*. Master of Science Thesis, Auburn University, AL.

Westman, G. 1999. *Concrete Creep and Thermal Stresses*. Doctoral Dissertation. Luleå University of Technology, Luleå, Sweden.

Xu, Y., and D.D.L. Chung. 2000. Cement of High Specific Heat and High Thermal Conductivity, Obtained by Using Silane and Silica Fume as Admixtures. *Cement and Concrete Research*. Vol. 30, Issue 7, pp. 1175-1178.

Appendix A

Aggregate Gradations

Table A-1: Coarse aggregate gradation

Sieve Size	Percent Passing	
	Normalweight Coarse Aggregate (Auburn, AL)	**Lightweight Coarse Aggregate (Norlite, NY)**
1 in.	100.0	100.0
¾ in.	95.2	97.0
½ in.	64.3	65.4
3/8 in.	39.2	22.4
# 4	1.2	2.9
# 8	0.1	0.4
# 16	0.0	0.0

Table A-2: Fine aggregate gradation

Sieve Size	Percent Passing	
	Normalweight Fine Aggregate (Auburn, AL)	**Lightweight Fine Aggregate (Norlite, NY)**
½ in.	100.0	–
3/8 in.	100.0	100.0
# 4	99.7	100.0
# 8	90.7	98.8
# 16	69.4	59.5
# 30	32.8	38.3
# 50	5.9	15.6
# 100	1.5	0.3
Pan	0.0	0.0

Appendix B

Concrete Mechanical Properties

Table B-1: Match-cured compressive strength results for all concretes

Concrete	Compressive strength (psi)					
	½ day	1 day	2 days	3 days	7 days	28 days
REF 0.45	1150	2340	3090	3800	4270	4710
REF 0.38	1765	3070	4410	4830	5400	5970
ICC 0.45	1180	2320	3120	3870	4330	4900
ICC 0.38	2120	3460	5140	5470	5870	6180
ISLWC 0.45	1090	1510	2710	3730	3970	4160
ISLWC 0.38	1000	1760	3790	4620	4920	5200
SLWC 0.45	910	2120	3370	3770	4310	4640
SLWC 0.38	1670	2560	3710	4710	5210	5850
AWC 0.45	810	1560	2820	3320	3720	3980
AWC 0.38	960	1670	2980	3780	4100	4370

Table B-2: Match-cured splitting tensile strength results for all concretes

Concrete	Splitting Tensile Strength (psi)					
	½ day	1 day	2 days	3 days	7 days	28 days
REF 0.45	160	260	350	390	350	430
REF 0.38	230	340	390	400	460	510
ICC 0.45	160	240	310	360	460	470
ICC 0.38	220	310	360	380	480	530
ISLWC 0.45	130	140	220	280	300	330
ISLWC 0.38	120	210	240	320	340	340
SLWC 0.45	160	280	270	360	370	460
SLWC 0.38	160	230	340	340	430	480
AWC 0.45	140	190	240	250	280	360
AWC 0.38	160	230	230	260	310	380

Table B-3: Match-cured modulus of elasticity results for all concretes

Concrete	Modulus of Elasticity (ksi)					
	½ day	1 day	2 days	3 days	7 days	28 days
REF 0.45	2200	3300	3450	3900	4000	4050
REF 0.38	2600	3450	4150	4350	4500	4550
ICC 0.45	2050	2950	3300	3700	4100	3950
ICC 0.38	2250	3300	4050	4350	4400	4500
ISLWC 0.45	1450	1900	2450	2400	2550	2750
ISLWC 0.38	1600	1850	2400	2800	2950	2950
SLWC 0.45	1650	2450	2700	2850	3450	3550
SLWC 0.38	1650	2400	3050	3300	3650	4000
AWC 0.45	1400	1700	2400	2350	2500	2650
AWC 0.38	1300	1750	2900	2450	3100	2950